4.4 GLOBAL SENSITIVITY ANALYSIS

The overall goal of Global Sensitivity Analysis (GSA) is to determine sensitivity of pavement performance prediction models to the variation in the design input values. The main difference between GSA and detailed sensitivity analyses is the way the levels of an input are considered. While extreme values (only two levels) of the input ranges are considered in the detailed sensitivity analysis, GSA utilizes the entire domain for the input ranges. In this section, the details of the GSA process are presented first followed by the findings and discussion of results for the four rehabilitation options.

4.4.1 GSA Methodology

The process for GSA analysis involves various steps.

1. The first step is to define a base case for all the rehabilitation options. The base cases consist of the pavement cross-section, material properties and climate information. These base cases should cover the design practices and climatic conditions in the State of Michigan.
2. The second step is to determine the ranges of input variables in order to cover the entire problem domain.
3. The third step is to sample input combinations from the problem domain.
4. The fourth step includes generating the predicted performance to the sampled inputs from the third step.
5. The fifth step involves fitting response surface models (RSM) to the generated data in step four.
6. Finally, the sensitivity metric is determined for the fitted RSM to quantify the impact of input variables on predicted performance measures.

The details of the analysis related to all the above steps are presented next.

4.4.1.1. Base cases

Similarly to the previously described analyses, the GSA analysis was conducted on the rehabilitation options currently used in Michigan DOT practice; i.e., HMA over HMA, HMA over PCC (composite), HMA over rubblized PCC, and unbonded PCC overlay. Also two different weather stations (Pellston and Detroit) were used to represent the effect of climate in Michigan. The effect of traffic was evaluated in the previous MDOT studies (*2*, *8*, *9*); hence in this analysis, the traffic was held constant at a typical interstate traffic level. The eight base cases evaluated in this study are shown in Table 4-40.

Table 4-40 Base cases for global sensitivity analysis

Rehabilitation type	Climate
HMA over HMA	Pellston Detroit
Composite (HMA over PCC)	
HMA over Rubblized PCC	
Unbonded PCC overlay	

Figure 4-16 shows the climatic data for the two locations considered in the State of Michigan. It can be observed that these climates cover different ranges of temperatures and freezing indices.

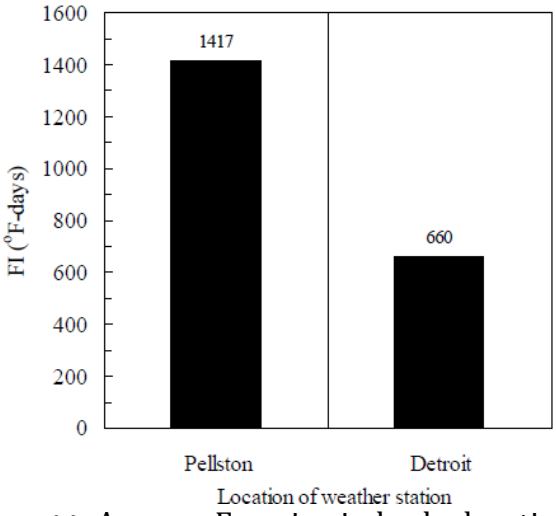

(a) Average Freezing index by location

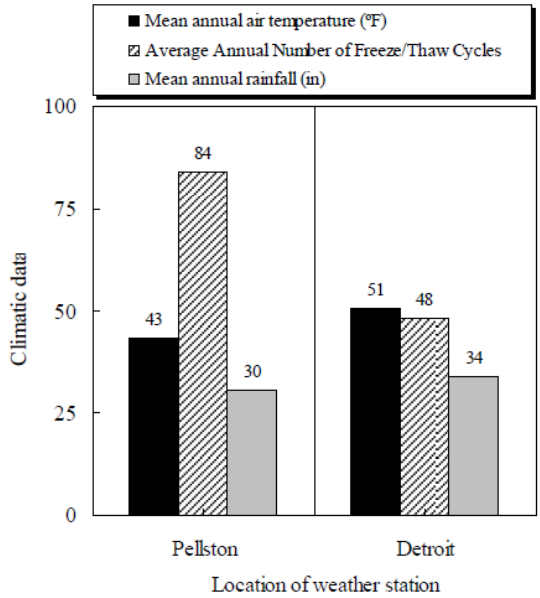

(b) Mean annual air temperature, number of F/T cycles and average precipitation by location

Figure 4-16 Summary of climatic properties by location within Michigan (*1*)

4.4.1.2. Design inputs

The MEPDG inputs represent a wide range of categories including traffic characterization, climatic data, and pavement structural and material information. Some of the inputs related to material characterization need special considerations. For example, characterizing existing pavement damage involves different input levels for the HMA over HMA rehabilitation option. Therefore, some decisions are needed to determine the specific input for the selected

level. The following section presents some of such cases for HMA over HMA rehabilitation option.

Characterizing HMA over HMA layer

HMA dynamic modulus (*E**) of the asphalt mixture is an input for level 1 characterization of the asphalt mixtures in the MEPDG. Details of *E** were presented and discussed in the Task 1 report of this study. In the *E** equation, α and δ are fitting parameters that determine the minimum and maximum values of *E**[δ represents the minimum value (lower shelf) for dynamic modulus and ($\alpha + \delta$) represents the maximum value (upper shelf)]. The level 1 characterization of *E** is preferred because it is a direct way of evaluating E*; i.e., no prediction or correlation is involved. However, several issues were encountered, which led the research team to use level 3 for HMA mixture characterization. This is explained below.

Equations 1 to 3 show the *E** prediction model in the MEPDG (*5*).

$$log(E^*) = \delta + \frac{\alpha}{1 + e^{\beta + \gamma \log(t_r)}} \quad (1)$$

$$\alpha = 3.871977 - 0.0021\rho_4 + 0.003958\rho_{38} - 0.000017\rho^2_{38} + 0.005470\rho_{34} \quad (2)$$

$$\delta = 3.750063 + 0.02932\rho_{200} - 0.001767\rho^2_{200} - 0.002481\rho_4 - 0.058097V_a - 0.802208\left[\frac{Vb_{eff}}{V_{beff} + V_a}\right] \quad (3)$$

where,

ρ_4 = cumulative % retained on No. 4 sieve.

ρ_{200} = % passing the No. 200 sieve.

ρ_{38} = cumulative % retained on 3/8 in sieve.

ρ_{34} = cumulative % retained on ¾ in sieve.

V_{beff} = effective bitumen content, % by volume.

V_a = air void content, %

From Equation 3 it can be seen that there is a strong correlation between δ , % air voids and % binder content. In GSA, an Artificial Neural Network (ANN) is used to predict the pavement performances. However, having independent variables which are correlated should not be considered together because of collinearity concerns. In addition, it is not possible to run ANN without including % air voids and % effective binder because these variables are further used in the cracking transfer function to predict cracking. Therefore, to characterize the asphalt mixture, level 3 inputs (aggregate gradation and asphalt volumetric properties) were used instead of mixture master-curves.

Characterizing the existing HMA layer

For level 1 input for characterizing the existing pavement structural capacity, HMA back-calculated modulus is required to measure the current damage. The overall procedure for damage calculations and existing pavement characterization for different rehabilitation levels is summarized in Chapter 2. However, to clarify the possible relationship between level 1 and

level 3 rehabilitation levels, the amount of overlay cracking was obtained using the MEPDG for these levels. In this exercise, the permanent deformation input was kept constant while the pavement condition rating was varied to determine the corresponding back-calculated modulus to produce the same amount of cracking. Thin (3 in) and thick (6 in) overlays were used for the comparison and the results are shown in Figures 4-17 and 4-18. The results show that each pavement condition rating corresponds to a specific range of the existing HMA back-calculated moduli. For example, very poor condition rating for an existing pavement corresponds to 250 ksi modulus as both rehabilitation levels exhibited the same amount of longitudinal and alligator cracking regardless of the overlay thickness. On the other hand, a modulus of 600 ksi for existing HMA yielded the same amount of cracking similar to excellent pavement condition rating. Based on these results, it is possible to relate the level 3 existing pavement condition ratings with the level 1 back-calculated moduli of the existing HMA layer. Therefore, in this study level 3 rehabilitation was utilized in all analyses. Also, if there is a fair estimate of the existing pavement modulus, level 3 (pavement condition rating) can be used instead of the level 1 (back-calculated modulus).

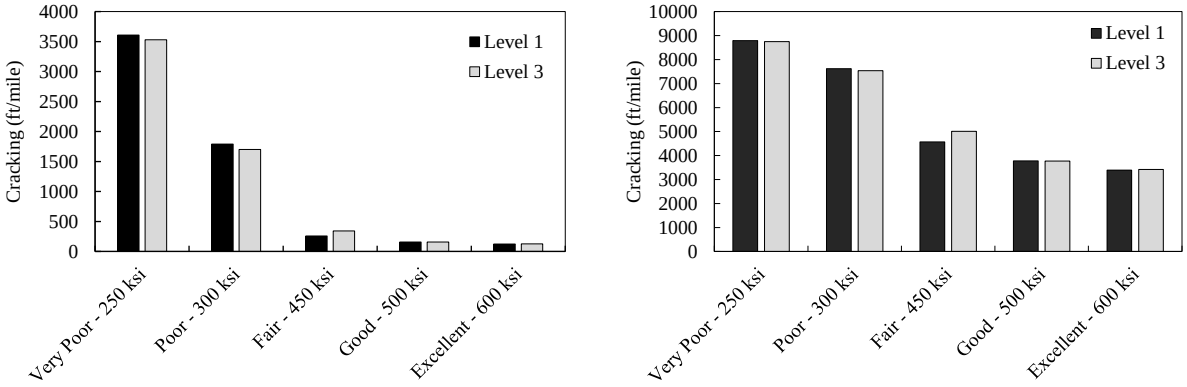

(a) Longitudinal cracking for 6 in overlay (b) Longitudinal cracking for 3 in overlay

Figure 4-17 Comparison between levels 1 and 3 rehabilitation for longitudinal cracking

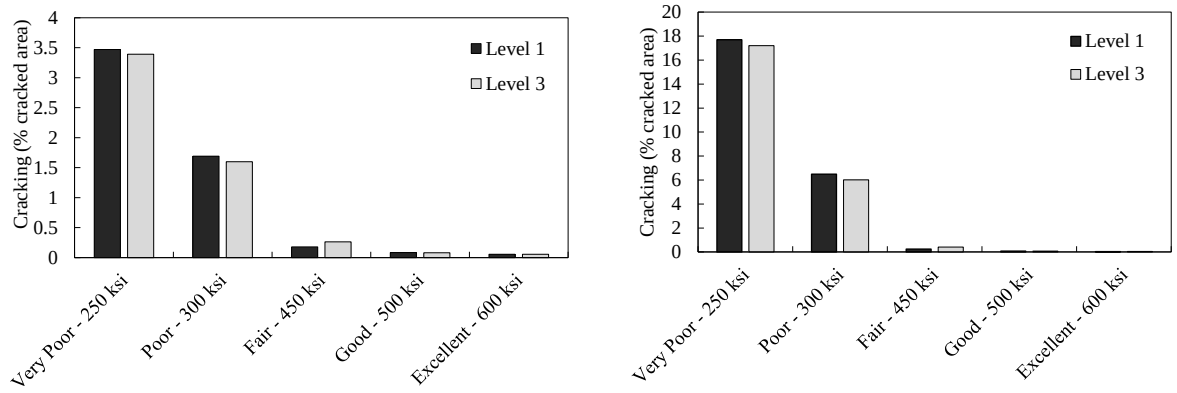

(a) Fatigue cracking for 6 in overlay (b) Fatigue cracking for 3 in overlay

Figure 4-18 Comparison between levels 1 and 3 rehabilitation for fatigue cracking

Rehabilitation options design inputs and ranges

The results of the preliminary sensitivity analysis were used here to determine the potentially significant inputs for different rehabilitation options. The final list of design inputs and their ranges were finalized with MDOT. Tables 4-41 to 4-44 summarize the design inputs, their ranges, and the baseline values for all rehabilitation options considered in this study. For the one-at-a-time (OAT) sensitivity analysis, the value of each input variable was varied over its entire range (from lower to upper limits) while all other input variables were held constant at their baseline values.

Table 4-41 List of design inputs for HMA over HMA

No.	Input variables		Baseline values	Lower limit	Upper limit
1	Overlay thickness (inch)		5	2	8
2	Overlay effective binder (% by volume)		10.5	7	14
3	Overlay PG		PG 58-22[1]	PG 58-22	PG 76-28
4	Overlay AV (%)		8.5	5	12
5	Overlay aggregate gradation (%)	3/4" sieve	100	100	100
		3/8" sieve	88.6	86.8	88.6
		#4 sieve	73.2	79.2	73.2
		passing # 200	4.9	5.6	4.9
6	Existing condition rating		Poor	Very poor	Excellent
7	Existing HMA thickness (inch)		8	4	12
8	Existing base modulus (psi)		27500	15000	40000
9	Existing Sub-base modulus (psi)		20000	15000	30000
10	Subgrade modulus (psi)		13750	2500	25000
11	Climate		Pellston[2]	Pellston	Detroit

Table 4-42 List of design inputs for composite

No.	Input variables		Baseline values	Lower limit	Upper limit
1	Overlay thickness (inch)		5	2	8
2	Overlay effective binder (% by volume)		10.5	7	14
3	Overlay PG		PG 76-28	PG 58-22	PG 76-28
4	Overlay AV (%)		8.5	5	12
5	Overlay aggregate gradation (%)	100	100	100	100
		88.6	86.8	86.8	88.6
		73.2	79.2	79.2	73.2
		4.9	5.6	5.6	4.9
6	Existing PCC thickness (inch)		9	7	11
7	Existing PCC MOR (psi)		650	550	900
8	Subgrade reaction modulus (psi/in)		175	50	300
9	Climate		Detroit	Pellston	Detroit

[1] Only two levels for PG were considered; therefore, the baseline value is identical to the lower limit.
[2] Pellston was used as a baseline in this case.

Table 4-43 List of design inputs for HMA over fractured JPCP (Rubblized)

No.	Input variables		Baseline values	Lower limit	Upper limit
1	Overlay thickness (inch)		5	2	8
2	Overlay effective binder (% by volume)		10.5	7	14
3	Overlay PG		PG 76-28	PG 58-22	PG 76-28
4	Overlay AV (%)		8.5	5	12
5	Overlay aggregate gradation (%)	3/4" sieve	100	100	100
		3/8" sieve	86.8	86.8	88.6
		#4 sieve	79.2	79.2	73.2
		passing # 200	5.6	5.6	4.9
6	Existing PCC thickness (inch)		9	7	11
7	Existing PCC elastic modulus (psi)		100000	35,000	1,500,000
8	Climate		Detroit	Pellston	Detroit

Table 4-44 List of design inputs for JPCP over JPCP (unbonded overlay)

No.	Input variable	Baseline values	Lower limit	Upper limit
1	Overlay PCC thickness (inch)	9	7[1]	10
2	Overlay PCC CTE (per °F x 10^{-6})	5.5	4	7
3	Overlay joint spacing (feet)	15	10	15
4	Overlay PCC MOR (psi)	650	550	900
5	Modulus of subgrade reaction, *k* (psi/in)	175	50	300
6	Existing PCC thickness (inch)	9	7	11
7	Existing PCC elastic modulus (psi)	3000000	500,000	3,000,000
8	Climate	Detroit	Pellston	Detroit

[1]The minimum thickness for an unbonded concrete overlay within MEPDG is 7 inches. The upper bound was selected based on LTPP unbonded overlay thicknesses and to ensure that it is lower than the existing pavement layer.

4.4.1.3. Sampling from the problem domain

The Latin Hypercube Sampling (LHS) method is a powerful technique that can be used to generate stratified random samples within the range of all design inputs covering the entire problem domain. The LHS is a statistical method for generating samples of plausible collections of parameter values from a multidimensional distribution. Generally, the method is commonly used to reduce the number of runs necessary for a Monte Carlo simulation to achieve a reasonably accurate random distribution as shown graphically in Figure 4-19. In this Figure, x_1 and x_2 are two input parameters which form a two dimensional problem domain. In order to cover the entire domain shown in Figure 4-19a, Monte Carlo and LHS are used separately. For this example, Monte Carlo needs 100 samples (Figure 4-19b) while the LHS requires 25 samples (Figure 4-19c) to cover the same problem domain thus LHS significantly improves the efficiency yet maintaining similar accuracy. The LHS can be incorporated into an existing Monte Carlo model fairly easily, and works with variables having any probability distribution.

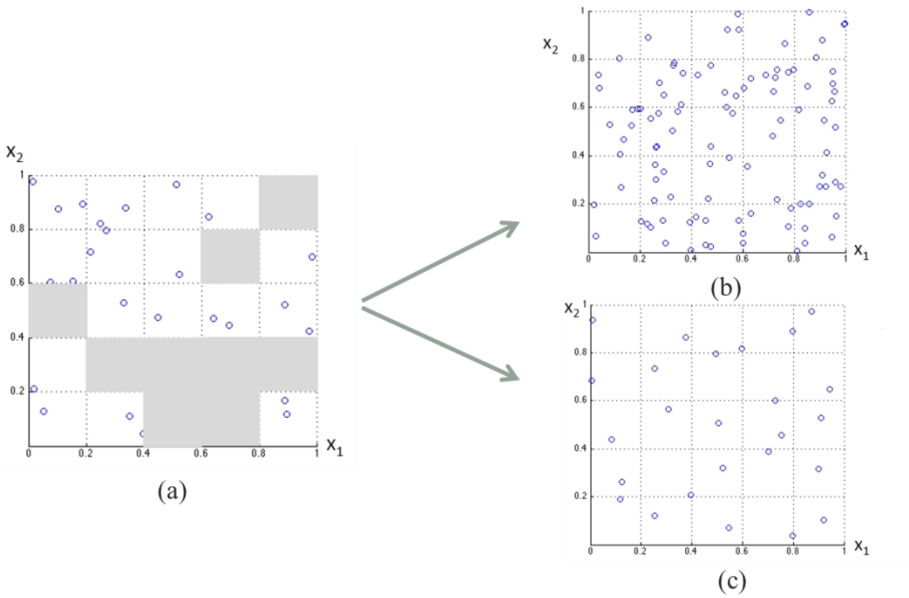

Figure 4-19 Comparison between Monte Carlo and LHS simulations

Figure 4-20 shows two design inputs (x_1 and x_2) with minimum value of zero and maximum value of a and b, respectively. For example if 3 samples are required, each input parameter range is divided into 3 equal intervals forming a square grid containing sample positions if (and only if) there is only one sample in each row and each column (which is referred as Latin Square as shown in Figure 4-20a). The concept can be extended for more design inputs by generalizing of Latin Square to an arbitrary number of dimensions (for e.g., 3 inputs as shown in Figure 4-20b), whereby each sample is the only one in each axis-aligned hyper-plane. By using this method, a fewer number of simulations are needed to adequately cover the domains of all inputs.

Once LHS sample combinations of all input variables are determined, they can be used as inputs in the MEPDG to obtain the predicted pavement performance over time. The number of required MEPDG runs is dependent on the number of design inputs used to generate LHS samples. Based on a limited parametric investigation performed in the NCHRP report 1-47 (*3*), the sufficient number of MEPDG runs to obtain stable results for GSA should be at least 20K (where K is the number of design inputs for each rehabilitation option). However, in this study, to increase the reliability of the networks predictions and accuracy, 30K simulations were used. These simulations cover the entire range of the problem domain, which means all the possible inputs combinations are considered. Table 4-45 shows the total number of the MEPDG runs needed for different rehabilitation options. As an example, Table 4-46 shows a portion of the randomly generated sample using LHs for the HMA over JPCP fractured.

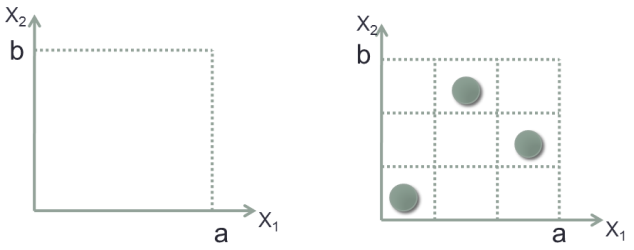

(a) Latin Square

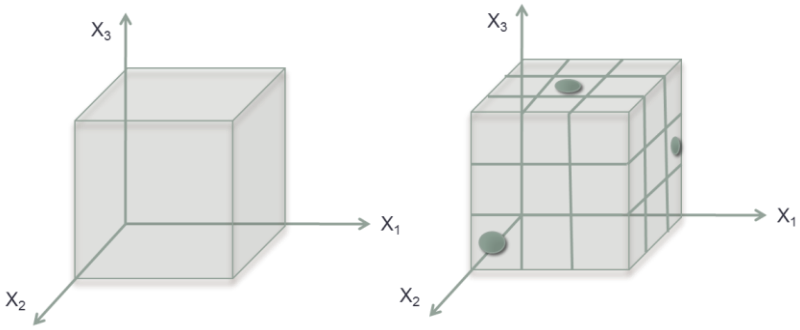

(b) Latin Cube

Figure 4-20 Example of sampling in LHS method

Table 4-45 Required number of simulations

Rehabilitation type	Number of inputs	Number of runs
HMA over HMA	11	330
HMA over PCC (Composite)	9	270
HMA over Rubblized PCC	8	240
Unbonded PCC overlay	8	240

Table 4-46 Generated samples for HMA over JPCP fractured

Run	Overlay Thickness	Overlay Effective Binder	Overlay PG	Overlay Air Voids	Overlay Aggregate	Existing Thickness	Existing Thickness	Climate
1	3.188	12.952	PG 76-28	6.489	Coarse	9.636	50924	Pellston
2	5.585	10.358	PG 76-28	11.371	Coarse	10.903	683920	Detroit
3	7.118	10.002	PG 76-28	5.864	Coarse	10.794	412611	Pellston
.	.	.	.	.	.	.	.	.
.	.	.	.	.	.	.	.	.
236	7.587	13.136	PG 58-22	7.946	Coarse	7.498	949310	Pellston
237	3.933	10.191	PG 76-28	5.298	Coarse	9.244	499617	Pellston
238	3.634	11.373	PG 58-22	10.032	Fine	7.691	475511	Detroit
239	6.086	7.794	PG 76-28	6.936	Coarse	8.153	142600	Pellston
240	7.703	11.393	PG 76-28	8.179	Coarse	9.332	1249368	Pellston

4.4.1.4. Response surface models (RSM)

The LHS generated input combinations (which are essentially random MEPDG design input scenarios) were used to make the MEPDG input files. The pavement performance prediction results were obtained after executing these input files using the MEPDG (version1.1). These results were used to provide a continuous surface of pavement performance at discrete locations in the problem domain. However, to obtain continuous performance measures other than the predefined discrete locations, a continuous surface should be fitted on these discrete points. Therefore, Artificial Neural Network (ANN) fitting tools were used to fit continuous surfaces. ANN consists of an interconnected group of artificial neurons, and it processes information using a connectionist approach for computation. Neural networks are used to model complex relationships between inputs and outputs or to find patterns in data. The ANN can be viewed as a nonlinear regression model except that the functional form of the fitting equation does not need to be specified necessarily (*3*). Subsequently, the RSMs estimated by using ANN were utilized to calculate sensitivity of different design inputs using the sensitivity metric called Normalized Sensitivity Index (NSI).

4.4.1.5. Sensitivity metric

The NSI can be used for a point estimation of sensitivity across a problem domain. The point-normalized sensitivity index S_{ijk} is defined as:

$$S_{ijk} = \left.\frac{dy_j}{dx_k}\right|_i \frac{x_{ki}}{y_{ji}} \tag{4}$$

where,

x_{ki} is the value of input *k* at point *i*

y_{ji} is the value of distress *j* at point *i*

$\left.\frac{dy_j}{dx_k}\right|_i$ is change of distress j with respect to change in input k at point i

Equation (4) can be simplified to:

$$S_{ijk} = \left.\frac{\frac{dy_j}{y_j}}{\frac{dx_k}{x_k}}\right|_i \tag{5}$$

Equation (5) shows that the sensitivity index is a ratio between rates of change in performance measure and design input. In some cases, predicted distress, y_{ji} is close to zero resulting in an artificially large sensitivity. Therefore, to overcome this problem S_{ijk} can be

normalized with the design limit for a distress. The final formula for sensitivity index is as follows (*3*):

$$NSI = S_{ijk}^{DL} = \frac{\Delta y_{ji}}{\Delta x_{ki}} \times \frac{x_{ki}}{DL_j} \tag{6}$$

where,

NSI is normalized sensitivity index for design limit at point i for distress j and input k

Δy_{ji} is change in distress *j* about point *i*

Δx_{ki} is change in input *k* about point *i*

x_{ki} is the value of input *k* at point *i*

DL_j is the design limit for distress *j*

The NSI was calculated using Equation (6) for most of the cases. However, for discrete design inputs (for e.g., climate, condition rating, PG grade etc.), a modified equation was implemented to determine the sensitivity index. Equation (7) still considers the design limit as reference for predicted distress; it normalizes the change in the performance with respect to the specified design limit for a certain distress if the design input is changed by one category. For example, if by changing PG grade from PG 58-22 to PG 76-28 rutting changes by 0.7 inches while all other inputs are held constant, the NSI for rutting will be 0.7/0.5=1.4. It should be noted that the difference in the predicted performance between categories should be higher than the threshold to obtain NSI greater than 1 to consider the input as significant.

$$NSI = \left. \frac{\Delta y_{ji}}{DL_j} \right|_{\Delta X_{ki} = 1 category} \tag{7}$$

The NSI for IRI also needs special attention because the lower bound for IRI is non-zero. The NSI formula for IRI when the design limit is 172 inch/mile and the initial IRI is 63 inch/mile is expressed in Equation (8). This equation was proposed in the NCHRP 1-47 study for performing the sensitivity analysis.

$$NSI = \frac{IRI - 63}{172 - 63} \tag{8}$$

The NSI can be interpreted as:

- If NSI=0, then there is no change in performance with respect to the change in input,
- If NSI=1, then the rates of change in performance and input are the same,
- If NSI >1, the performance rate of change is faster than the rate of change in the input.

The NSI interpretation is for OAT analysis, and only explains the main effect of an input on a given distress measure. Therefore, there was a need to explain the interactive effect of two variables for evaluating the joint effect of variables. Equations (9) and (10) were developed to evaluate NSI of an interaction where Equation (11) shows the numerical solution for Equation (10).

$$S_{ijklm}\Big|_{(i,j)} = \frac{\partial^2 y^m}{\partial x^k \partial x^l} \times \frac{x^k x^l}{y^m}\Bigg|_{(i,j)} \tag{9}$$

$$NSI^{DL}_{ijklm}\Big|_{(i,j)} = \frac{\partial^2 y^m}{\partial x^k \partial x^l} \times \frac{x^k x^l}{DL^m}\Bigg|_{(i,j)} \tag{10}$$

$$NSI = S^{DL}_{ijklm}\Big|_{(i,j)} = \frac{x_i^k \times x_j^l}{\Delta x_i^k \times \Delta x_j^l} \times \frac{y^m{}_{x^k{}_{i+1},x^l{}_{j+1}} - y^m{}_{x^k{}_{i},x^l{}_{j+1}} - y^m{}_{x^k{}_{i+1},x^l{}_{j}} + y^m{}_{x^k{}_{i},x^l{}_{j}}}{DL^m} \tag{11}$$

where,

$S^{DL}_{ijklm}\Big|_{(i,j)}$ = sensitivity index for input *k* and *l*, distress *m*, at point (*i,j)* with respect to design limit (DL)

x_i^k = value of input x^k at point *i*

x_j^l = value of input x^l at point *j*

Δx_i^k = change in input x^k around point *i* $\left(x^k{}_{i+1} - x^k{}_{i-1}\right)$

Δx_j^l = change in input x^l around point *j* $\left(x^l{}_{j+1} - x^l{}_{j-1}\right)$

$y^m{}_{x^k{}_i,x^l{}_j}$ = value of distress *m*, for input x^k at point *i* and input x^l at point *j*

DL^m = design limit for distress *m*

4.4.1.6. Distress thresholds for GSA

The NSI calculation involves the design limit (threshold value) for each distress type. Tables 4-47 and 4-48 summarize recommended threshold values for various performance measures from the NCHRP Report 1-47(*3*) and MEPDG manual of practice (*10*), respectively . It should be noted that practically, the distress threshold values depend on the road class, and may vary among agencies based on their practices. Finally, Table 4-49 summarizes the threshold values adopted in this study based on discussions with MDOT (January 7, 2013).

Table 4-47 Recommended threshold values for performance measures—NCHRP 1-47

Pavement type	Performance measure	Threshold	Reference
Flexible	Alligator cracking	25%	1-47 NCHRP
	Longitudinal cracking	2000 ft/mile	
	Surface rutting	0.75 in	
	IRI	172 in/mile	
Rigid (JPCP)	% Slab cracked	15%	
	Faulting	0.12 in	
	IRI	172 in	
Rigid (CRCP)	Crack width	20 mils	
	Crack LTE	75%	
	Punchouts	10/mile	
	IRI	172 in/mile	

Table 4-48 Recommended threshold values for performance measures—AASHTO

Pavement type	Distress	Threshold	Reference
Flexible (New & Overlay)	Alligator cracking	I=10% P=20% S=35%	AASHTO manual of practice
	Surface rutting	I=0.4 inch P=0.5 inch S=0.65 inch	
	IRI	I=160 inch/mile P=200 inch/mile S=200 inch/mile	
Rigid (JPCP) (New & Overlay)	% Slab cracked	I=10% P=15% S=20%	
	Faulting	I=0.15 inch P=0.2 inch S=0.25 inch	
	IRI	I=160 inch/mile P=200 inch/mile S=200 inch/mile	

Note: I= interstate, P=primary, and S=secondary

Table 4-49 Distress threshold values used in this study based on discussion with MDOT

Pavement type	Distress	Threshold
Flexible (New & Overlay)	Alligator cracking	20%
	Longitudinal cracking	2000 ft/mi
	Thermal cracking	1000 ft/mi
	Surface rutting	0.5 in
	IRI	172 in/mi
Rigid (JPCP) (New & Overlay)	% Slab cracked	15%
	Faulting	0.25 in
	IRI	172 in/mi

As mentioned above, the point-normalized sensitivity index defined in Equation (6) is normalized with the design limit (threshold). Equation (6) shows that changing the threshold value will change the NSI value proportionally. The effect of the threshold value on the calculated NSI was investigated. Figure 4-21 shows the NSI curves for three different

threshold values. The results show that the change in threshold value will proportionally increase or decrease the NSI value for a given performance measure.

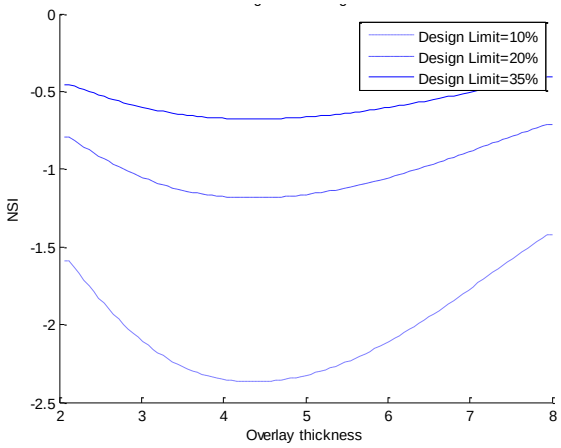

(a) Alligator cracking for HMA over HMA

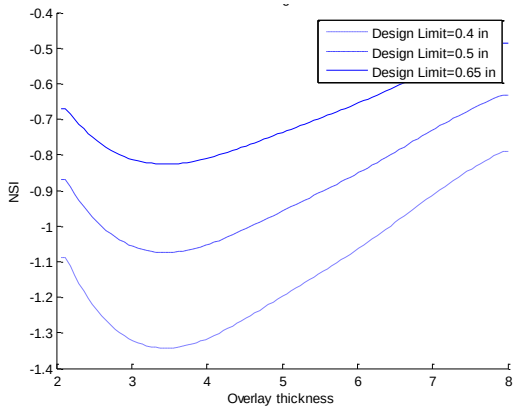

(b) Surface rutting for HMA over HMA

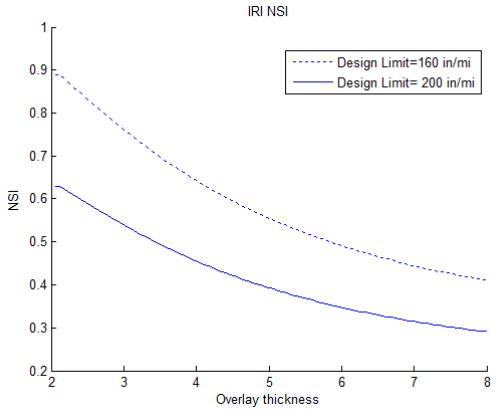

(c) Roughness (IRI) for HMA over HMA

Figure 4-21 Effect of different threshold values on NSI calculation

4.4.2 Global Sensitivity Analysis Results

In GSA, for each rehabilitation option both main and interactive effects of inputs on pavement distresses were investigated. More than 1000 ANN RSMs were performed for each input-distress combination and the RSMs were averaged to obtain an expected RSM to improve the accuracy of performance predictions. Subsequently, those RSMs were utilized to evaluate the NSI. Due to the variation in the ANN predictions for 1000 RSMs, a 95% confidence interval was provided for distress and NSI predictions. The GSA included the following components for each rehabilitation option:

1. The relative importance of design inputs were determined by using the Garson algorithm.
2. The main effects of each design input were evaluated by using NSI values.
3. The interaction effects of important design inputs were evaluated by using two-variable NSI values.

The results for each rehabilitation option are presented next.

4.4.2.1. HMA over HMA

Relative importance of design inputs

In order to obtain the overall relative significance of design inputs, all the inputs should be changed simultaneously to cover their entire possible combinations. Therefore, in this case despite an OAT analysis (where all results are based on a base case), no base case or baseline values for design inputs are needed. However, it should be noted that such methodology only determines the relative ranking of inputs among each other. Garson algorithm was implemented to get the relative importance of the design inputs. Garson (*11*) proposed a method for partitioning the neural network connection weights in order to determine the relative importance of each input variable in the network. An example showing the application of Garson's algorithm in a single hidden layer feed forward multi-layer perceptron (MLP) with two processing elements (PEs) is shown in Figure 4-22.

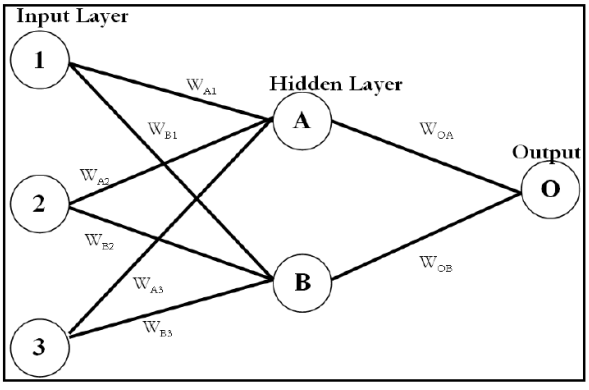

Figure 4-22 Network diagram (*11*)

The dataset used in this analysis are the LHS inputs generated for GSA. The LHS inputs cover the entire range of problem domain hence it takes into account all the possible input combinations. The relative importance of the design inputs is shown in Figure 4-23 for all pavement performance measures. The relative importance of an input can also be expressed as the percent participation of design inputs in the distress prediction models (i.e. for a given pavement distress each design input will have a percent contribution to the predicted distress). The results show that overlay thickness is the most important input and has the highest contribution in all predicted performance measures. The volumetric parameters for overlay HMA mixture (effective binder and air voids) are important for cracking, especially for alligator cracking. Existing condition rating for alligator cracking and existing HMA thickness for longitudinal cracking and rutting have important overall contributions.

The height of each bar graph shows the percent contribution of the input parameters (which adds up to 100%). In general, these numbers can be used to compare and quantify the contributions of each input for a specific performance measure.

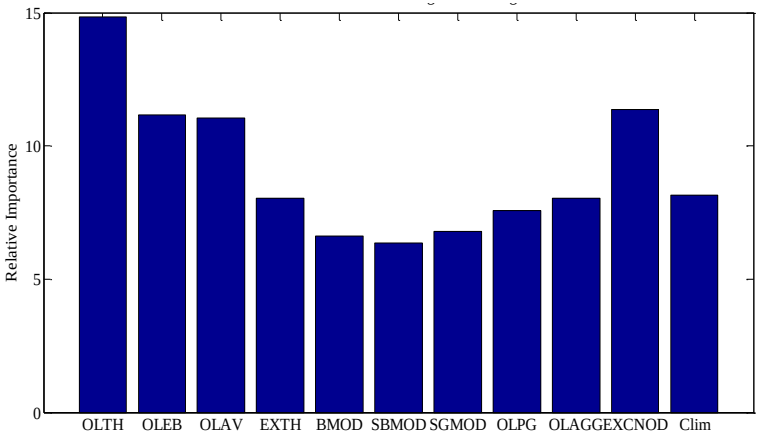

(a) Relative importance of design inputs for alligator cracking

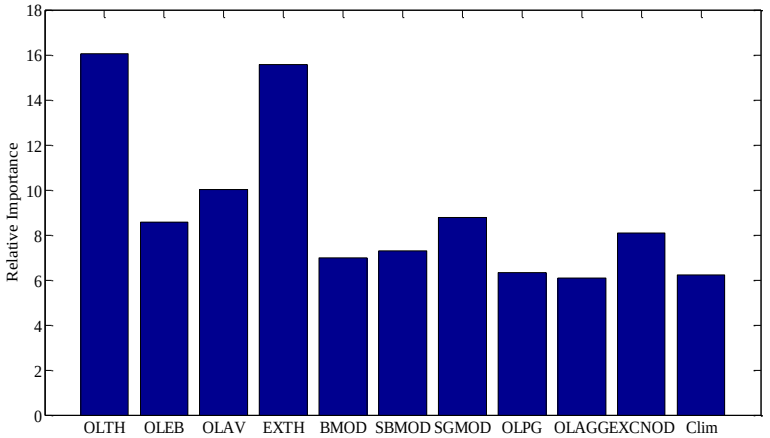

(b) Relative importance of design inputs for longitudinal cracking

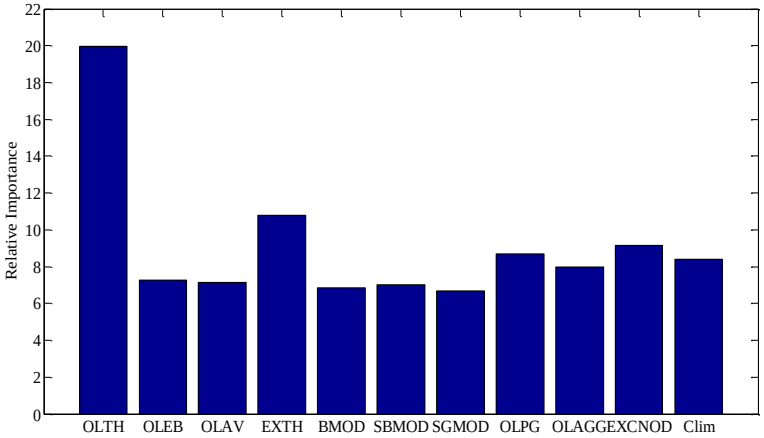

(c) Relative importance of design inputs for rutting

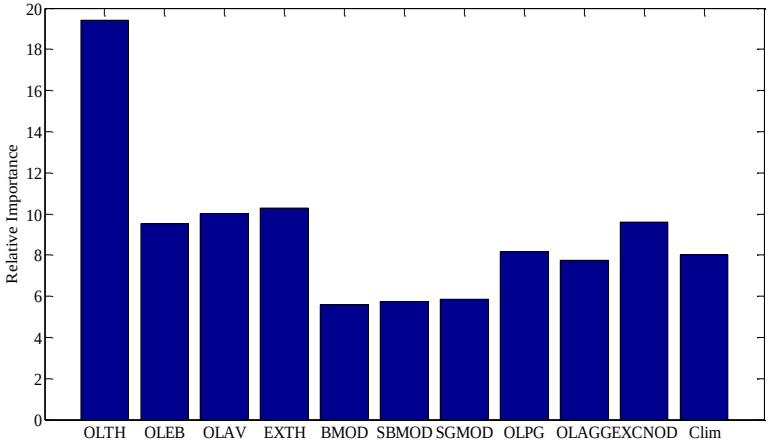

(d) Relative importance of design inputs for IRI

Figure 4-23 **Relative importance of design inputs for HMA over HMA**

Main effect of design inputs

As mentioned above, the relative importance of inputs can be used for determining their overall contribution to predicted pavement performance. In order to investigate the impact of the input variables with respect to a standard, a base case should be specified. In this scenario, each input variable of interest should vary over its range while other variables are held constant at their base values. The base cases, input ranges, and baseline values were presented before.

The neural networks were trained to fit the best surface on the discrete points from LHS simulations for each pavement performance measure. As the fitted surfaces cover the entire problem domain, those allow the evaluation of each variable over its entire range. Figure 4-24 shows an example of predicted alligator cracking for overlay thickness using the ANN RSM. Due to the variability in the ANN predictions, a 95% confidence interval is provided. This variability is a function of sampling process for the training of ANN. In each ANN run, 70% of the data set is sampled randomly for training and remaining is used for validation and testing. Using Equation (6) the NSI was calculated for overlay air void - alligator cracking combination. A 95% confidence interval is also provided for the NSI curve. The wider confidence interval band means an increase in the variability of ANN predictions.

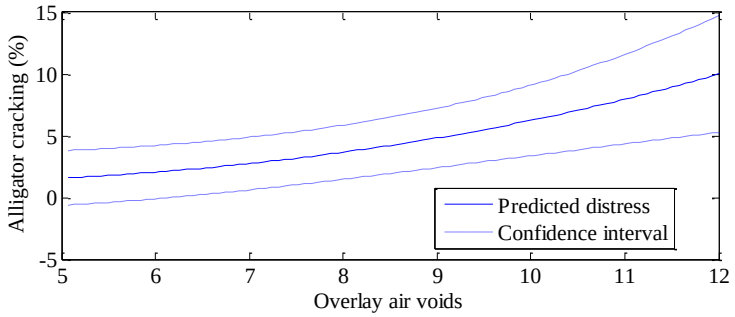

(a) Predicted alligator cracking

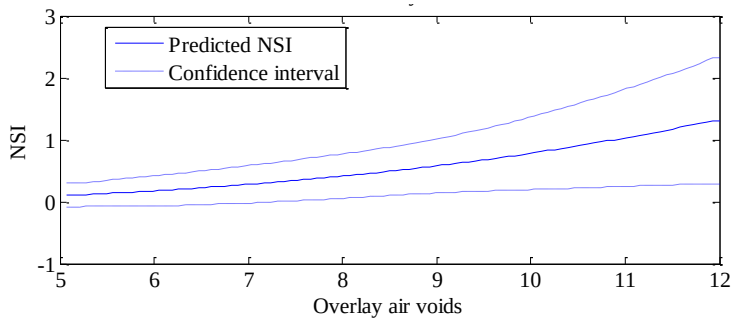

(b) Calculated NSI

Figure 4-24 Sensitivity of alligator cracking to HMA overlay air voids

The main effects of all the input variables on all predicted distresses were investigated. The distress and NSI plots for all of the inputs and distresses are presented in Appendix B. Figure 4-25 summarizes the main effects of all input variables on each pavement performance

measure by box plots. The results show that overlay air void percentage has a significant impact on cracking (NSI>1). An increase in air voids is associated with higher cracking. For longitudinal cracking; overlay and existing HMA thickness, effective binder content, unbound layer moduli and existing conditions all have a significant impact. The effect of a particular input on pavement performance measure can be interpreted as follows:

- If a NSI is positive, the distress magnitude will increase by increasing the input value.
- If a NSI is negative, the distress magnitude will decrease by increasing the input value.

For rutting and IRI, the NSI results show that all inputs have relatively lower impact as compared to cracking.

Interactive effect of design inputs

The detailed sensitivity analysis identified some practically significant interactions between input variables. Those interactions were further investigated in detail in this part. An interactive effect means that one input can amplify or reduce the effect of another input on the predicted pavement performance. Therefore, it is vital to consider the interactive effect of given design input variables when such interaction exists. It should be noted that only interactions between overlay design and existing design inputs were considered. Similar to the NSI for one variable, a NSI for interaction was developed as shown in Equation (11). Figures 4-26 to 4-28 show the significant interactions for alligator cracking and the corresponding NSI plots. The results shown in Figure 4-26a indicates that higher overlay thicknesses lower the impact of existing thickness on alligator cracking. For example, for an 8-inch overlay thickness, regardless of the existing HMA thickness, the predicted cracking will be negligible over the design life. On the other hand, for a thin overlay depending on the existing HMA thickness, the rehabilitation strategy will exhibit 10 to 20% alligator cracking over the design life. Figure 4-26b shows that the rate of change in cracking with respect to overlay thickness will increase as the existing thickness increases.

Other interactions in Figures 4-27 and 4-28 can be interpreted similarly. The maximum NSI for interactions can be used to rank the interactions. The results for alligator cracking of HMA over HMA as shown in Figure 4-26 to Figure 4-28 manifests that the interaction between overlay air voids and existing HMA thickness has the most important effect. The interaction between existing thickness and overlay thickness, and existing thickness and overlay effective binder content have somewhat similar effects on alligator cracking. It should be noted that in the interaction sensitivity plots, the magnitude of the NSI should be consider rather than the surface colors.

On each boxplot, the central mark (red line) is the median of the distribution; the lower and upper edges of the box are the 25th and 75th percentiles, respectively. The whiskers extend to the most extreme data points without considering outliers, and outliers are plotted individually as the red plus signs in the graph. It should be noted that box plots are used for continuous variables to represent a continuous distribution and do not apply to discrete variables.

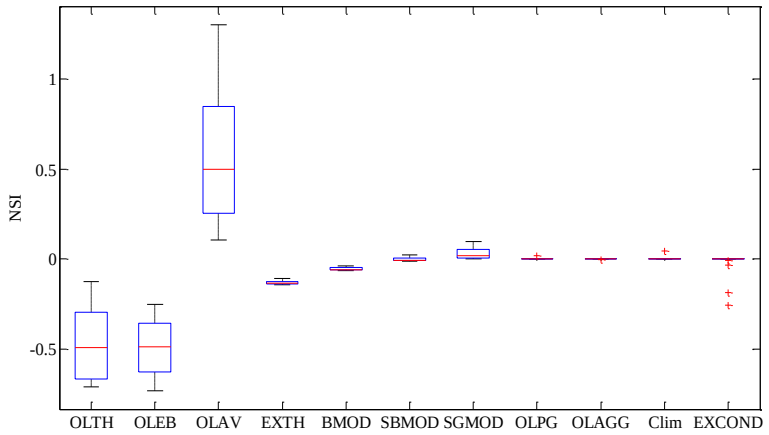

(a) Alligator cracking

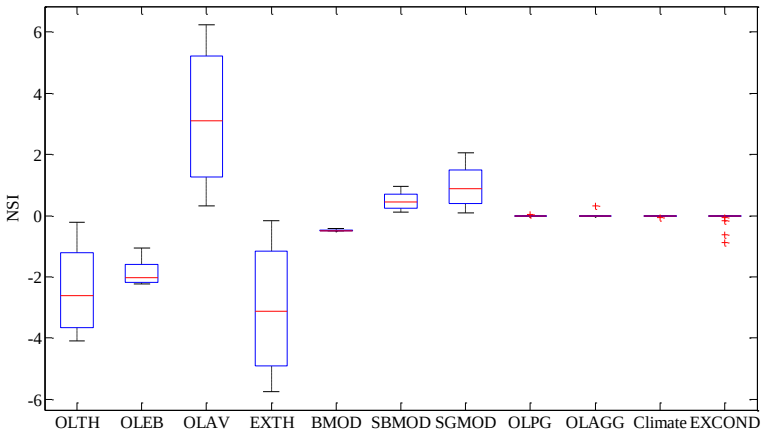

(b) Longitudinal cracking

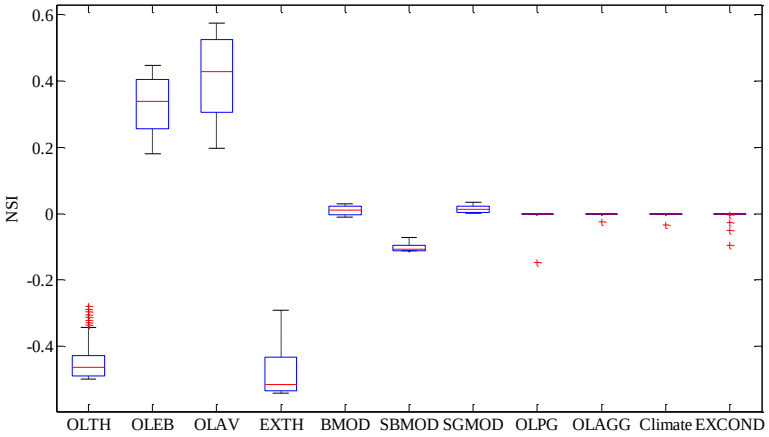

(c) Rutting

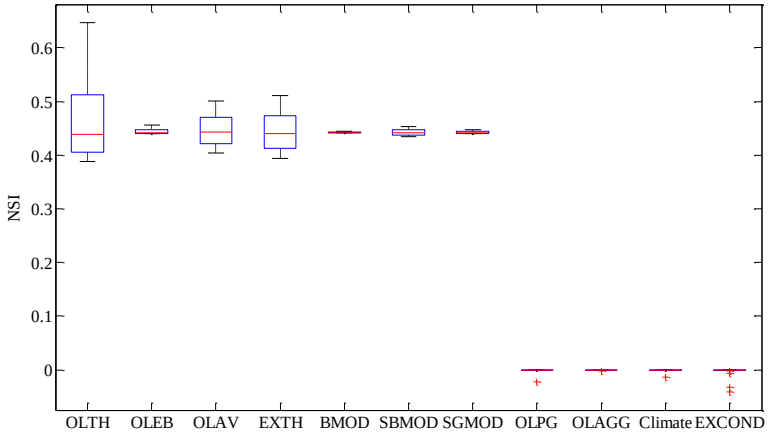

(d) IRI

Figure 4-25 Summary of NSI curves for HMA over HMA

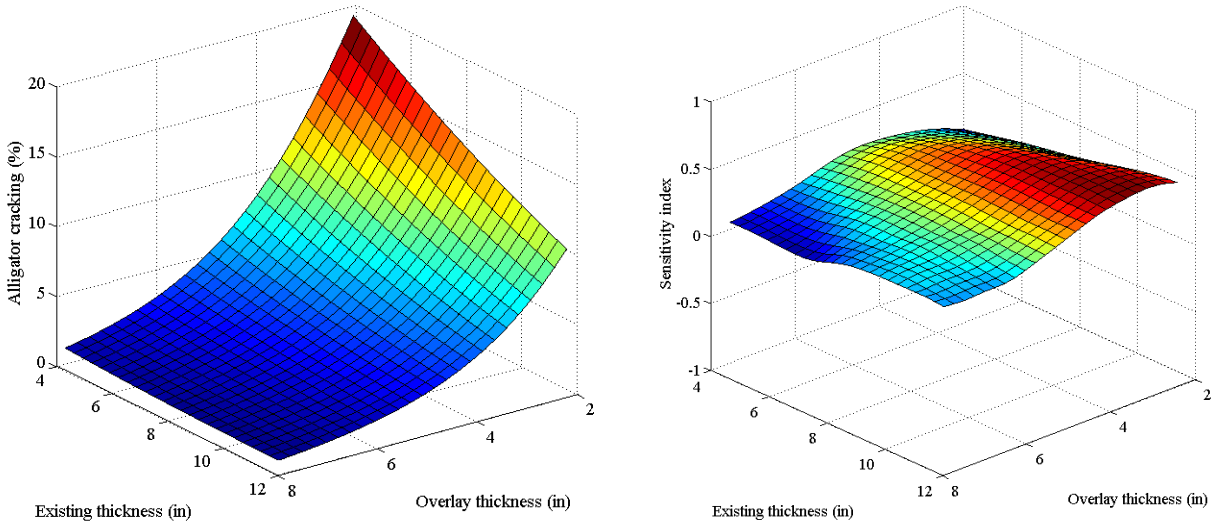

(a) Predicted alligator cracking (b) Calculated NSI

Figure 4-26 Interaction between HMA overlay thickness and existing thickness

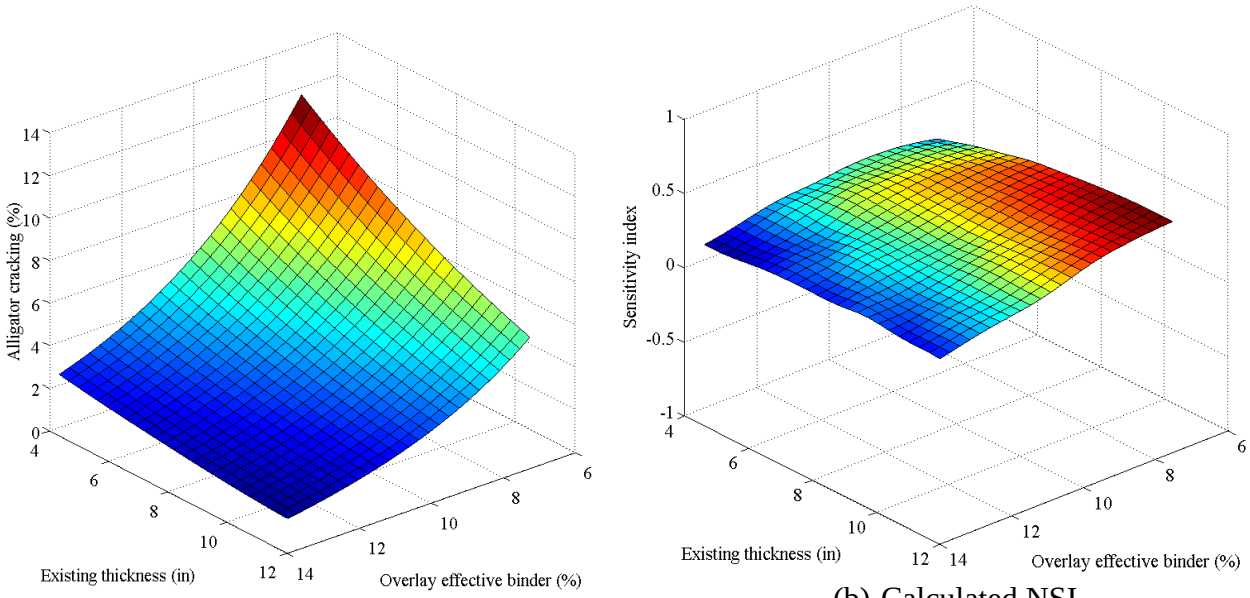

(a) Predicted alligator cracking (b) Calculated NSI

Figure 4-27 Interaction between HMA overlay effective binder and existing thickness

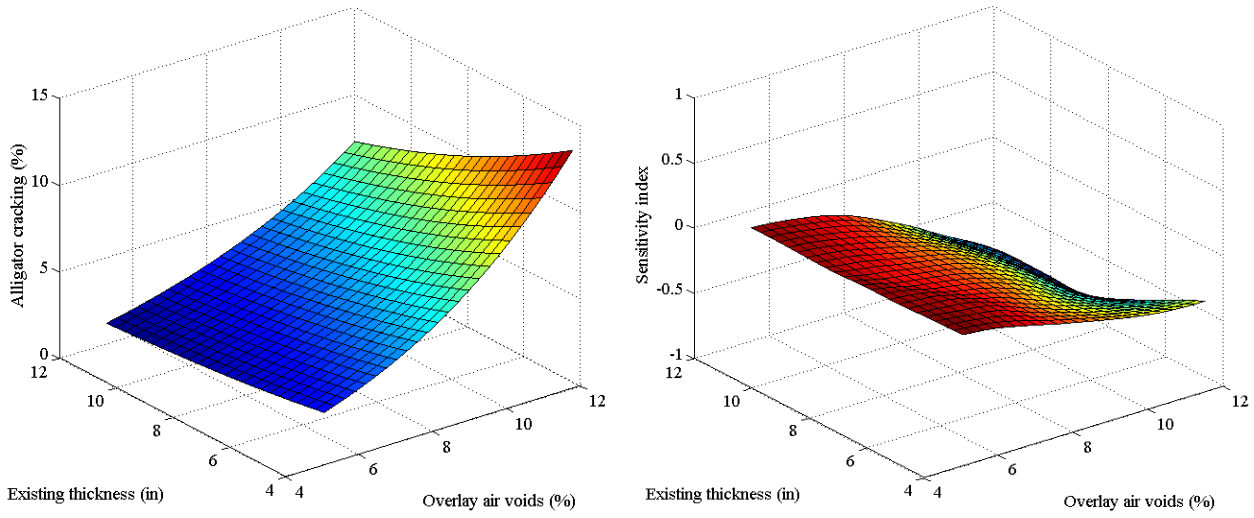

(a) Predicted alligator cracking (b) Calculated NSI

Figure 4-28 Interaction between HMA overlay air voids and existing thickness

4.4.2.2. Composite pavement

Relative importance of design inputs

Similar to HMA overlay, the relative importance of design inputs for this rehabilitation option is determined as shown in Figure 4-29. Since no alligator cracking was predicted by the MEPDG, the results are only shown for the remaining distresses. The results demonstrate the overlay thickness and overlay air voids have the highest contribution to all the predicted pavement performance measures. The volumetric parameters for overlay HMA mixture (effective binder content, air voids, and aggregate gradation) and PG grade are important for rutting and have somewhat similar contributions.

Main effect of design inputs

The summary of NSI plots for composite pavements is presented in Figure 4-30. The results show that the overlay thickness and overlay air voids have the highest impact on all predicted distress among design inputs. Existing PCC thickness has an important effect on longitudinal cracking. The NSI results show that all inputs have relatively lower impact on IRI as compared to cracking and rutting. The plots were generated using more than 100 points within the ranges of the design inputs; therefore, some of the inputs (e.g., OLAV) might show a noticeable number of outliers. However, such outliers were much less than the total number of data point for generating these plots. It should be noted that box plot summarizes a NSI curve for each design input range. In some cases if there is a rapid change in NSI due to a specific input value, the point will be shown as an outlier in the box plot (see Figure B-59 for overlay air voids NSI). Therefore, the maximum value of NSI was used as the criteria for identifying a significant input variable.

Interactive effect of design inputs

Interaction effects between input variables and NSI for this rehabilitation option are presented in Appendix B. Figures B-66 and B-67 show significant interactions for longitudinal cracking. The results show that thinner overlay will lower the impact of existing thickness on longitudinal cracking. For example, for a 2-inch overlay, regardless of the existing PCC slab thickness, the predicted cracking will be negligible over the design life. On the other hand, for a thick overlay depending on the existing PCC thickness, longitudinal cracking may vary from low to very high (2000 ft/mile), which is the threshold for longitudinal cracking. Figure B-66 for NSI interaction shows that the rate of change in cracking with respect to overlay thickness will increase as the existing thickness increases. Other interactions can be interpreted similarly. The maximum NSI for interactions can be used to rank the interactions. The results for longitudinal cracking for composite rehabilitation option show that the interaction between overlay air voids and existing PCC thickness has the most significant effect among other interactions (see Figure B-67). The interaction between existing thickness and overlay thickness, and existing thickness and overlay air voids have somewhat similar effects on rutting.

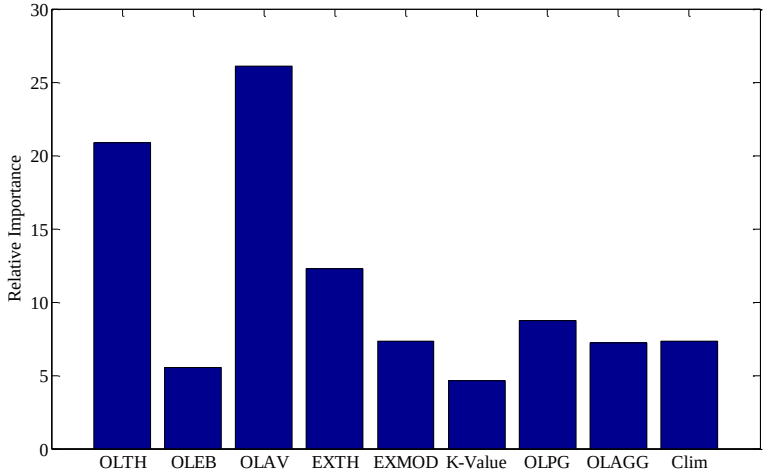

(a) Relative importance of design inputs for longitudinal cracking

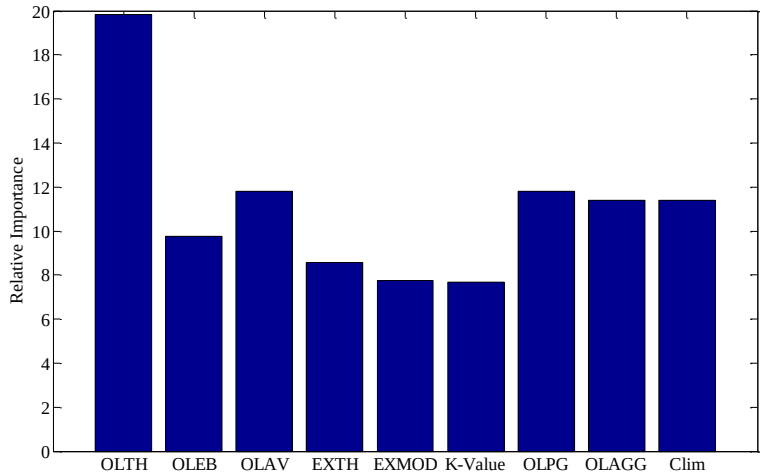

(b) Relative importance of design inputs for rutting

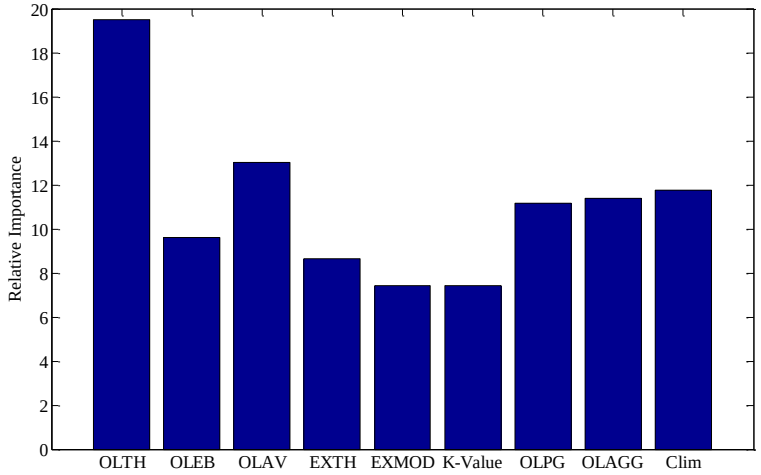

(c) Relative importance of design inputs for IRI

Figure 4-29 Relative importance of design inputs for composite pavement

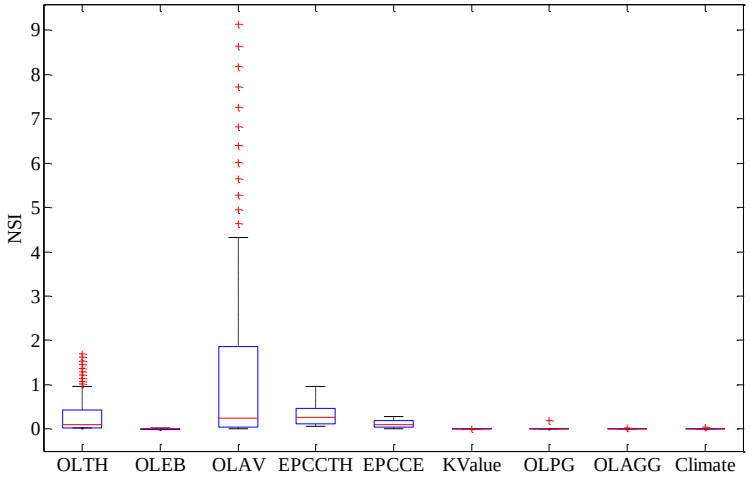

(a) Relative importance of design inputs for longitudinal cracking

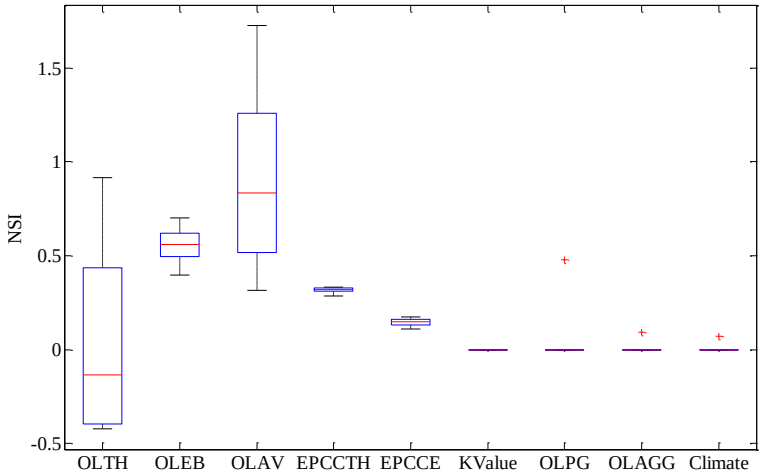

(b) Relative importance of design inputs for rutting

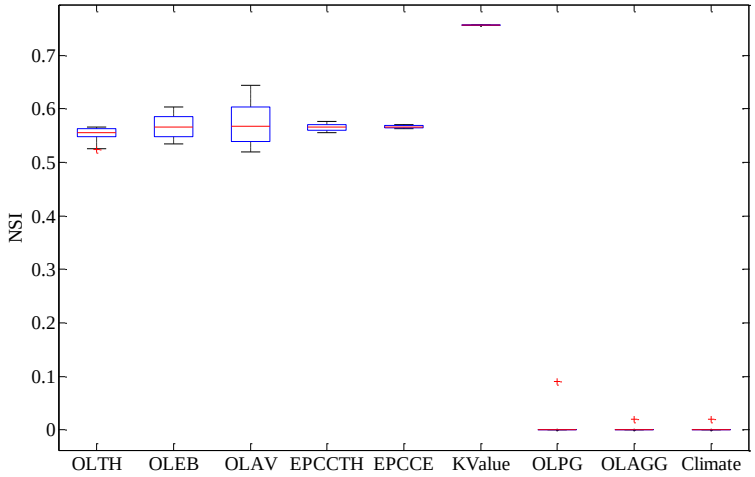

(c) Relative importance of design inputs for IRI

Figure 4-30 Summary of NSI curves for composite pavement

4.4.2.3. Rubblized pavement

Relative importance of design inputs

Figure 4-31 illustrates the relative importance of design inputs for HMA over rubblized PCC pavement. The results show that the existing PCC fractured modulus has the highest impact on the pavement distresses except for rutting. Overlay thickness has the most significant effect on the rutting prediction. Overlay HMA mixture volumetric parameters (overlay air voids and aggregate gradation) and PG grade have important contributions to rutting besides overlay thickness.

Main effect of design inputs

The main effects of all the input variables on all predicted distresses were investigated, as shown in Figure 4-32. The distress and NSI plots for all of the inputs and distresses are presented in Appendix B. The results show that overlay air voids has a significant impact on all the pavement performance measures (NSI>1 for all cases). Overlay thickness, effective binder content, and existing PCC modulus all have a significant impact on alligator cracking. In the case of rutting, overlay effective binder content shows a significant impact. For IRI all design inputs except overlay air voids show relatively lower contribution. It should be noted that box plot summarizes a NSI curve for each design input range. In some cases if there is a rapid change in NSI due to a specific input value, the point will be shown as an outlier in the box plot. Therefore, the maximum value of NSI was used as the criteria for identifying a significant input variable.

Interactive effect of design inputs

Interaction between input variables for distress and NSI for this rehabilitation option are presented in Appendix B. Figures B-96 to B-98 show the significant interactions for alligator cracking and the corresponding NSI plots. The results in Figure B-96 show that lower overlay air voids will reduce the impact of existing modulus on alligator cracking. For example, for low overlay air voids and fair to high existing rubblized PCC modulus, the predicted cracking will be negligible over the design life. On the other hand, for high overlay air voids depending on the existing rubblized PCC modulus; the HMA layer may exhibit 0 to 50% alligator cracking over the design life. Figure B-96 also shows that the rate of change in cracking w.r.t overlay air voids will increase as the existing rubblized PCC modulus decreases. The maximum NSI for interactions can be utilized to rank the interactions. The interactions are compared based on the maximum NSI later in the summary of this section.

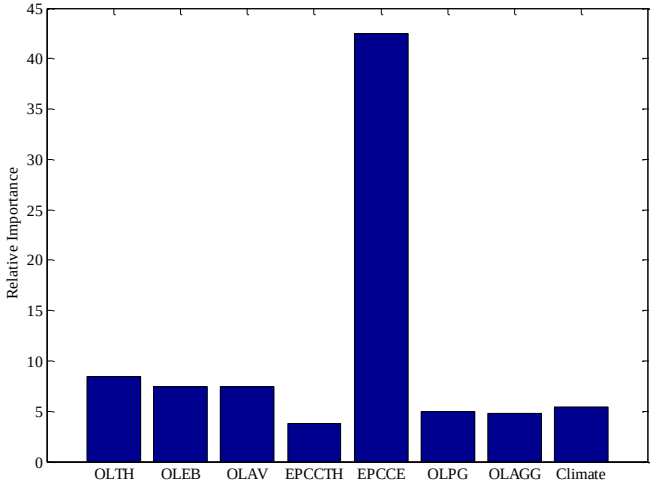

(a) Relative importance of design inputs for alligator cracking

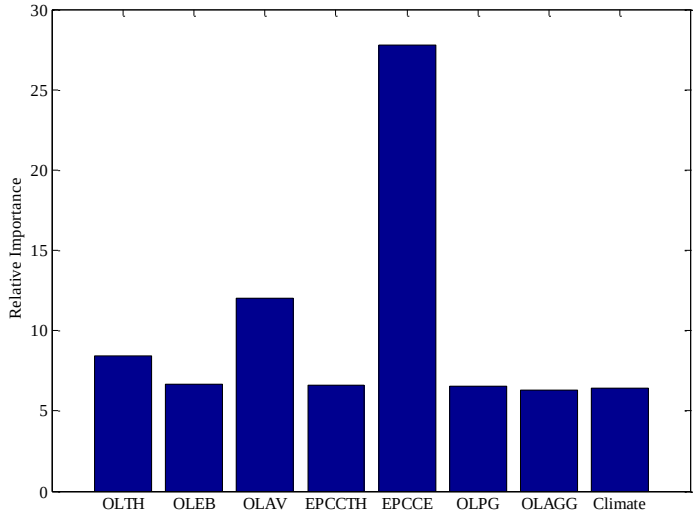

(b) Relative importance of design inputs for longitudinal cracking

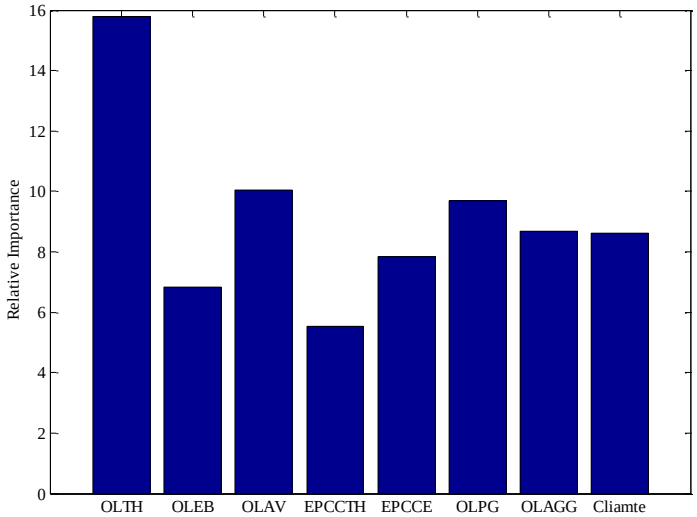

(c) Relative importance of design inputs for rutting

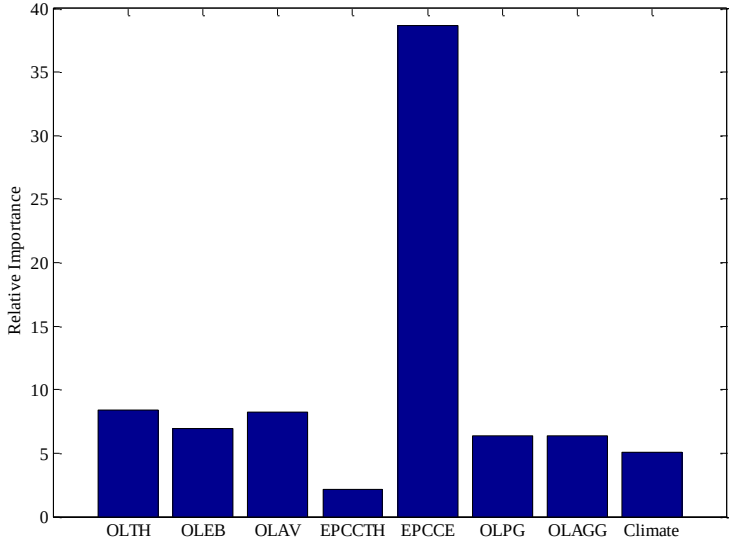

(d) Relative importance of design inputs for IRI

Figure 4-31 Relative importance of design inputs for rubblized PCC pavement

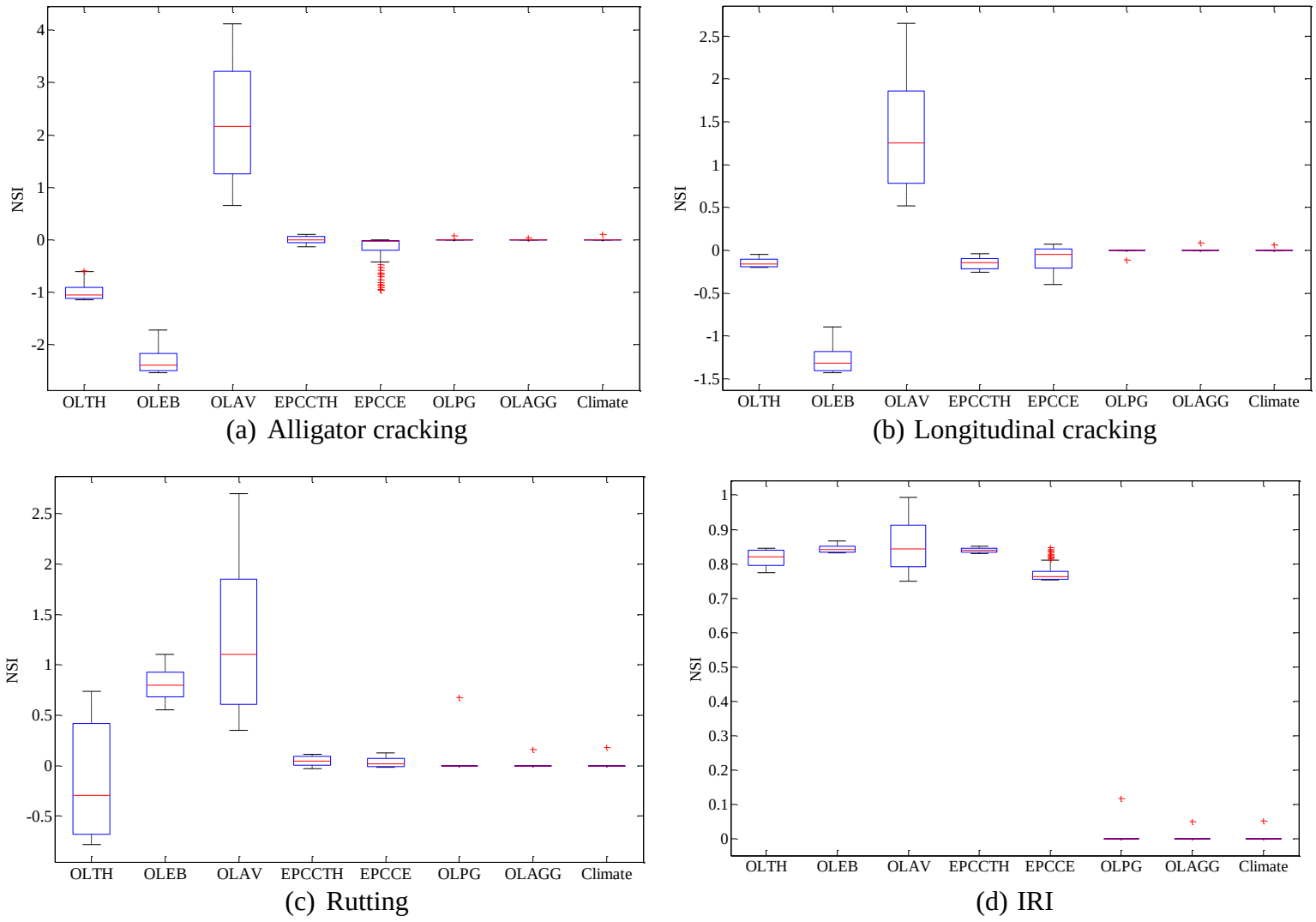

(a) Alligator cracking

(b) Longitudinal cracking

(c) Rutting

(d) IRI

Figure 4-32 Summary of NSI curves for rubblized PCC pavement

4.4.2.4. Unbonded PCC overlay

Relative importance of design inputs

Figure 4-33 presents the relative importance of input variables for different pavement performance measures. The results show that for cracking, overlay thickness, overlay MOR, and subgrade modulus of reaction (*k*-value) have the most significant contributions. For faulting, overlay CTE and climate are the major contributors. For IRI, overlay CTE, *k*-value, and climate have important but somewhat similar contributions in predicted roughness.

Main effect of design inputs

The summary of NSI plots for unbonded PCC overlay is presented in Figure 4-34. The main effects of all the design inputs on all predicted distresses were investigated similarly to other rehabilitation options and are presented in Appendix B. The results demonstrate that overlay CTE has a significant impact on all pavement performance measures. For cracking, overlay thickness has the highest effect followed by overlay MOR, CTE and joint spacing. Faulting and IRI showed lower sensitivity to design inputs compared to cracking. However, overlay thickness and existing PCC modulus show relatively large impact on IRI.

Interactive effect of design inputs

Figures B-140 to B-142 show the significant interactions for cracking and the corresponding NSI interaction plots. Figure B-141 shows that higher overlay MOR will lower the impact of existing PCC modulus on cracking. For example, for 900 psi overlay MOR, regardless of the existing PCC modulus, the predicted cracking will be close to zero over the design life. On the other hand, for low overlay MOR depending on the existing PCC modulus, the unbonded PCC overlay will exhibit 20-40% cracking over the design life. Figure B-141 also shows that the rate of change in cracking with respect to overlay MOR will decrease as the existing PCC modulus increases. The interaction between existing modulus and overlay thickness has a significant effect on cracking. The interaction between design inputs for faulting and IRI showed lower effects. The maximum NSI for interactions can be used to rank the interactions.

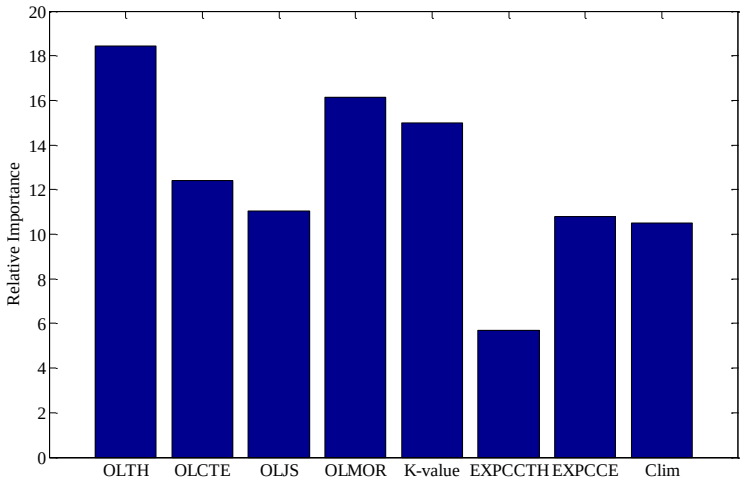

(a) Relative importance of design inputs for cracking

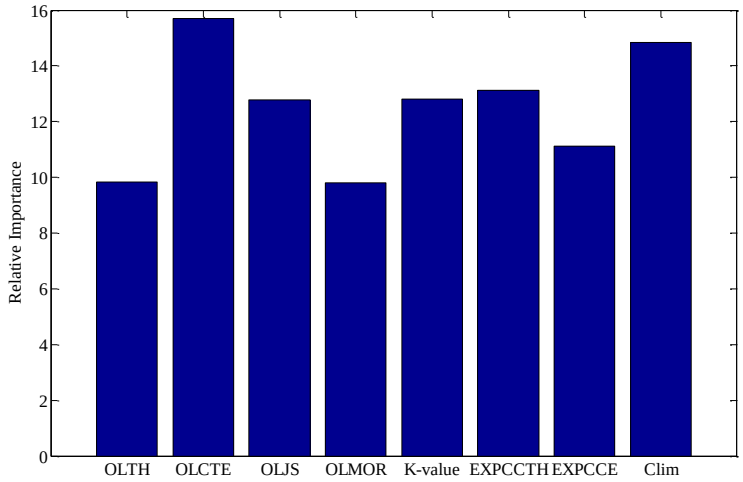

(b) Relative importance of design inputs for faulting

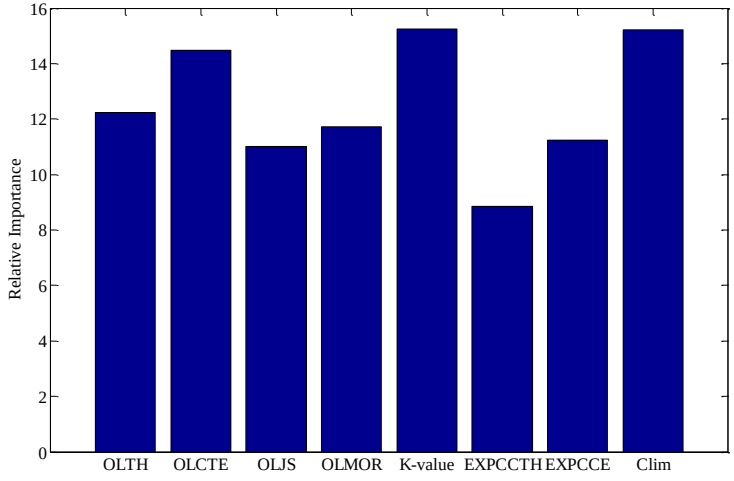

(c) Relative importance of design inputs for IRI

Figure 4-33 Relative importance of design inputs for unbonded PCC overlay

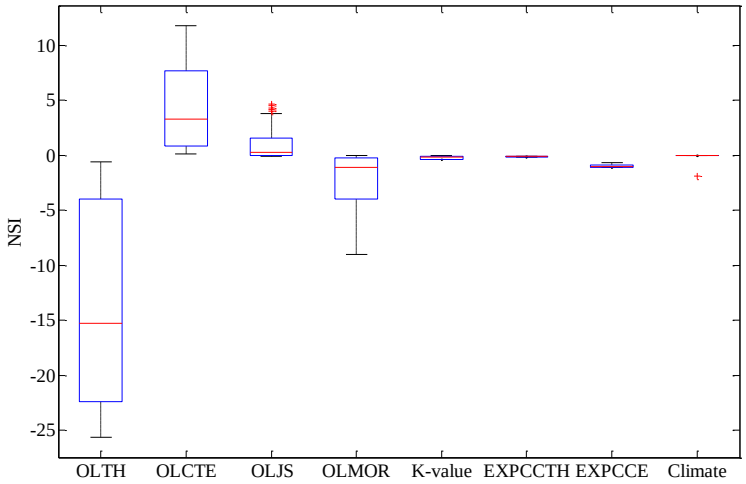

(a) Relative importance of design inputs for cracking

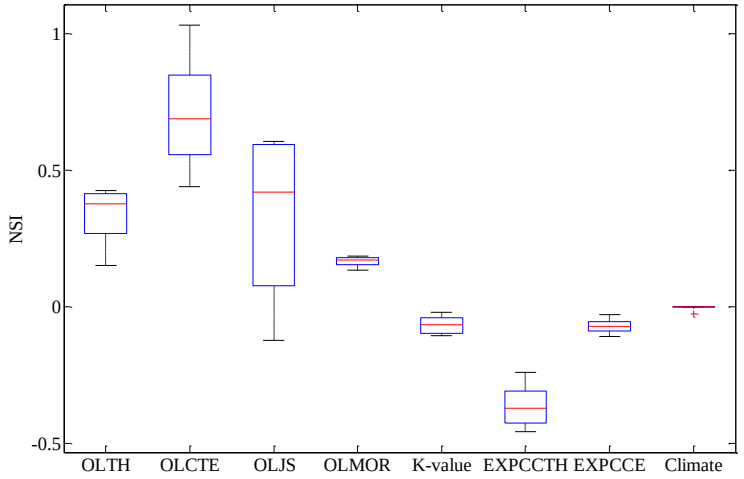

(b) Relative importance of design inputs for faulting

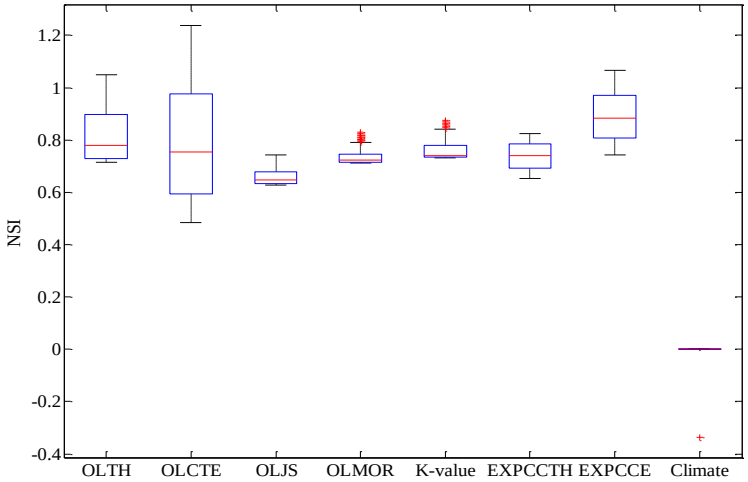

(c) Relative importance of design inputs for IRI

Figure 4-34 Summary of NSI curves for unbonded PCC overlay

4.4.2.5. Summary Results

The four rehabilitation options were considered in GSA similarly to the preliminary and the detailed sensitivity analyses. First, the relative contributions of the design inputs for various pavement performance measures were identified and discussed. Second, the main effect of design inputs for a base case was investigated. Finally the interactive effect of the design inputs was studied for all pavement performance measures within each rehabilitation option.

The results are summarized based on the main effects determined through the maximum NSI values from GSA. The input variables are ranked based on NSI which indicates their impact on the difference in pavement performance measures. Table 4-50 shows the inputs for HMA over HMA. The results can be summarized as follows:

- In general, the overlay thickness and HMA volumetrics are the most significant inputs for the overlay layer.
- The existing thickness and condition rating have an important effect among the existing pavement inputs.

Table 4-50 The MEPDG inputs ranking for HMA over HMA

Input variables	Alligator cracking ranking (NSI)	Longitudinal cracking ranking (NSI)	Rutting ranking (NSI)	IRI ranking (NSI)
Overlay thickness	3 (0.6)	3 (4)	2 (0.5)	1 (0.65)
Overlay air voids	1 (1.2)	1 (6)	1 (0.52)	2 (0.51)
Overlay effective binder	2 (0.7)	5 (2)	3 (0.47)	4 (0.51)
Existing thickness	5 (0.15)	2 (5)	4 (0.47)	3 (0.51)
Base modulus	9 (0.05)	8 (0.4)	7 (0.05)	6 (0.44)
Subbase modulus	8 (0.05)	7 (1)	5 (0.35)	5 (0.45)
Subgrade modulus	6 (0.1)	6 (2)	9 (0.05)	7 (0.44)
Existing pavement condition rating	4 (0.5)	4 (3.8)	6 (0.2)	10 (0.05)
Overlay aggregate gradation	10 (0)	9 (0.25)	10 (0.05)	8 (0.05)
Overlay PG	11 (0)	11 (0)	8 (0.05)	11(0.05)
Climate	7 (0.1)	10 (0.05)	11 (0.05)	9 (0.05)

Note: The shaded cells show the most important input variables (|NSI|>1)

Table 4-51 shows the inputs for HMA over PCC composite rehabilitation option. The results can be summarized as follows:

- The overlay thickness and HMA air voids are the most significant inputs for the overlay layer.
- The existing thickness has an important effect among the existing pavement inputs.

Table 4-51 The MEPDG inputs ranking for composite pavement

Inputs	Longitudinal cracking ranking (NSI)	Rutting ranking (NSI)	IRI ranking (NSI)
Overlay thickness	2 (1.8)	2 (1)	6 (0.56)
Overlay air voids	1 (8.5)	1 (1.75)	3 (0.61)
Overlay effective binder	7 (0)	3 (0.7)	2 (0.64)
Overlay PG	5 (0.2)	4 (0.6)	7 (0.5)
Overlay aggregate gradation	9 (0)	7 (0.1)	8 (0.5)
Existing PCC thickness	3 (1)	5 (0.3)	4 (0.58)
Existing PCC modulus	4 (0.25)	6 (0.2)	5 (0.57)
Subgrade reaction modulus	8 (0)	9 (0)	1 (0.75)
Climate	6 (0.1)	8 (0.05)	9 (0.5)

Note: The shaded cells show the most important input variables (|NSI|>1)

Table 4-52 shows the inputs for HMA over rubblized PCC rehabilitation option. The results can be summarized as follows:

- The HMA thickness, air voids and effective binder content are the most significant inputs for the overlay layer.

Table 4-52 The MEPDG inputs ranking for rubblized PCC pavement

Inputs	Alligator cracking ranking (NSI)	Longitudinal cracking ranking (NSI)	Rutting ranking (NSI)	IRI ranking (NSI)
Overlay thickness	3 (1)	5 (0.1)	3 (0.8)	3 (0.85)
Overlay air voids	1 (4)	1 (6)	1 (2.8)	1 (1)
Overlay effective binder	2 (2.1)	2 (1.2)	2 (1.1)	2 (0.87)
Overlay PG	6 (0.05)	7 (0.05)	4 (0.4)	6 (0.84)
Overlay aggregate gradation	7 (0.05)	8 (0.05)	5 (0.2)	8 (0.84)
Existing PCC thickness	5 (0.05)	4 (0.1)	8 (0.1)	4 (0.85)
Existing PCC modulus	4 (0.8)	3 (0.4)	6 (0.15)	5 (0.85)
Climate	8 (0.05)	6 (0.05)	7 (0.1)	7 (0.84)

Note: The shaded cells show the most important input variables (|NSI|>1)

Table 4-53 presents the inputs for unbonded PCC overlay rehabilitation option. The results can be summarized as follows:

- All overlay related inputs seem to significantly impact the cracking performance.
- The existing PCC elastic modulus is the most important input among all inputs related to existing layers.

Table 4-53 The MEPDG inputs ranking for unbonded PCC overlay

Design inputs	Cracking ranking (NSI)	Faulting ranking (NSI)	IRI ranking (NSI)
Overlay PCC thickness (inch)	1 (23)	4 (0.4)	2 (1.05)
Overlay PCC CTE (per °F x 10-6)	2 (12)	1 (1.1)	1 (1.2)
Overlay joint spacing (ft)	4 (5)	2 (0.55)	8 (0.75)
Overlay PCC MOR (psi)	3 (8)	5 (0.2)	5 (0.82)
Modulus of subgrade reaction (psi/in)	5 (0.5)	8 (0.1)	4 (0.88)
Existing PCC thickness (inch)	8 (0.1)	3 (0.45)	6 (0.81)
Existing PCC elastic modulus (psi)	6 (1)	7 (0.1)	3 (1.05)
Climate	7 (1)	6 (0.1)	7 (0.8)

Note: The shaded cells show the most important input variables (|NSI|>1)

Tables 4-54 to 4-57 rank the interactions between input variations from overlay and existing layer for all the rehabilitation options based on the maximum NSI. The results can be summarized as follows:

- The interaction between overlay air voids and existing pavement thickness seems to be the most important in impacting all pavement performance measures among HMA rehabilitation options. A higher air void in the overlay layers on a thin existing layer seems to be the worst combination for predicted cracking.
- The interaction between overlay thickness and existing PCC layer modulus seems to have the most significant effect on unbonded PCC overlay performance. A thicker overlay may hide the impact of weak existing PCC layer on pavement predicted performance.

All the interactions studied here are practically and statistically significant. Therefore all of them should be considered in the design and analysis.

Table 4-54 Interaction ranking for HMA over HMA

Interaction	Alligator cracking ranking (NSI)	Longitudinal cracking ranking (NSI)	Rutting ranking (NSI)	IRI ranking (NSI)
Overlay air voids and existing thickness	1 (0.8)	1 (15)	3 (0.3)	3 (0.1)
Overlay effective binder and existing thickness	2 (0.5)	3 (7)	2 (0.3)	2 (0.1)
Overlay thickness and existing thickness	3 (0.5)	2 (10)	1 (0.4)	1 (0.2)

Table 4-55 Interaction ranking for composite pavement

Interaction	Longitudinal cracking ranking (NSI)	Rutting ranking (NSI)
Overlay thickness and existing thickness	2 (25)	2 (1.5)
Overlay air voids and existing thickness	1 (44)	1 (1.7)

Table 4-56 Interaction ranking for rubblized PCC pavement

Interaction	Alligator cracking ranking (NSI)	Longitudinal cracking ranking (NSI)	Rutting ranking (NSI)	IRI ranking (NSI)
Overlay air voids and existing thickness	1 (3.7)	1 (2.4)	2 (0.8)	2 (0.1)
Overlay effective binder and existing thickness	2 (2.1)	2 (1.1)	1 (1)	1 (0.1)
Overlay thickness and existing thickness	3 (0.8)	3 (0.5)	3 (0.8)	3 (0.1)

Table 4-57 Interaction ranking for unbonded PCC overlay

Interaction	Cracking ranking (NSI)	Faulting ranking (NSI)	IRI ranking (NSI)
Overlay thickness and existing modulus	1 (28.5)	1 (0)	1 (1.5)
Overlay MOR and existing thickness	3 (6)	2 (0)	3 (0.7)
Overlay MOR and existing modulus	2 (14.5)	3 (0)	2 (0.7)

4.5 SATELLITE STUDIES

Several additional clarification studies were performed to evaluate the sensitivity of input variables in the MEPDG/DARWin-ME. These investigations were important to understand intricate details about the following topics:

1. Impact of HMA gradation on the predicted performance of flexible pavement
2. Effect of binder's *G** on predicted performance of HMA over HMA
3. Influence of unbound layers gradation on predicted performance of flexible and rigid pavements

4.5.1 Effect of different HMA Gradations on Predicted Pavement Performance

The main objective for this investigation was to evaluate the impact of HMA gradations (level 3) on the predicted pavement performance based on the specification limits. Different HMA gradations were obtained for the specific MDOT mixtures from Part 1 of the study. The process for the selection of the HMA mixtures included the following steps:

a. Evaluate all HMA mixtures used in Part 1 of the project
b. Sort the mixtures by course type i.e., top, leveling, and base
c. Plot the aggregate gradation for each HMA mixture
d. Select a coarse, fine and intermediate gradation based on step c
e. Perform DARWin-ME analysis using the specific volumetric properties of the selected HMA mixtures in step d
f. Compare the predicted pavement performance measures to evaluate the effect of gradation.

A typical pavement cross-section used in this investigation is shown in Table 4-58. Table 4-59 presents the volumetric properties of different MDOT mixtures selected for this evaluation. The base case consisted of mid gradations for all HMA layers. The HMA gradations were changed one-at-a-time while all others were held constant.

Table 4-58 Typical flexible pavement cross-section

Layer Type	Thickness (in)	Modulus (psi)	Type
HMA Top	2	N/A	PG 58-28
HMA Leveling	2		
HMA Base	2		
Base	4	30,000	A-1-A
Subbase	10	20,000	A-3
Subgrade	semi inf	17,000	A-4

Figures 4-35 to 4-37 show the predicted alligator cracking, surface rutting and IRI, respectively. Based on the results, it can be seen that only HMA base course gradation has some effect on the predicted bottom-up alligator cracking. The base case values lie directly under one of the other curves indicating no performance differences. Therefore, it can be

concluded that for level 3 inputs, HMA gradation doesn't significantly impact the predicted pavement performance. In addition, the average gradation from the specification limits can be used for initial pavement design. However, it should be noted that these findings are valid for the range of HMA gradations obtained in this study.

Table 4-59 Volumetric properties of the selected mixtures

Course type	Gradation	MDOT HMA mixture types		
		Mid (base case)	Fine	Coarse
Top	3/4"	100	100	100
	3/8"	95.7	99.5	99.7
	No. 4	80.1	76.2	84.1
	No. 200	5.8	5.4	6
	Eff AC	12.58	11.4	12.06
Leveling	3/4"	100	100	100
	3/8"	87.6	89.9	87.1
	No. 4	66.5	69.3	76.4
	No. 200	5.7	5.6	5.3
	Eff AC	10.62	10.9	10.58
Base	3/4"	100	100	99.9
	3/8"	76.1	72.3	82.6
	No. 4	56.9	47.3	65
	No. 200	3.5	5	5.1
	Eff AC	9.78	9.8	10.4

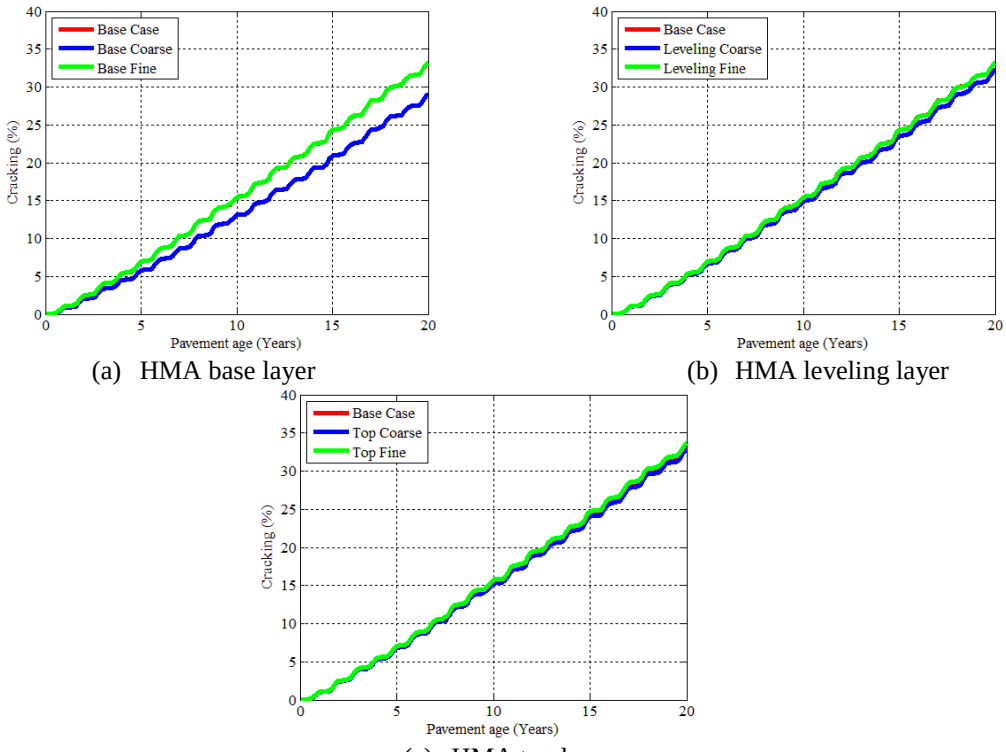

(a) HMA base layer

(b) HMA leveling layer

(c) HMA top layer

Figure 4-35 Alligator cracking predictions

(a) HMA base layer

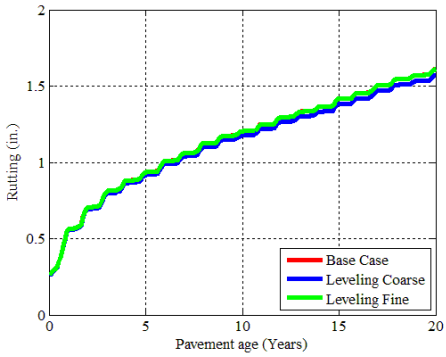

(b) HMA leveling layer

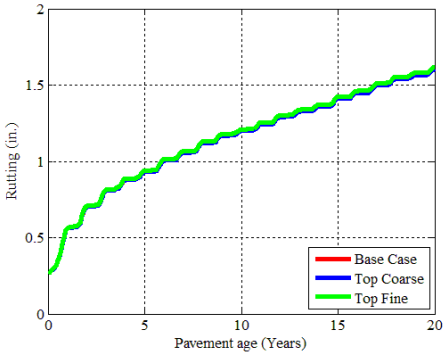

(c) HMA top layer

Figure 4-36 Rutting predictions

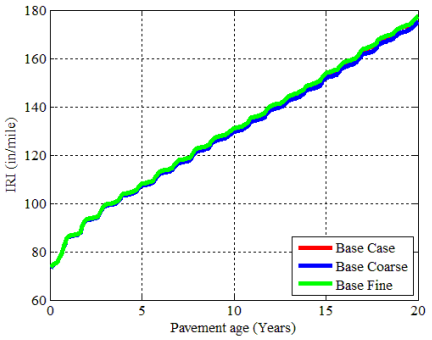

(a) HMA base layer

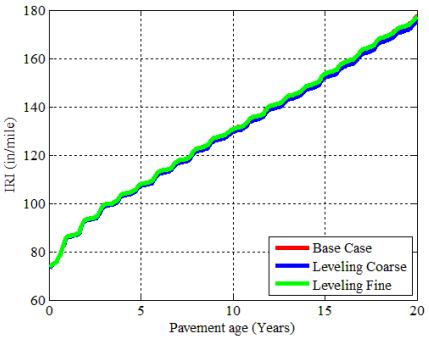

(b) HMA leveling layer

(c) HMA top layer

Figure 4-37 IRI predictions

4.5.2 Impact of Binder *G** Variations on Predicted Pavement Performance

In Part 1 of the study, several binders being used by MDOT were tested and characterized. It was observed that multiple binders with similar PG can have significantly different rheological behavior; i.e., master curves for dynamic shear modulus (*G**). The main objective of this investigation was to assess the variations in the MEPDG pavement performance predictions due to multiple binders having the same PG but different *G** master curves. Figure 4-38 shows the *G** master curves for two binders with the same PG grading (PG 64-28). The two binders have different G* magnitude at different frequencies.

In order to evaluate the effect of *G** on predicted performance of HMA over HMA, a typical cross-section was selected. All inputs were held constant while *G** data was used to characterize the binder at level 1. Figure 4-39 shows the predicted pavement performance. The results show that the effect of *G** variation is only important for rutting prediction. Therefore, it is recommended that *G** master curve (level 1) should be used if available, especially if rutting is a dominant distress. The variations in *G** master curve could be attributed to different binder sources for the same PG. However, it is anticipated that if a binder from the same source is utilized for mix design at a specific location, the level 1 *G** master curve should not vary significantly. Therefore, an average can be used for multiple G* master curves. Part 1 of this study addressed this issue in more detail.

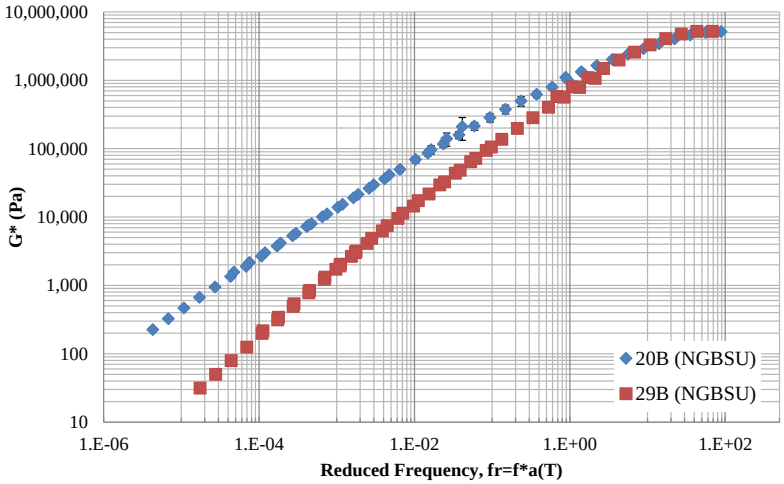

Figure 4-38 The G* master curves for two binders with same PG

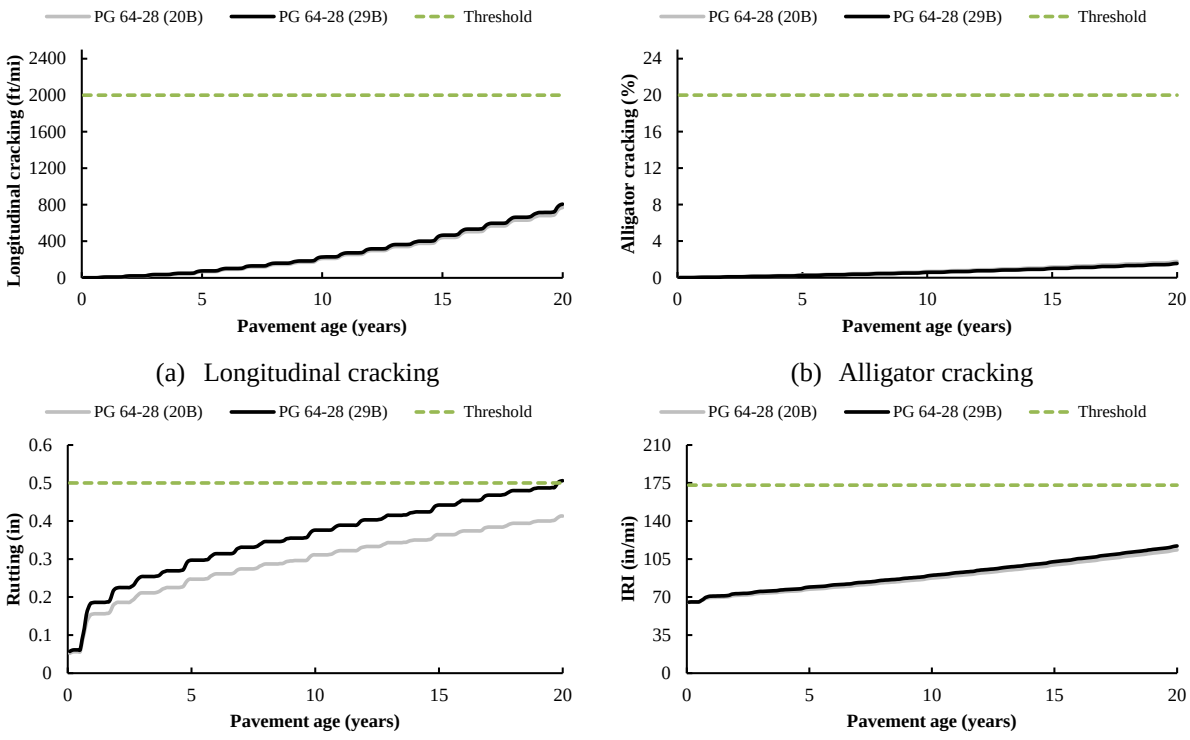

(a) Longitudinal cracking

(b) Alligator cracking

(c) Rutting

(d) IRI

Figure 4-39 The effect of G* variation on predicted HMA over HMA pavement performance

4.5.3 Impact of Unbound Layer Gradations on Predicted Performance

The main objective of this investigation is to study the impact of aggregate base and subbase gradations on the predicted performance. A sensitivity analysis was performed to study the effects. Three gradations each were selected for base and subbase materials. The gradations were selected for fine and coarse aggregates for each material type from the MDOT specifications. In addition, the default gradation based on A-3 and A-1-a in the DARWin-ME was considered for base and subbase materials, respectively. It should be noted that a pavement structure can be designed based on several combinations of these materials with different gradations. The design matrix for the sensitivity study is shown in Table 4-60. The following procedure was used to select the coarse, and fine aggregate gradations:

1. Determine materials used for base and subbase from MDOT specifications
    a. Base course – 22A, 21AA,
    b. Subbase – Class II materials
2. Determine gradations from the MDOT specifications
    a. Table 902-1 and 902-2 for base materials
    b. Table 902-4 for subbase materials
3. Perform DARWin-ME analysis for both new JPCP and HMA pavements with coarse (lower) and fine (upper) specification limits for base and subbase materials.

Table 4-60 Design matrix for sensitivity analysis

Material type	Pavement scenario							
	1	2	3	4	5	6	7	8
Base material (A-3)	Coarse	Fine	Default	Default	Coarse	Coarse	Fine	Fine
Subbase material (A-1-a, A-1-b)	Default	Default	Coarse	Fine	Coarse	Fine	Coarse	Fine

Figure 4-40 shows the gradations for the selected base and subbase layers. The analyses were performed for new JPCP and flexible pavements. The cross-section information is summarized in Table 4-61. For each pavement type the time to reach a threshold for a specific distress was determined. Figure 4-41 shows the pavement performance predictions and time to reach threshold for new rigid pavement. The results show that the difference in time to failure for transverse cracking is less than 2 years for any combination shown in Table 4-60. The faulting and IRI predictions did not reach the threshold limit in the 20 year design life and therefore are not shown. Similar analysis for unbonded overlay showed no difference in the predicted performance for all combinations. Figure 4-42 shows the results for alligator and reflective cracking as well as for surface rutting. Longitudinal cracking and IRI did not reach the threshold limit in the 20 year design and therefore are not shown. Based on these results it is recommended that for the same material type and climate, the base and subbase aggregate gradations can be selected within the limits of the specifications or just use the default values.

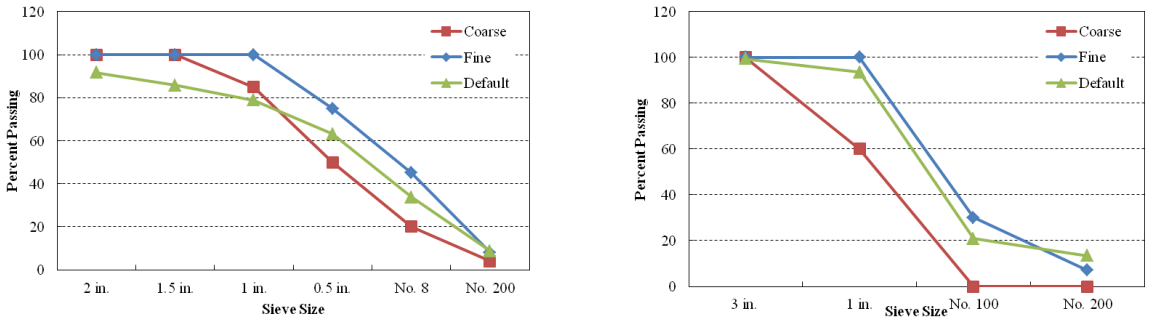

(a) base (b) subbase

Figure 4-40 Coarse, fine and default gradations

Table 4-61 Cross-section information

Pavement type	Layer type	Thickness (inches)
Rigid	JPCP	9
	Base	4
	Subbase	10
Flexible	HMA	6
	Base	8
	Subbase	15

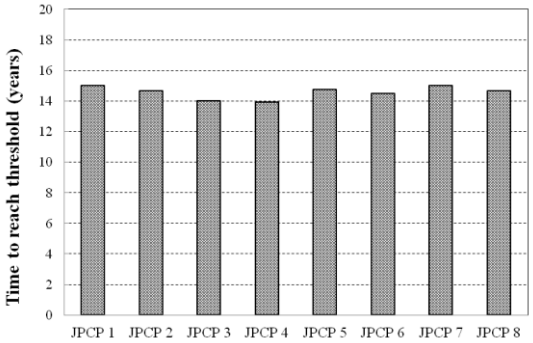

(a) Time to threshold

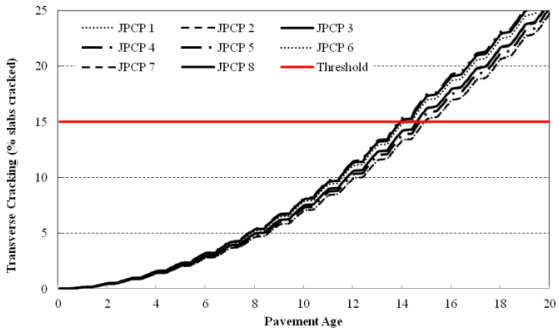

(b) Transverse cracking

Figure 4-41 Impact of aggregate gradation on rigid pavement performance

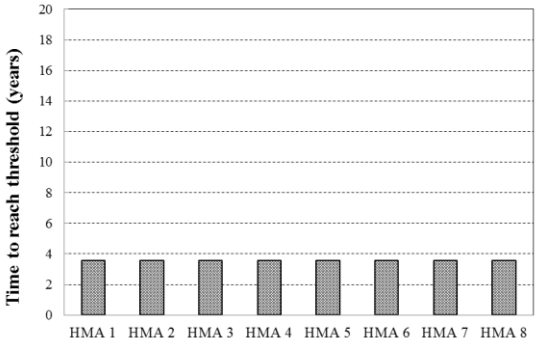

(a) Time to threshold

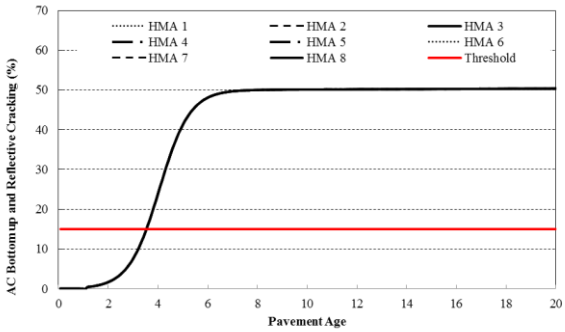

(b) Alligator and reflective cracking

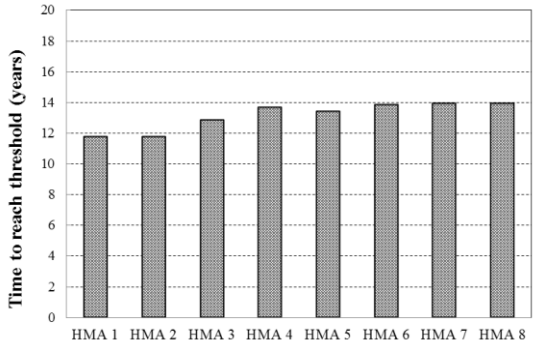

(c) Time to threshold

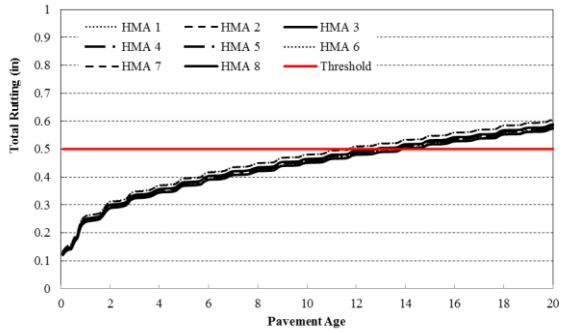

(d) Surface rutting

Figure 4-42 Impact of aggregate gradation on HMA over HMA pavement performance

CHAPTER 5 - VERIFICATION OF REHABILITATION DESIGN

5.1 INTRODUCTION

Validation of the MEPDG/DARWin-ME performance models is necessary to determine how well the models predict measured pavement performance in the State of Michigan. The first step in the verification process is to identify projects across different regions in the State based on local pavement design and construction practices. The second step involves extraction of the measured pavement performance data for each project from the MDOT Pavement Management System (PMS) and Sensor (laser measured IRI, rutting and faulting) database. The third step entails documentation of all input data related to pavement materials, cross-section, traffic and climatic conditions for the identified projects. The accuracy of these input data is important in determining the true predictability of the performance models in the MEPDG/DARWin-ME. Finally, measured and predicted performances are compared for each project to evaluate the existing performance models and to identify the local calibration needs. It should be noted, that only DARWin-ME was used for the verification of the rehabilitation models. In this chapter, the work related to the following tasks as outlined in Chapter 1 is presented:

- Task 2-4: Project identification and selection
    - Project selection criteria and matrix
    - Project information by rehabilitation option
- Task 2-5: Verification of rehabilitation performance models
    - Project performance
        - Available distresses in MDOT's PMS and conversion to match DARWin-ME
        - Project field performance
    - Project Inputs for verification
    - Verification results
        - Predicted vs. measured
        - Model accuracy
        - Need for local calibration

5.2 PROJECT IDENTIFICATION & SELECTION

In-service pavement projects were identified and selected to determine the validity of the performance prediction models for Michigan. It should be noted that some identified pavement projects may not be selected because they lack sufficient performance data or adequate construction records. The project selection criteria, design matrix, and a summary of the selected projects are discussed in the subsequent sections.

5.2.1 Project Selection Criteria and Design Matrix

MDOT identified and provided rehabilitation projects (unbonded, rubblized and composite overlays) for the verification of the rehabilitation models. The MSU research team identified HMA over HMA projects and MDOT provided the needed inputs. The HMA over HMA pavement projects to be included in the study were selected based on the following criteria:

- Site factors: The site factors will address the various regions in the state, climatic zones and subgrade soil types.
- Traffic: Three traffic levels were selected; level 1, less than 1000 AADTT, level 2, 1000 to 3000 AADTT; and level 3 more than 3000 AADTT. The three levels were selected based on pavement class, trunk routes, US routes and Interstate routes.
- Overlay thicknesses: The range of constructed overlay thicknesses.
- Open to traffic date: The information is needed to determine the performance period.
- As built cross-section: Includes details of the existing structure and the overlay.
- Pre-overlay repairs performed on the existing pavement (such as partial and/or full depth repairs, dowel bar retrofit)
- Material properties of both the existing and the new structure

Table 5-1 summarizes the number of selected pavement projects based on the selection criteria presented above. A total of 42 projects were selected representing various rehabilitation options. It can be seen that each rehabilitation option contains more than 5 projects.

Table 5-1 Selection matrix displaying selected projects

Rehabilitation type	Traffic level*	Overlay thickness level*	Age (years)			Total
			<10	10 to 20	>20	
Composite overlay	1	2		1	1	7
	2	2		2	2	
	3	2			1	
HMA over HMA	1	1			8	16
		2	1	5		
	2	2	1		1	
Rubblized overlay	1	2		4	2	11
		3		2		
	2	2			1	
	3	2			1	
		3		1		
Unbonded overlay	2	2		1		8
		3		1		
	3	3	1	5		
*Levels		1	2	3		
Traffic (AADTT)		<1000	1000-3000	>3000		
Overlay thickness (in)		<3	3-6	>6		

5.2.2 Project Information by Rehabilitation Option

Pavement cross-section and material related information for each selected pavement project are essential to generate the most representative project in the DARWin-ME. In addition, the validity of the performance predictions using the software depends on how well the overlay and existing pavement layers are defined. This section outlines the overlay, existing pavement cross-section, and the geographical location information of the selected projects.

5.2.2.1. Unbonded Overlays

Figure 5-1 presents the locations of the eight unbonded concrete overlay pavement projects selected for this study. Geographically, the eight projects are located on the east and west sides of the Lower Peninsula of Michigan. Since there are no unbonded JPCP pavements built prior to 1998 in the State of Michigan, the selected projects were constructed between 1998 and 2004. Table 5-2 provides a detailed summary of the selected projects based on traffic, overlay thickness, and pavement age. Table 5-3 summarizes the cross-section information for each selected project. The data in the table indicate that:

- The overlay thickness ranges from 6 to 8 inches
- The existing PCC pavement thickness for all projects is 9 inches.
- The existing base and subbase thicknesses ranged from 3 to 4 inches and from 10 to 14 inches, respectively.
- The asphalt interlayer thickness for all unbonded overlay projects is 1-inch, except for one project that had a variable interlayer thickness from 1- to 2.5-inch because crown correction was done with the separator layer.
- The average annual daily truck traffic (AADTT) for each project is greater than 1000.

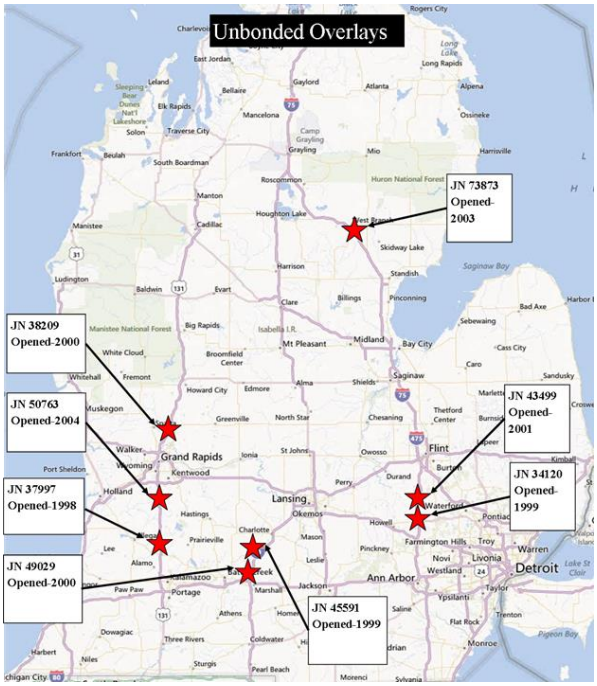

Figure 5-1 Geographic location of the eight unbonded overlay projects

Table 5-2 Complete project matrix for unbonded overlays

Rehab type	Traffic (AADTT)	Age (years)	OL thickness (in)	No. of projects
Unbonded overlays	<1000	<10	<3	
			3 to 6	
			>6	
		10 to 20	<3	
			3 to 6	
			>6	
		>20	<3	
			3 to 6	
			>6	
	1000 to 3000	<10	<3	
			3 to 6	
			>6	
		10 to 20	<3	
			3 to 6	1
			>6	1
		>20	<3	
			3 to 6	
			>6	
	>3000	<10	<3	
			3 to 6	
			>6	1
		10 to 20	<3	
			3 to 6	
			>6	5
		>20	<3	
			3 to 6	
			>6	
Total				8

Table 5-3 Unbonded overlay cross-section information

Job number	Control section	Overlay thickness (in)	Existing thickness (in)	Base thickness (in)	Subbase thickness (in)	Interlayer thickness (in)	Interlayer PG Grade
37997	3111	7.1	9 (1960)	3	11	1	PG 58-28
34120	47014	7.9	9 (1960)	3	14	1	PG 58-28
49029	13074	7.1	9 (1969/1972)	4	10	1	PG 58-28
45591	13074 23061	7.1	9 (1972)	4	10	1	PG 58-28
38209	41132 41133	6.3	9 (1970/1973)	4	10	1	PG 58-28
43499	47014	7.1	9 (1960)	3	14	1	PG 70-28
73873	65041	6	9 (1974)	4	10	1	PG 64-28
50763	39014 3111	6.5	9 (1963)	4	10	1-2.5	PG 58-28

5.2.2.2. Rubblized Overlays

Figure 5-2 shows the locations of the 11 selected rubblized projects. Geographically, all projects are located in the Lower Peninsula of Michigan. The projects were constructed between 1989 and 2000. The existing JRCP pavement was rubblized prior to applying an HMA surface. Table 5-4 presents a detailed summary of the selected projects based on traffic, overlay thickness, and pavement age. Table 5-5 lists the cross-section information for each project. The data in the table indicate that:

- The overlay thickness ranges from 4 to 9.5 inches.
- The existing PCC pavement thicknesses ranged from 8 to 9 inches.
- The existing base and subbase thicknesses range from 0 to 4 inches and from 0 to 18 inches, respectively.

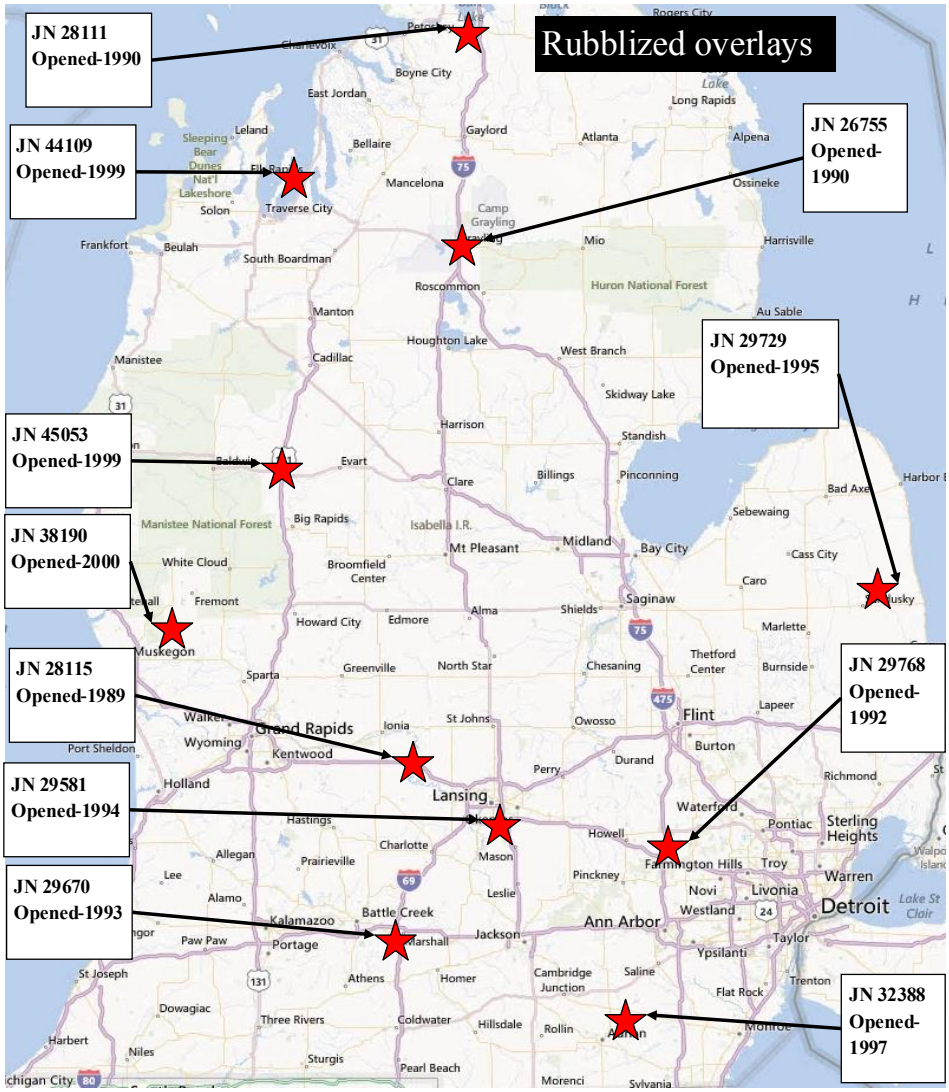

Figure 5-2 Geographic location of the eleven rubblized overlay projects

Table 5-4 Complete project matrix for rubblized overlays

Rehab type	Traffic (AADTT)	Age (years)	OL thickness (in)	No. of projects
Rubblized overlays	<1000	<10	<3	
			3 to 6	
			>6	
		10 to 20	<3	
			3 to 6	4
			>6	2
		>20	<3	
			3 to 6	
			>6	
	1000 to 3000	<10	<3	
			3 to 6	
			>6	
		10 to 20	<3	
			3 to 6	
			>6	
		>20	<3	
			3 to 6	3
			>6	
	>3000	<10	<3	
			3 to 6	
			>6	
		10 to 20	<3	
			3 to 6	
			>6	1
		>20	<3	
			3 to 6	1
			>6	
Total				11

Table 5-5 Rubblized overlay cross-section information

Job Number	Overlay thickness (in)	Existing thickness (in) (construction. date)	Base thickness (in)	Subbase thickness (in)	Penetration or PG Grade
28115	5	9 (1959)	3	9	120-150
26755	4.25	8 (1955)	0	0	120-150
29768	5.25	9 (1962)	4	14	85-100
29670	6.25 @ Center Line, 5.5 @ rt edge	9 (1960)	3	9	85-100
29581	7.5 min to 9.5(crown correction.)	9 (1963/64)	4	10	85-100
28111	4	9-7-9 (1936/37)	0	0	200-250
29729	5 @ edge; 7.2” @ Center Line	9-7-9 (1939)	0	18 average; (8 min)	120-150
45053	5.5 minimum	9 (1958)	3	12	64-28 (T)
44109	7.5	8 (1954)	0	9	58-28
38190	5.5	9 (1963)	4	14	58-28
32388	6 @ Center Line; 7 @ edge	8 (1953)	0	6 min, up to 12	58-28

5.2.2.3. Composite Overlays

Figure 5-3 shows the location of the 7 composite overlay projects selected for this study. Geographically, the seven projects are located in the Lower Peninsula of Michigan. The projects were constructed between 1987 and 2000. The composite overlay projects are built over an intact JRCP. Table 5-6 presents a detailed summary of the selected projects based on traffic, overlay thickness, and pavement age. Table 5-7 summarizes the cross-section information for each project. The data in the table indicate that:

- The overlay thickness ranges from 3.5 to 4.5 inches.
- The existing PCC pavement thicknesses are between 7 and 9 inches.
- The existing base and subbase thicknesses range from 0 to 4 inches and from 0 to 15 inches, respectively.

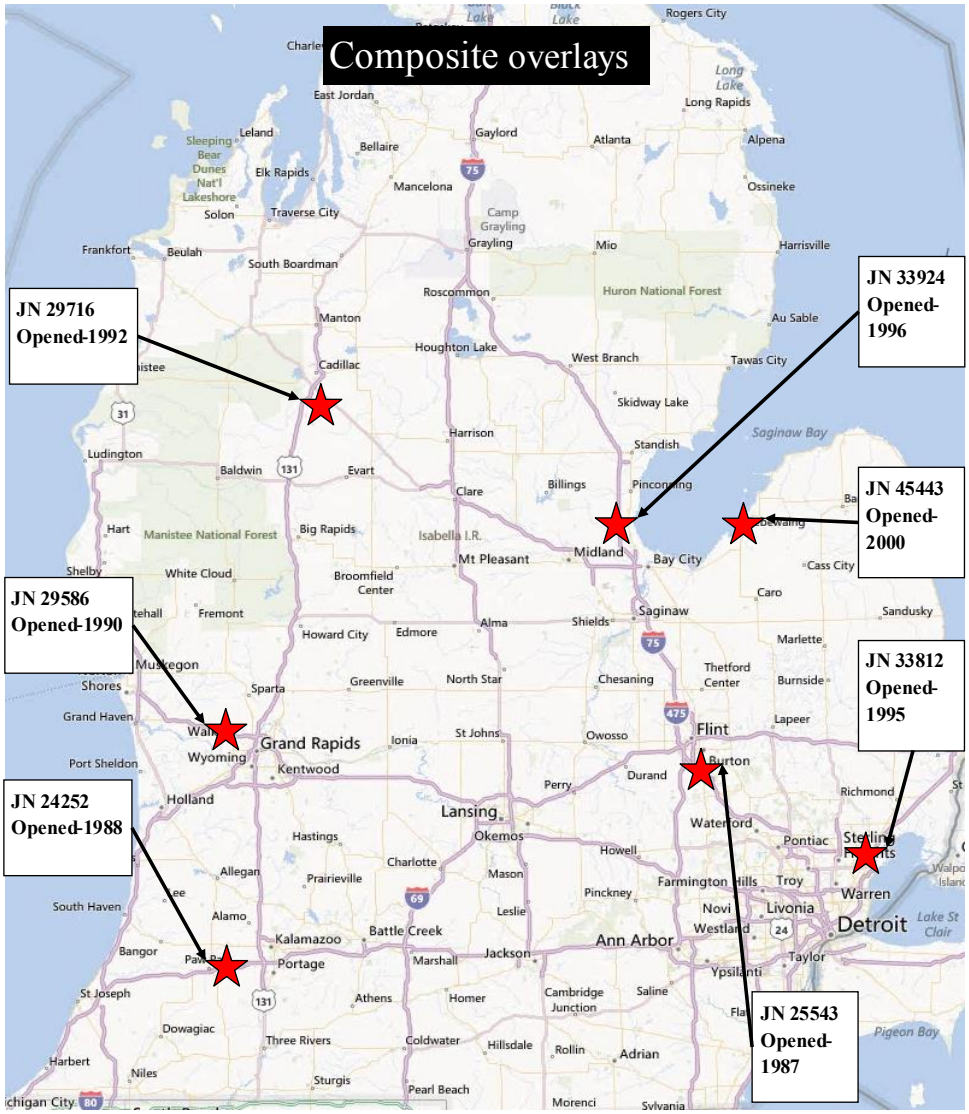

Figure 5-3 Geographical location of the seven composite overlay projects

Table 5-6 Complete project matrix for composite overlays

Rehab type	Traffic (AADTT)	Age (years)	OL thickness (in)	No. of projects
Composite	<1000	<10	<3	
			3 to 6	
			>6	
		10 to 20	<3	
			3 to 6	1
			>6	
		>20	<3	
			3 to 6	1
			>6	
	1000 to 3000	<10	<3	
			3 to 6	
			>6	
		10 to 20	<3	
			3 to 6	2
			>6	
		>20	<3	
			3 to 6	2
			>6	
	>3000	<10	<3	
			3 to 6	
			>6	
		10 to 20	<3	
			3 to 6	
			>6	
		>20	<3	
			3 to 6	1
			>6	
Total				7

Table 5-7 Composite overlay cross-section information

Job number	Overlay thickness (in)	Existing thickness (in) (construction date)	Base thickness (in)	Subbase thickness (in)	Penetration or PG Grade
25543	4	9 (1963)	4	10	85-100
24252	4.5	9 (1959)	3	9	85-100
29586	3	9 (1961)	3	12 minimum	85-100
29716	3.5	9-7-9 (1938)	0	0	120-150
33812	3	9 (1959)	3	14 min	85-100
33924	4	8 (1964/67)	4	Sloped Lt to Rt 3-10	120-150
45443	3.5 min	8 (1949)	0	15	64-28

5.2.2.4. HMA over HMA

Figure 5-4 shows the location of 14 out of 15 HMA over HMA pavement projects selected for this study. One of the projects did not meet all criteria and was excluded from the verification study. Geographically, 14 projects are located in the Lower Peninsula and one project in the Upper Peninsula of Michigan. In the Lower Peninsula, six projects are located in the South West, five in the North West, and three projects are located in the Southern part of the State. All projects were constructed between 1983 and 2005. The HMA over HMA projects are built over existing flexible pavements. Table 5-8 presents a detailed summary of the selected projects based on traffic, overlay thickness, and pavement age, while Table 5-9 summarizes the cross-section information. The data in the latter table indicate that:

- The overlay thickness ranges from 2 to 3.5 inches.
- The existing HMA pavement thicknesses range between 1.5 and 7.5 inches.
- The existing base and subbase thicknesses range from 4 to 11 inches and from 0 to 28 inches respectively.

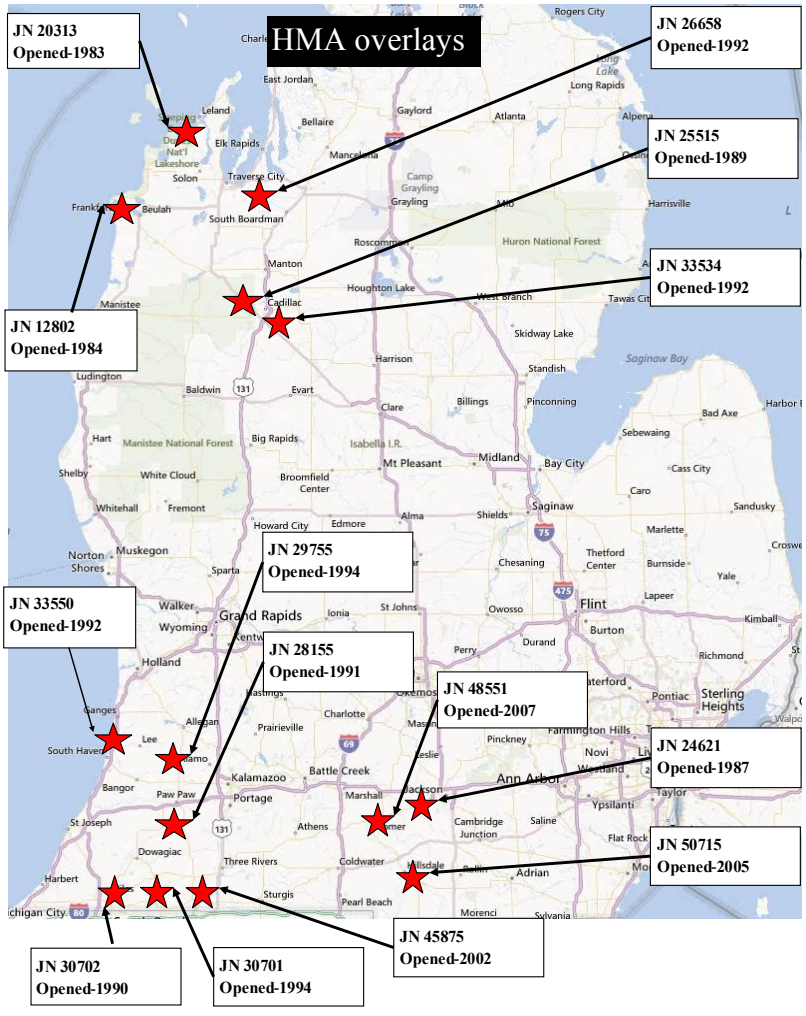

Figure 5-4 Geographical location of 14 HMA over HMA projects

Table 5-8 Complete project selection matrix for HMA over HMA

Rehab type	Traffic (AADTT)	Age (years)	OL thickness (in)	No. of projects
HMA over HMA	<1000	<10	<3	
			3 to 6	1
			>6	
		10 to 20	<3	
			3 to 6	5
			>6	
		>20	<3	7
			3 to 6	
			>6	
	1000 to 3000	<10	<3	
			3 to 6	
			>6	
		10 to 20	<3	
			3 to 6	
			>6	
		>20	<3	
			3 to 6	2
			>6	
	>3000	<10	<3	
			3 to 6	
			>6	
		10 to 20	<3	
			3 to 6	
			>6	
		>20	<3	
			3 to 6	
			>6	
Total				15

Table 5-9 HMA over HMA cross-section information

Job number	Overlay thickness (in)	Existing thickness	Base thickness (in)	Subbase thickness (in)	PG Grade
33534	2.5	3.25	11	25	85-100 ex, 120-150 OL
33550	3	6.4	11	28	85-100
28155	2.5	5.2	7	12	120-150
26658	2.5				120-150
29755	3	4-5.5	4 or 5 stabilized	0 or 15	120-150
30701	3	4.5	7 or 7+3 select	0 or 18	85-100
31047	3	3.3	10	13.7	120-150
32361	3	3.7	5-7-5	0 or 15	120-150
45875	2	4.5	6-11	8	64-28
50715	3.5	7.59	6		64-28
20313	2.25	1.5	5	0 or 12	120-150
12802	2.5	2.25 or 4.75	7		120-150
24621	2.5	3.75	8		120-150
25515	2.5	2.25	10		120-150
30702	2.5	7.1	5		85-100

5.3 PROJECT FIELD PERFORMANCE

Once all the projects were selected, the next step was to determine the measured time series performance for each project. MDOT collects distress and laser based measurement (sensor) data on their pavement network every other year. The distress data in the MDOT PMS are represented by different principle distress codes (PD's). Each PD corresponds to a visually measured surface distress observed in the field. Certain distress types collected by MDOT are expressed in a form that is not compatible with the DARWin-ME; therefore, conversions were necessary to make the data comparable. The distress types collected by MDOT and the necessary conversion process are discussed in this section. Furthermore, the current condition of each pavement section is also presented.

5.3.1 Selected Distresses and Conversion

The necessary distress information was identified and extracted from the MDOT PMS and sensor database. The extraction process of all the necessary distress and sensor data needed assistance from MDOT. The MDOT PMS Current Distress Manual was used to determine all the PD's corresponding to predicted distresses in the DARWin-ME. The latest version of the document outlining all the different distress calls can be found in Appendix D. It should be noted that, all PD's were included since MDOT began collecting this data (1992), earlier versions of the PMS manual were consulted to ensure that the correct data was extracted for all years.

The necessary steps for PMS data extraction include:

1. Identify the PD's that corresponds to the MEPDG/DARWin-ME predicted distresses,
2. Convert (if necessary) MDOT PD's to units compatible with the MEPDG/DARWin-ME
3. Extract PD's, and sensor data for each project
4. Summarize time-series data for each project

The identified and extracted pavement distresses and conditions for flexible and rigid pavements are summarized in Tables 5-10 and 5-11. A detailed discussion of the conversion process is detailed for both, flexible and rigid overlays.

Table 5-10 Flexible pavement distresses

Flexible pavement distresses	MDOT principle distresses	MDOT units	DARWin-ME units	Conversion needed?
IRI	Directly measured	in/mile	in/mile	No
Top-down cracking	204, 205, **724, 725**	miles	ft/mile	Yes
Bottom-up cracking	234, 235, **220, 221, 730, 731**	miles	% area	Yes
Thermal cracking	**101,** 103, 104, 114, **701, 703, 704,** 110	No. of occurrences	ft/mile	Yes
Rutting	Directly measured	in	in	No
Reflective cracking	No specific PD	None	% area	No

*Bold numbers represent older PD's that are not currently in use

Table 5-11 Rigid pavement distresses

Rigid pavement distresses	MDOT principle distresses	MDOT units	DARWin-ME units	Conversion needed?
IRI	Directly measured	in/mile	in/mile	No
Faulting	Directly measured	in	in	No
Transverse cracking	112, 113	No. of occurrences	% slabs cracked	Yes

5.3.1.1. Distresses conversion for HMA designs

It should be noted that only the distress types predicted by the DARWin-ME were considered for the verification exercise. The corresponding MDOT PD's were determined and compared to distress types predicted by the DARWin-ME to determine if any conversions were necessary. The MDOT measured pavement distresses that are related to HMA overlays are listed in Table 5-10. The conversion process (if necessary) for all distress types is as follows:

IRI: The IRI measurements in the MDOT sensor database are compatible to those in DARWin-ME. Therefore, no conversion or adjustments was need and the data were used directly.

Top-down cracking: Top-down cracking is defined as load related cracking in the wheel-path (longitudinal cracking). The PD's 204, 205, 724, and 725 are assumed to correspond to top down cracking in the MDOT PMS database because those may not have developed an indication of alligator cracking; however, these cracks could be bottom-up. The PD's are recorded in miles and needs conversion to feet/mile. Data from the wheel-paths were summed into one value and divided by the total project length.

Bottom-up cracking: The bottom up cracking is defined as alligator cracking in the wheel-path. The PD's 234, 235, 220, 221, 730 and 731 match this requirement in the MDOT PMS database. The PD's have units of miles; however, to make those compatible with the DARWin-ME alligator cracking units, conversion to percent total area is needed. This can be achieved by using the following Equation (1):

$$\%AC_{bottom-up} = \frac{\text{Length of cracking} \times \text{width of wheelpaths}}{\text{Length of project} \times \text{Lane width}} \quad (1)$$

Thermal cracking: Thermal cracking corresponds to transverse cracking in flexible pavements. The DARWin-ME predicts thermal cracking in feet/mile. The PD's 101, 103, 104, 114, 701, 703 and 704 were utilized to extract transverse cracking in flexible and rubblized pavements. For the composite pavement, PD's 101, 110, 114 and 701 were used. The transverse cracking is recorded as the number of occurrences. In order to convert transverse cracking in feet/mile, the number of occurrences was multiplied by the lane width for PD's 101, 103 and 104. For the PDs 114 and 701, the number of occurrences was multiplied by 3 feet because these PD's are defined as "tears" (short cracks) that are less than

half the lane width. All transverse crack lengths are summed and divided by the project length to get feet/mile.

Rutting: This is the total amount of surface rutting contributed by all the pavement layers. The average rutting (left & right wheel-paths) was determined for the entire project length. No conversion was necessary. It is assumed that the measured rutting corresponds to total surface rutting, and was compared to the total rutting in the DARWin-ME.

Reflective cracking: MDOT does not have any specific PDs for reflective cracking. It is difficult to determine the difference between a thermal and a reflective crack at the surface. Therefore, the total transverse cracking observed can be compared to the total combined thermal and reflective cracking. Reflective cracking was not included in verification for this reason and due to the limitations in the prediction model.

5.3.1.2. Distress conversion for JPCP Designs

As mentioned before, only the distresses that are predicted in the DARWin-ME were considered for verification. The corresponding MDOT PD's were determined and necessary conversions were made if needed. Table 5-11 summarizes the distresses related to JPCP overlays and the conversion process is discussed below:

IRI: The IRI in the MDOT sensor database does not need any conversion; the values were used directly

Faulting: The faulting is predicted as average joint faulting by the DARWin-ME. The faulting values reported in the MDOT sensor database corresponds to the average height of each fault for both cracks and joints. However, the DARWin-ME faulting prediction does not distinguish between faulting at cracks or joints and only predicts faulting at the joints. Therefore, only measured average joint faulting should be compared with the predicted faulting by DARWin-ME. However, because MDOT's data does not discern between faults at cracks and faults at joints, no conversions were made and the measured faulting at joints and cracks was directly compared to the predicted faulting from DARWin-ME.

Transverse cracking: The transverse cracking distress is predicted as % slabs cracked in the DARWin-ME. However, MDOT measures transverse cracking as the number of transverse cracks. PD's 112 and 113 correspond to transverse cracking. The measured transverse cracking needs conversion to percent slabs cracked by using Equation (2).

$$\%\ \text{Slabs Cracked} = \frac{\sum PD_{112,113}}{\left(\frac{\text{Project Length(miles)} \times 5280\ ft}{\text{Joint Spacing (ft)}}\right)} \times 100 \qquad (2)$$

5.3.2 Measured Field Performance

A customized PMS and sensor databases were created in order to query the selected PD's. The databases include all the distress and sensor data for multiple years in respective

Microsoft Access databases. These databases allowed the research team efficient performance data extraction for any project length. The databases included measured PMS performance data from 1992 to 2011 and the sensor data from 1996 to 2011, respectively. The sensor data prior to 1996 were not in a consistent format and could not be included in the custom database. The time series condition data were extracted for each selected project. The divided highway can have an increasing and a decreasing direction to indicate north/south or east/west bounds directions. Therefore, for such projects, both directions are included in the time-series data. Distress data for undivided highways are collected in one direction only. The threshold value of each distress and condition type is indicated by the horizontal straight line on each figure. The distress threshold values were discussed in Chapter 4.

5.3.2.1. Unbonded Concrete Overlays

The current performance of each unbonded overlay project is summarized in Figure 5-5. The magnitude represents the latest distress amount of each project regardless of maintenance fixes performed throughout the project life. The overlay pavement age is displayed in parentheses below the project number. It can be seen that none of the projects reached the distress thresholds for percent slabs cracked, IRI and faulting. It should be noted that all the project ages are below the design life of 20 years.

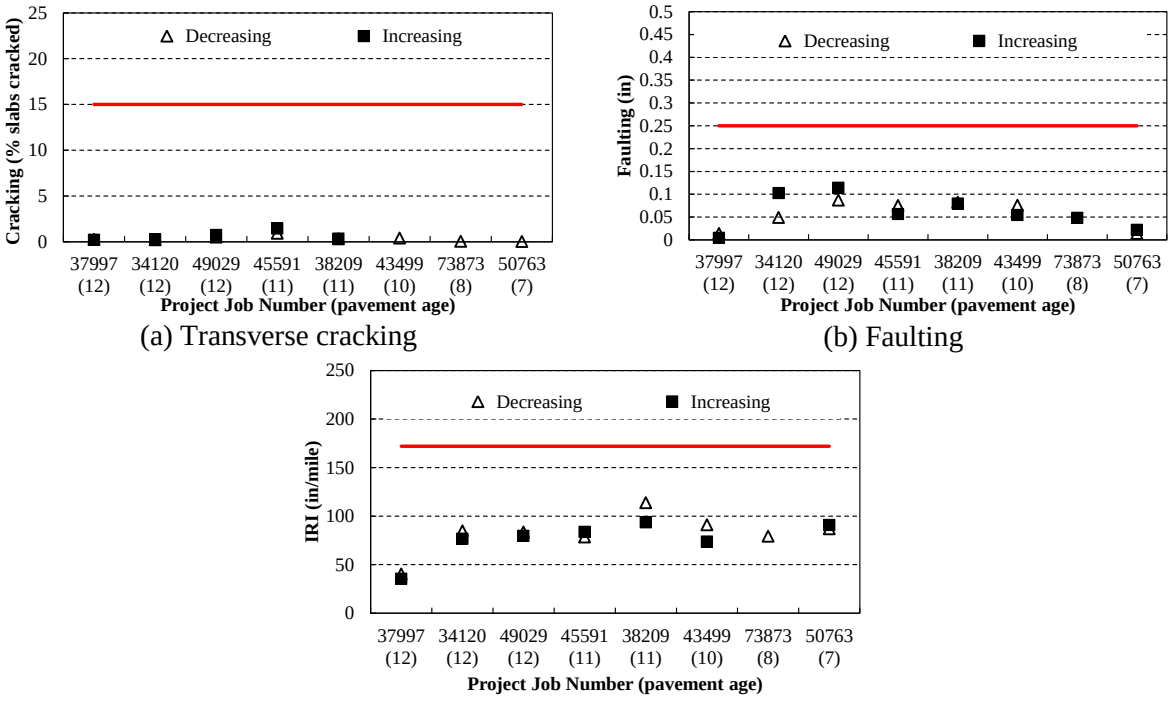

(a) Transverse cracking

(b) Faulting

(c) IRI

Figure 5-5 Current pavement distress and condition of unbonded overlay projects

Figure 5-6 shows an example of the extracted time-series data for Job number 37997. The distress data is plotted versus age for both the increasing and decreasing direction depending on the project. The divided highway can have increasing and decreasing direction to indicate north/south or east/west bounds. The vertical dashed lines indicate a maintenance action

performed on the pavement. For this particular pavement project, diamond grinding was performed in 2001, 2 years after construction, and joint sealing and concrete pavement restoration (CPR) were performed in 2006, 7 years after construction. It can be seen from the figure, that the maintenance fixes did not affect the magnitude of percent slabs cracked, but did affect IRI over time. It is possible that the IRI measurements were performed prior to the diamond grinding. However, it is reported for the same year as a fix. The time-series distress figures (in the same format) for all unbonded overlay projects can be found in Appendix C.

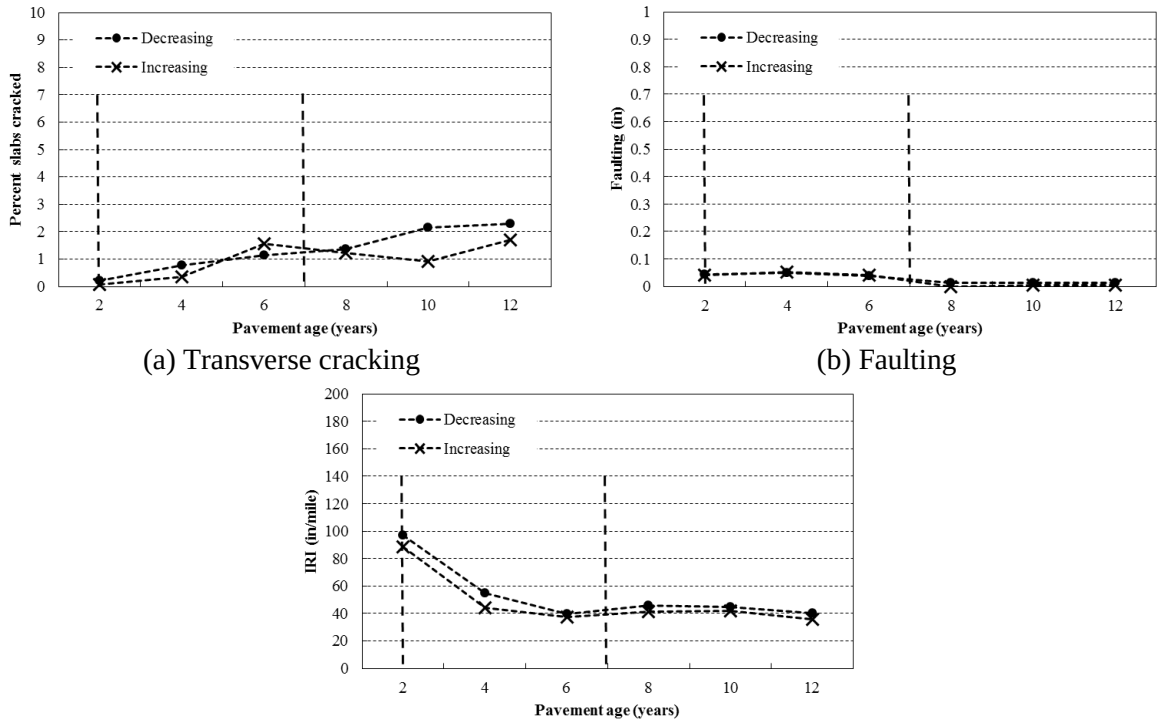

(a) Transverse cracking (b) Faulting

(c) IRI

Figure 5-6 Performance of unbonded overlay project 37997

5.3.2.2. Rubblized Overlays

The current performance of each rubblized overlay project is summarized in Figure 5-7. The distress magnitudes represent the latest distress value of each project regardless of maintenance fixes. The pavement age is displayed in parentheses below the project number. It can be seen that only thermal cracking exceeded the distress threshold value. It should be noted that it is not possible to determine the differences between thermal and reflective cracking from MDOT's PD's as they do not represent reflective cracking directly. Depending on the rubblization techniques used (badger or sonic breaker), joints could still be intact, and could cause reflective cracking in rubblized overlays.

As an example, Figure 5-8 shows the extracted time-series data for Job number 28115. The extracted distress data is plotted versus age for both the increasing and decreasing directions. The vertical dashed lines indicate a maintenance action performed on the pavement. For this particular pavement project, a chip seal was performed in 1998, 9 years after construction and an overband crack fill was performed in 2000, 11 years after construction. The figure

also shows that the number of distress points for both directions are not always equal. Both directions were included if the information was available. The IRI and rutting data were only available beyond 1996, and since this particular project was constructed prior to 1996, no data were available prior to the 9th year of the project. The time-series distress figures for all rubblized overlay projects can be found in Appendix C.

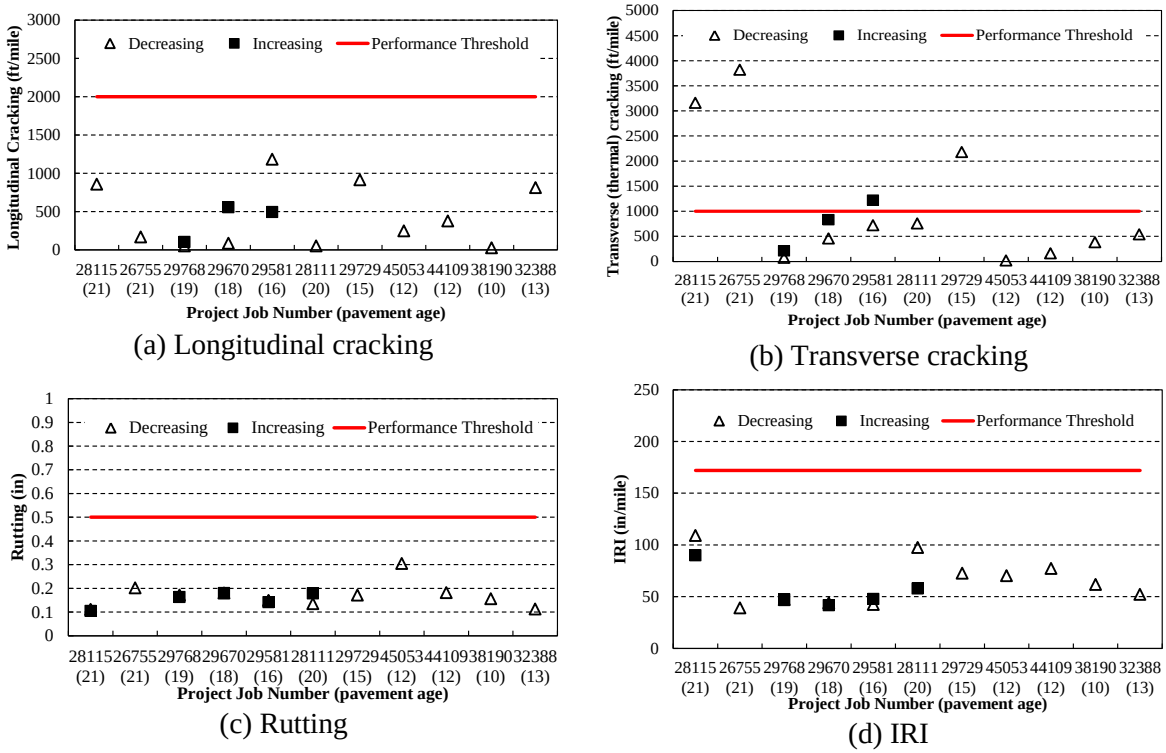

(a) Longitudinal cracking

(b) Transverse cracking

(c) Rutting

(d) IRI

Figure 5-7 Current pavement distress and condition for rubblized overlays

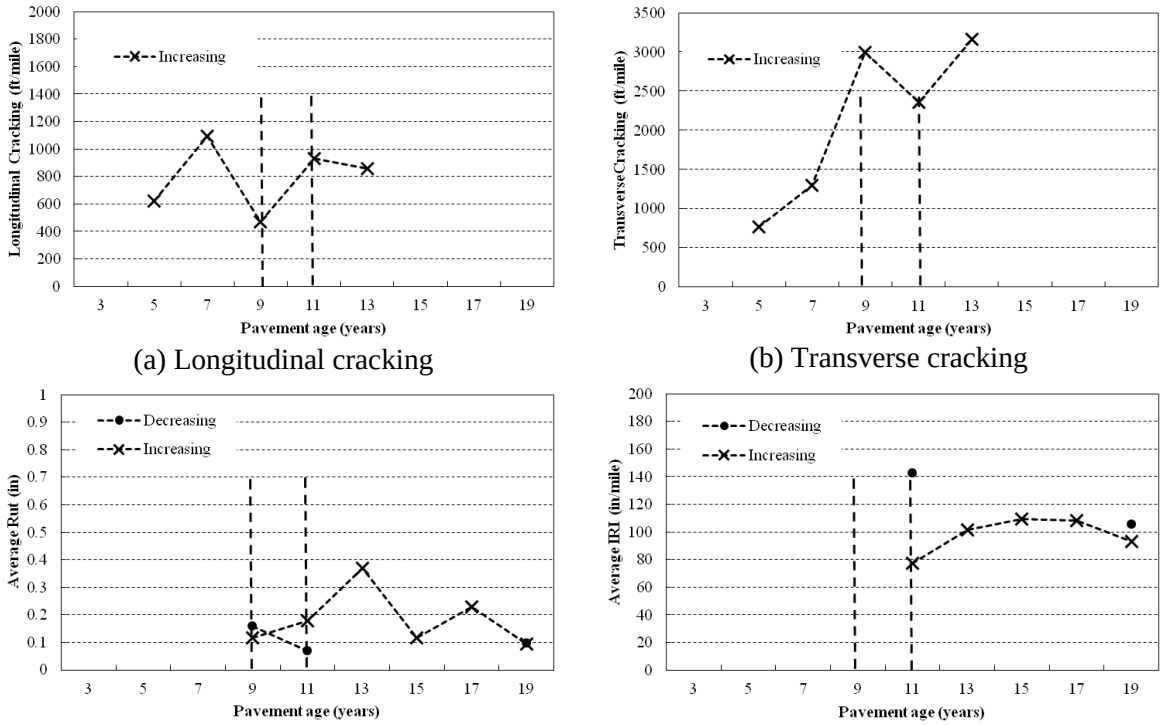

(a) Longitudinal cracking (b) Transverse cracking

(c) Rutting (d) IRI

Figure 5-8 Performance of rubblized overlay project 28115

5.3.2.3. Composite Overlays

The current performance of each composite overlay project is summarized in Figure 5-9. The distress magnitudes represent the latest distress value of each project regardless of the maintenance fixes. It can be seen that only thermal transverse cracking exceeded the distress threshold. Similar to rubblized overlays, it is not possible to distinguish between reflective cracking and thermal cracking in MDOT's PMS database. It is possible that some of the thermal cracking is actually reflective cracking.

Figure 5-10 shows the extracted time-series data for Job number 29586. The extracted distress data is plotted versus age for both the increasing and decreasing directions. The vertical dashed lines indicate if a maintenance action has been performed on the pavement. For this particular pavement project, a cold mill and resurfacing was performed in 1999, 9 years after construction. As mentioned for rubblized overlays, the missing IRI and rutting data is due to the age of the project. The time-series distress figures for all composite overlay projects can be found in Appendix C.

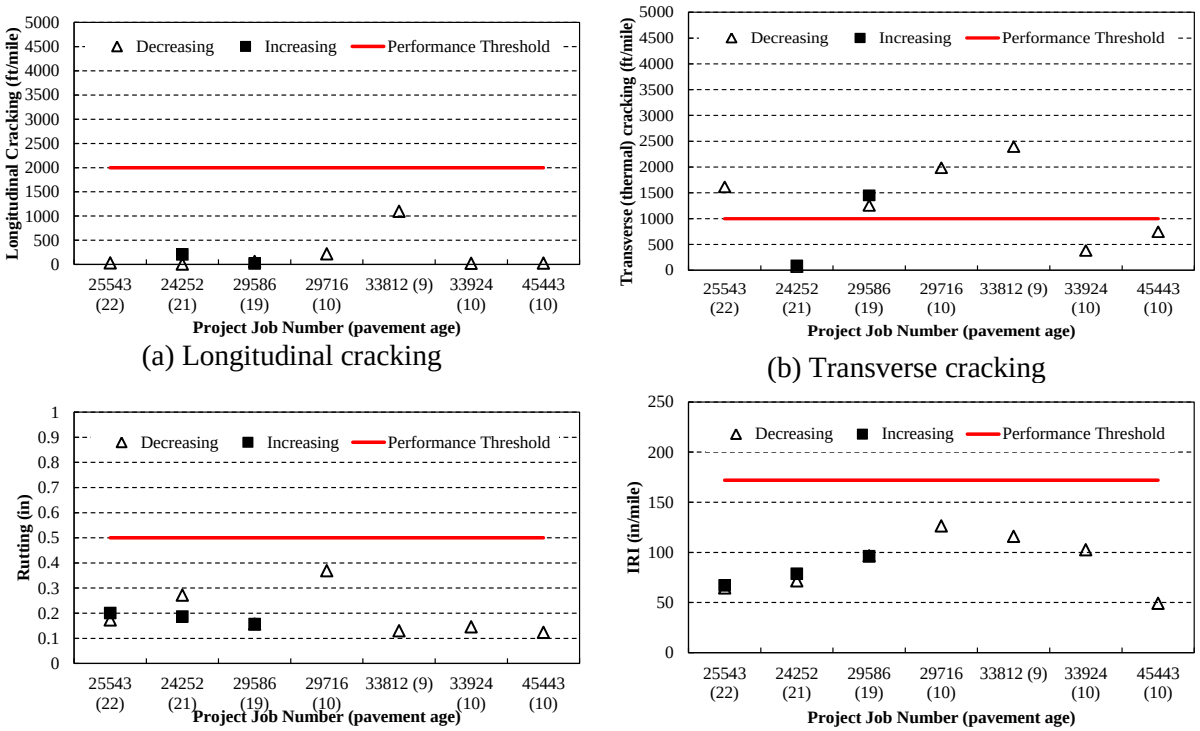

(a) Longitudinal cracking

(b) Transverse cracking

(c) Rutting

(d) IRI

Figure 5-9 Current pavement distress and condition of composite overlay projects

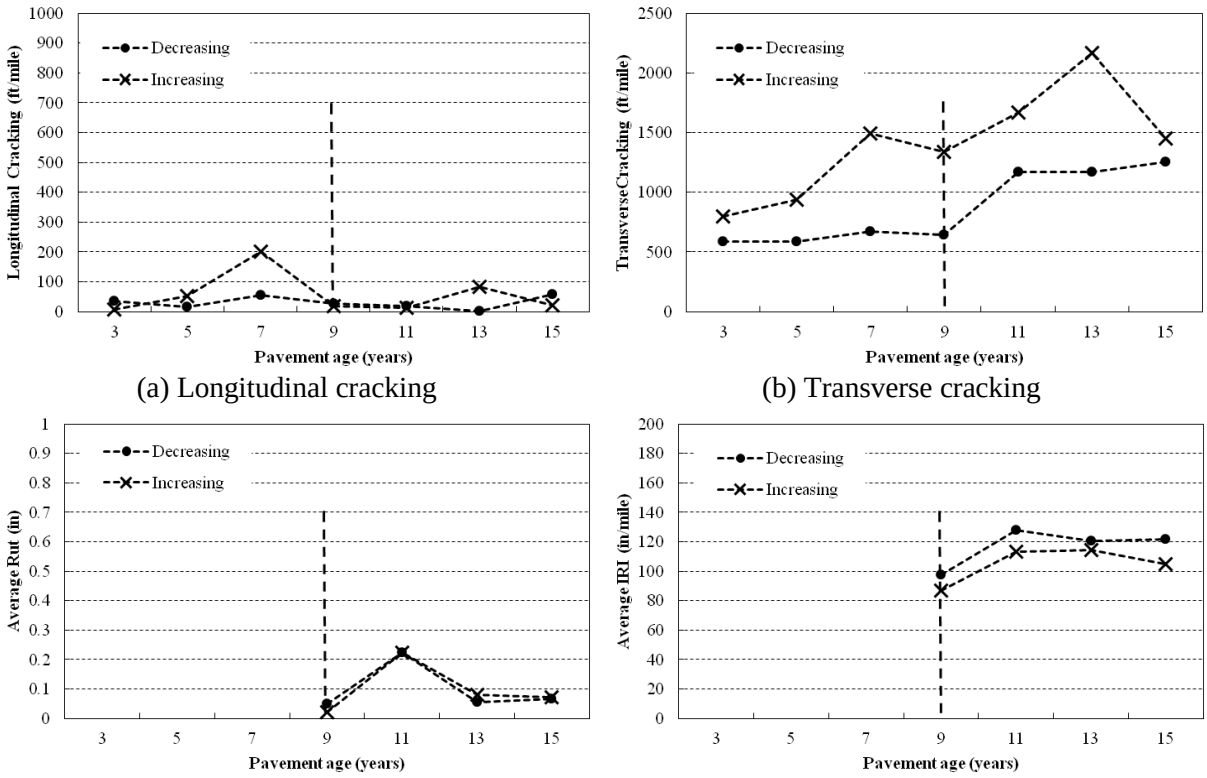

(a) Longitudinal cracking

(b) Transverse cracking

(c) Rutting

(d) IRI

Figure 5-10 Performance of composite overlay project 29586.

5.3.2.4. HMA over HMA

The current performance of each HMA over HMA project is summarized in Figure 5-11. The values represent the latest distress magnitude for each project regardless of maintenance fixes. It can be seen that one project exceeds the threshold for IRI and four projects exceeded the thermal transverse cracking distress threshold. As with rubblized and composite overlays, it is not possible to distinguish between thermal and reflective cracking.

Figure 5-12 shows the extracted time-series data for Job number 28155. The vertical dashed lines indicate the maintenance performed. For this particular project, crack treatments were performed in 1997 (5 years after construction) and 2000 (8 years after construction), a cold mill and resurfacing was performed in 2006 (14 years after construction). The time-series distress figures for all composite overlay projects can be found in Appendix C.

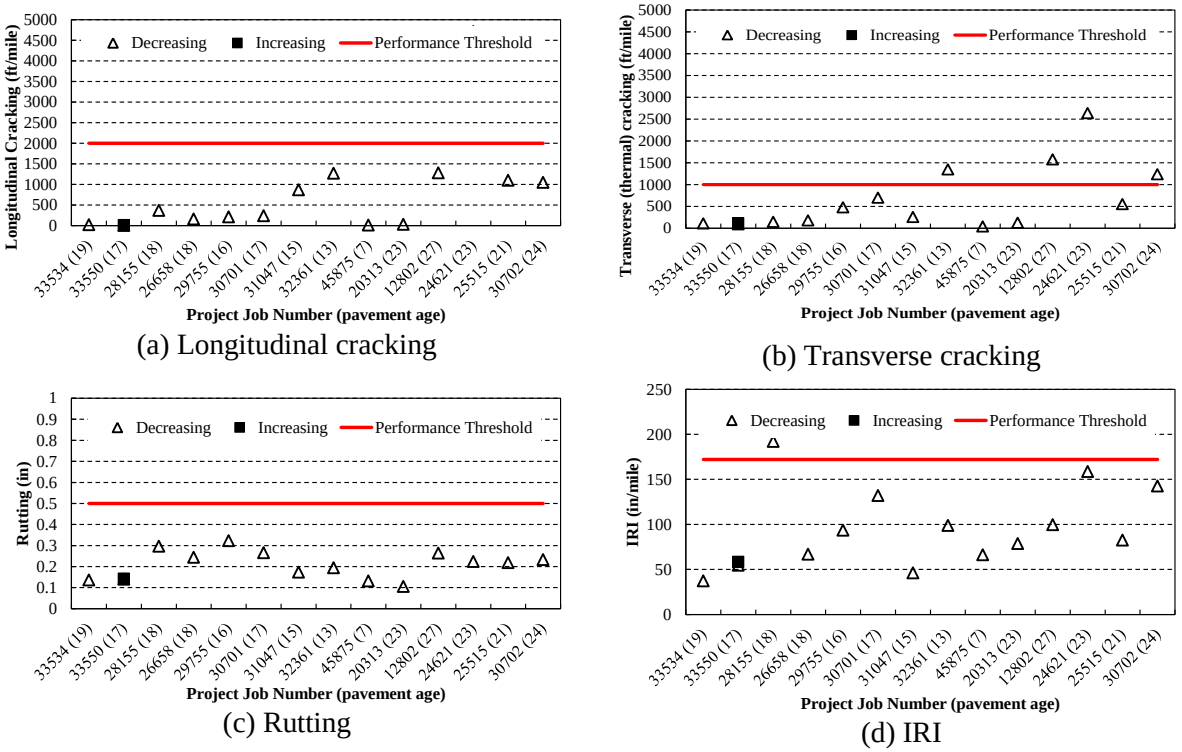

(a) Longitudinal cracking

(b) Transverse cracking

(c) Rutting

(d) IRI

Figure 5-11 Current pavement distress and conditions of the selected HMA over HMA projects

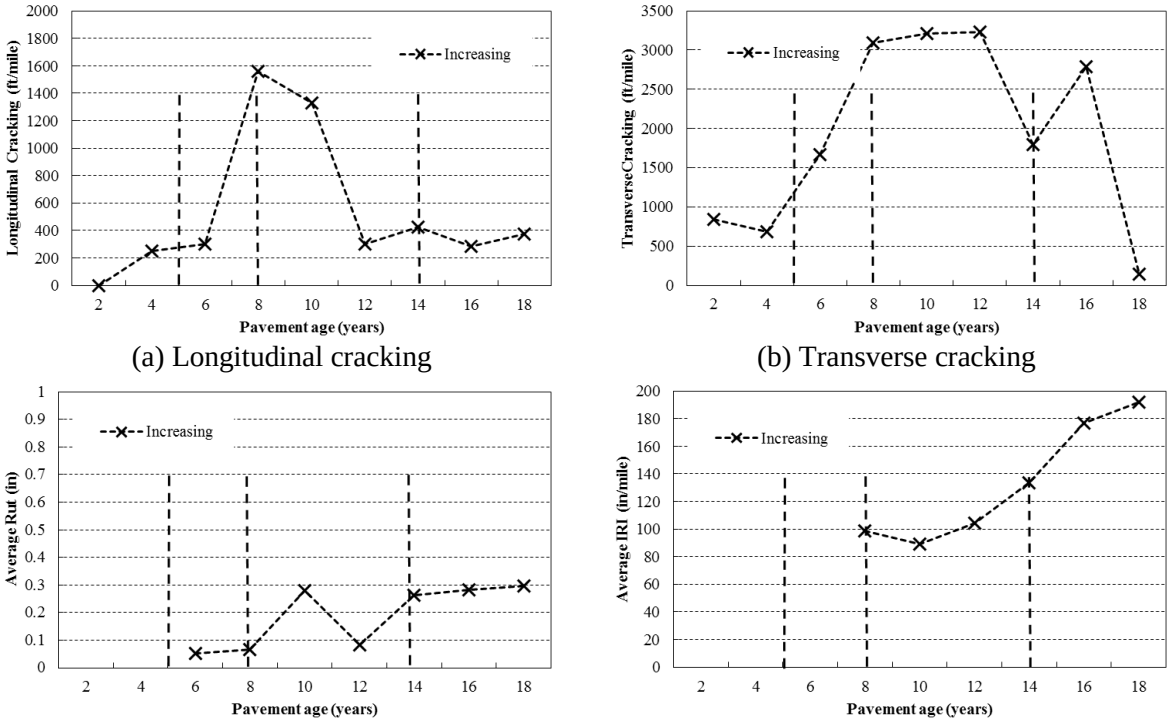

(a) Longitudinal cracking (b) Transverse cracking

(c) Rutting (d) IRI

Figure 5-12 Performance of HMA over HMA project 28155.

The time-series plots presented here show the results of the extraction process from the customized MDOT PMS and Sensor database. The magnitudes of the measured performance data are critical for comparing the measured and predicted performance. The next section discusses the process for identifying and collecting all the necessary input data to create the most representative pavement project in DARWin-ME.

5.4 PROJECT INPUTS FOR VERIFICATION

The next step of the validation process consists of identifying and documenting input variables for each selected project. The material, cross-section, climate, traffic, and existing pavement condition information are essential to create the most representative project to be analyzed in the DARWin-ME. The collection of required inputs needed extensive collaboration with the MDOT RAP to ensure the appropriateness of the selected values. The inputs for each project were obtained from MDOT historical records (project plans, material records), the previous MDOT studies (Report numbers: RC-1516, RC-1531, and RC-1537), and geographical location to select climate conditions.

5.4.1 Unbonded Overlays

The inputs for all unbonded overlay projects are summarized in Table 5-12. The inputs needed to represent the as-constructed designs are discussed below.

Cross-section information

The pavement cross-section information was collected from the project design drawings provided by MDOT. The cross-section for unbonded overlays consisted of thickness of overlay layer, asphalt interlayer, existing PCC, base and subbase. Some projects did not have all the necessary layer thicknesses; however, the missing pavement layer thicknesses were determined after consultation with the RAP, or a typical design values for the time period of project construction (new and existing) were recommended by MDOT.

Material related information

The material related information necessary for each pavement layer consisted of the following:

- Overlay PCC modulus of rupture (MOR)
- Asphalt interlayer binder type and volumetric properties
- Existing PCC elastic modulus
- Base/subbase material type and resilient modulus
- Subgrade soil type and resilient modulus

The overlay PCC modulus of rupture values were selected from the previous MDOT study, RC-1516 because the study included typical values agreed upon by MDOT. The asphalt interlayer binder type was determined from the mix design information extracted from the MDOT historical records for each project. The existing PCC elastic modulus value is the only way to characterize the condition of the underlying PCC pavement. The value of 3,000,000 psi was assumed because it is the upper limit suggested by the software as discussed in Chapter 3. The base/subbase type and modulus values were also obtained from a previous MDOT study (RC-1516) because the values were agreed upon by MDOT. The subgrade soil type and resilient moduli values were obtained from a previous MDOT study (RC-1531) which outlined the subgrade soil type and moduli values for the entire State of Michigan.

Climate information

The climate information for each project was determined by their geographical location. The DARWin-ME has a database for specific weather stations across the State of Michigan. The closest weather station to the actual project was selected. If none of the pre-loaded weather stations were located near the project, an interpolation was performed by selecting two or more weather stations in the vicinity of the project.

Traffic information

The traffic information is essential and one of the most important inputs to analyze pavements using the DARWin-ME. The annual average daily truck traffic (AADTT) was determined from as-constructed project design drawings and by collaboration with the RAP.

When such information was not available, current traffic values were obtained from the traffic maps specific to the project location which are available on MDOT's website (<http://www.michigan.gov/mdot/0,4616,7-151-9622_11033-22141--,00.html>). The AADTT values obtained from the website were back-casted to reflect the traffic at the time of construction using a growth rate of two percent.

5.4.2 Rubblized Overlays

The inputs for all rubblized overlay projects are summarized in Table 5-13. The inputs needed to represent the as-constructed projects as much as possible and are discussed below.

Cross-section information

The pavement cross-section information was collected from the project design drawings provided by MDOT. The cross-section for rubblized overlays consisted of thickness of the HMA overlay layer, existing fractured PCC layer, base and subbase. Some projects did not have all the necessary layer thicknesses; however, the missing pavement layer thicknesses were determined after consultation with the RAP, or typical design values for the time period of project construction (new and existing) were recommended by MDOT.

Material related information

The material related information necessary for each pavement layer consisted of the following:

- Asphalt overlay binder type, mixture gradation, effective binder content, and air voids
- Fractured PCC slab elastic modulus
- Base/subbase material type and resilient modulus
- Subgrade soil type and resilient modulus

The asphalt overlay layer properties were determined from the project job mix formula information extracted from the historical data provided by MDOT. The HMA volumetric properties were obtained from the job mix formula data sheets. The existing rubblized PCC elastic modulus is the only way to classify the existing condition of the rubblized layer. It was difficult to estimate this value; therefore, a value of 70,000 psi was assumed based on discussions with MDOT. The base/subbase and subgrade soil types and moduli values were obtained using the same procedure as for unbonded overlays.

Climate information

The climate information for each project was determined as discussed in the unbonded overlay section.

Traffic information

The traffic information for each project was determined similar to unbonded overlay section.

5.4.3 Composite Overlays

The inputs for all composite overlay projects are summarized in Table 5-14. The inputs that are needed to represent the as-constructed projects are discussed below.

Cross-section information

The pavement cross-section information was collected from the project design drawings provided by MDOT. The cross-section for composite overlays consisted of thickness for the overlay layer, existing intact PCC layer, base and subbase. Some projects did not have all the necessary layer thicknesses; however, the missing pavement layer thicknesses were determined after consultation with the RAP, or a typical design values for the time period of project construction (new and existing) were recommended by MDOT.

Material related information

The material related information necessary to characterize each layer consisted of the following:

- Asphalt overlay binder type, mixture gradation, effective binder content, and air voids
- Existing PCC MOR or elastic modulus
- Base/subbase material type and resilient modulus
- Subgrade soil type and resilient modulus

The asphalt overlay layer volumetric properties were determined from the project job mix formulas obtained from the historical project data provided by MDOT. The existing pavement is classified by the measured cracking, and how much of the measured cracking was fixed during pre-overlay repairs. The PCC MOR was used to characterize the strength of the existing layer similar to the unbonded overlay layer MOR. The base/subbase and subgrade soil types and moduli values were obtained using the same procedure as for unbonded overlays discussed previously.

Climate information

The climate information for each project was determined as discussed in the unbonded overlay section.

Traffic information

The traffic information for each project was determined in a similar method as discussed in the unbonded overlay section.

5.4.4 HMA over HMA

The inputs for all HMA over HMA projects are summarized in Table 5-15. The inputs needed to represent the as-constructed projects are discussed below.

Cross-section information

The pavement cross-section information was collected from the project design drawings provided by MDOT. The cross-section for HMA over HMA projects consisted of thickness for the overlay layer, existing HMA layer, base and subbase. Some projects did not have all the necessary layer thicknesses; however, the missing pavement layer thicknesses were determined after consultation with the RAP, or a typical design values recommended by MDOT were used.

Material related information

The material related information necessary to characterize each layer consisted of the following:

- Asphalt overlay binder type, mixture gradation, effective binder content, and air voids
- Existing HMA pavement binder type, mixture gradation, effective binder content, and air voids
- Base/subbase material type and resilient modulus
- Subgrade soil type and resilient modulus

The asphalt overlay layer properties were determined from the project historical data provided by MDOT. The HMA volumetric properties of the overlay were obtained from the job mix formula data sheets. The existing pavement was characterized by selecting the condition rating of each project consisting of poor, fair and good conditions. Since the existing condition is difficult to determine, the verification was performed for all three conditions ratings. The HMA mixture properties for the existing pavement were obtained from the job mix formula data sheets if available, otherwise, the values were assumed based on projects in a similar climate, or by selecting properties from the MDOT specifications. The specifications in effect during the time of original construction were used. The base/subbase and subgrade soil types and moduli values were obtained using the same procedure as for unbonded overlays discussed previously.

Climate information

The climate information for each project was determined as discussed in the unbonded overlay section.

Traffic information

The traffic information for each project was determined in a similar method as discussed in the unbonded overlay section.

Table 5-12 Unbonded overlay input data

Unbonded Overlay Projects								
Project Number	37997	34120	49029	45591	38209	43499	73873	50763
Year opened	1998	1999	1999	2000	2000	2001	2003	2004
Traffic								
Two way AADTT	4250	4279	5700	5595	2744	5004	1458	3185
ESALs (millions) (DARWin-ME)	19.14	25.44	36.73	36.06	14.4	29.75	7.43	14.34
Lanes in design direction	2	2	2	2	2	2	2	2
Climate	Kalamazoo	Ann Arbor	Kalamazoo	Battle Creek	Grand Rapids	Ann Arbor	Houghton Lake	Kalamzoo
Overlay Layer								
PCC Thickness (in)	7.1	7.9	7.1	7.1	6.3	7.1	6	6.5
PCC Modulus of Rupture (psi)	650	650	650	650	650	650	650	650
AC Interlayer								
AC Thickness (in)	1	1	1	1	1	1	1	1
AC PG or Penetration Grade	PG 58-28	PG 58-28	PG 58-28	PG 58-28	PG 58-28	PG 70-28	PG 64-28	PG 58-28
Existing PCC								
PCC Thickness (in)	9	9	9	9	9	9	9	9
PCC Elastic Modulus (ksi)	3000	3000	3000	3000	3000	3000	3000	3000
Base Layer								
Thickness (in)	3	3	4	4	4	3	4	4
Material type	Crushed Stone	Crushed Stone	Crushed Stone	Crushed Stone	Crushed Stone	Crushed Stone	Crushed Stone	Crushed Stone
Modulus (psi)	30000	30000	30000	30000	30000	30000	30000	30000
Subbase Layer								
Thickness (in)	11	14	10	10	10	14	10	10
Material type	A-3	A-3	A-3	A-3	A-3	A-3	A-3	A-3
Modulus (psi)	13500	13500	13500	13500	13500	13500	13500	13500
Subgrade								
Material type (by loc.)	SP1-A-3	SP2-A-3	SP1-A-3	SP1-A-3	A-4	SP2-A-3	SP2-A-3	SP1-A-3
Modulus (psi) (backcalc /design-Baladi project)	27739/ 7000	25113/ 6500	27739/ 7000	27739/ 7000	20314/ 5000	25113/ 6500	25113/ 6500	27739/ 7000

Note: Gray cells represent assumed values

Table 5-13 Rubblized overlay input data

Rubblized Projects											
Project Number	28115	26755	29768	29670	29581	28111	29729	45053	44109	38190	32388
Year opened	1989	1990	1992	1993	1994	1990	1995	1999	1999	2000	1997
Traffic											
Two way AADTT	490/340	1550	3390	856	3707	280	370	675	279	575	455
ESALs (millions) (DARWin-ME)	3.11	8.9	19.44	4.51	23.51	1.87	2.47	4.51	1.86	3.84	3.04
Lanes in design direction	2	2	2	2	2	1	1	1	1	1	1
Climate	Grand Rapids	Houghton Lake	Ann Arbor	Battle Creek	Lansing	Pellston	Flint	Reed City	Traverse City	Muskegon	Adrian
Overlay Layer											
HMA Thickness (in)	5	4.25	5.25	6.25	7.5	4	5 Edge, 7.2 Center Line	5.5	7.5	5.5	6 Center Line, 7 Edge
HMA binder type	Pen 120-150	Pen 120-150	Pen 85-100	Pen 85-100	Pen 85-100	Pen 200-300	Pen 120-150	PG 64-28 (T) PG 58-28(B+L)	PG 58-28	PG 58-28	Pen 85-100
Existing PCC (fractured)											
PCC Thickness (in)	9	8	9	9	9	9	9	9	8	9	8
PCC Fractured Elastic Modulus (psi)	70000	70000	70000	70000	70000	70000	70000	70000	70000	70000	70000
Base Layer											
Thickness (in)	3		4	3	4			3		4	
Material type	Crushed Stone		Crushed Stone	Crushed Stone	Crushed Stone			Crushed Stone		Crushed Stone	
Modulus (psi)	30000		30000	30000	30000			30000		30000	
Subbase Layer											
Thickness (in)	9		14	9	10		18	12	9	14	12
Material type	A-3		A-3	A-3	A-3		A-3	A-3	A-3	A-3	A-3
Modulus (psi)	13500		13500	13500	13500		13500	13500	13500	13500	13500
Subgrade											
Material type	A-4	SP2-A-3	SP2- A-3	SP1-A-3	CL - A-6	SP1-A-3	SM - A-4	SP1- A-3	SP1-A-3	SP1-A-3	CL-A-6
Modulus (psi) (backcalc/design -Baladi project)	20314/ 5000	25113/ 6500	25113/ 6500	27739/ 7000	17600/ 4400	27739/ 7000	24764/ 5200	27739/ 7000	27739/ 7000	27739/ 7000	17600/ 4400

Note: Gray cells represent assumed values

Table 5-14 Composite overlay input data

Composite Overlay Projects							
Project Number	25543	24252	29586	29716	33812	33924	45443
Year opened	1987	1988	1990	1992	1995	1996	2000
Traffic							
Two way AADTT	2250	6064	2882	672	1380	1000	512
ESALs (millions)	15.66	43.49	20.05	4.68	9.6	6.96	3.56
Lanes in design direction	2	2	2	2	2	2	2
Climate	Flint	Kalamazoo	Grand Rapids	Reed City	Detroit	Bay City	Bay City
Overlay Layer							
HMA Thickness (in)	4	4.5	3	3.75	3	4	3.5
HMA binder type	85-100	85-100	85-100	120-150	85-100	120-150	PG 64-28
HMA aggregate Gradation	Top course	Top course	Top course		Top course	Top course	Top course
Cumulative % Retained 3/4	0	0	0	0	0	0	0
Cumulative % Retained 3/8	11.4	12	11.6	13	38.3	14.4	15.5
Cumulative % Retained #4	31.7	31.9	36.2	40	56	51.5	23.3
% Passing 200	6.5	5.4	6.5	6	5.6	5.4	5.3
Existing PCC							
PCC Thickness (in)	9	9	9	9	9	8	8
PCC Compressive Strength (psi)	5000	5000	5000	5000	5000	5000	5000
Base Layer							
Thickness (in)	4	3	3		3	4	
Material type	Crushed Stone	Crushed Stone	Crushed Stone		Crushed Stone	Crushed Stone	
Modulus (psi)	30000	30000	30000		30000	30000	
Subbase Layer							
Thickness (in)	10	9	12		14	10	15
Material type	A-3	A-3	A-3		A-3	A-3	A-3
Modulus (psi)	13500	13500	13500		13500	13500	13500
Subgrade							
Material type	SM - A-4	SP1-A-3	A-4	SP1- A-3	SP1-A-3	SC - A-6	SC - A-6
Modulus (psi) (backcalc/design - Baladi project)	24764/ 5200	27739/ 7000	20314/ 5000	27739/ 7000	27739/ 7000	17600/ 4400	17600/ 4400

Note: Gray cells represent assumed values

Table 5-15 HMA over HMA input data

HMA over HMA Projects															
Project Number	33534	33550	28155	26658	29755	30701	31047	32361	45875	50715	20313	12802	24621	25515	30702
Year opened	1992	1992	1991	1992	1994	1994	1996	1997	2002	2005	1983	1984	1987	1989	1990
Traffic															
Two way AADTT	450	1564	185	130	185	408	260	3900 ADT	805	350	300	3800 ADT	238	315	365
ESALs (millions)	3.09	10.75	1.27	0.89	1.27	2.8	1.79	1.37	5.53	2.41	3.88	1.37	3.08	4.08	4.73
Lanes in design direction	2	2	2	1	1	1	1	1	1	1	1	1	1	1	1
Climate	Reed City	Kalamzaoo	Kalamazoo	Traverse City	Traverse City	Kalamazoo	Marquette/ Iron Mountain	Flint	South Bend	Jackson/ Battle Creek	Traverse City	Traverse City	Battle Creek	Cadillac/ Gaylord	South Bend
Overlay Layer															
HMA Thickness (in)	2.5	3	2.5	2.5	3	3	3	3	4	3.5	2.25	2.5	2.5	2.5	2.5
HMA binder type	120-150	85-100	120-150	120-150	120-150	85-100	120-150	120-150	PG 64-28	PG 64-28	120-150	120-150	120-150	120-150	85-100
HMA aggregate Gradation	3b	3c	1100T	1100T	1100T	3c	1100T	1100T	5E3	5E3	1100T	1100L	1100T	1100T	1500T
Mixture Air Voids (as const)	6	6.6	7	5	4.8	6.6	4.8	4.8	8	8	6	7	7	7	7
HMA Effective binder	9.4	10	12	12	12	10	12	12	12	12	12	11.2	11.2	11	11.2
Cumulative % Retained 3/4	0	0	0	0	0	0	0	0	0	0	0	0	0	0	0
Cumulative % Retained 3/8	28.6	36	36	18.6	18.6	36	18.6	18.6	2.5	2.5	15.4	15	14.2	10.2	11.2
Cumulative % Retained #4	50.2	45.6	45.6	40.4	40.4	45.6	40.4	40.4	32.8	32.8	32.9	36	36.4	38.4	32.2
% Passing 200	4.8	6.5	6.5	5.4	5.4	6.5	5.4	5.4	5.4	5.4	7.4	6.4	6.9	5.6	6
Existing HMA															
Existing HMA Thickness (in)	3.25	4.5	5.2	5	4-5.5	4.5	3	3.7	4.5	7.5	1.5	2.25 or 4.75	3.75	2.25	7.1
HMA binder type	85-100	85-100	120-150	120-150	120-150	85-100	120-150	120-150	PG 64-28	PG 64-28	120-150	120-150	120-150	120-150	85-100
HMA aggregate Gradation	3b	3c	1100L	1100L	1100L	3C	1100L		4E3	4E3		1100L			
Mixture Air Voids (as const)	7	7	7	7	7	7	7	7	7	7	7	7	7	7	7
HMA Effective binder	11.6	12	11	11.4	11	11	11	11	11	11	11	11	11	11	11
Cumulative % Retained 3/4	0	0	0	0	0	0	0	0	0	0	0	0	0	0	0
Cumulative % Retained 3/8	28.6	36	10.6	18.6	17.3	36	17.3	17.3	13.2	13.2	13.4	15	13.3	12	11.2
Cumulative % Retained #4	50.2	45.6	31.5	40.4	37.4	45.6	37.4	37.4	35.1	35.1	37	36	34.1	35.2	32.2
% Passing 200	4.8	6.5	5.4	5.4	5.7	6.5	5.7	5.7	4.6	4.6	5.8	6.4	8.5	5.6	6
Base Layer															
Thickness (in)	11	8	7	7	4/5 stabilized	7	10	7	11	6	5	7	8	10	5
Material type	Crushed Stone	Crushed Stone	Crushed Stone	Crushed Stone		Crushed Stone	Crushed Stone	Crushed Stone	Crushed Stone	Crushed Stone	Crushed Stone	Crushed Stone	Crushed Stone	Crushed Stone	Crushed Stone
Modulus (psi)	30000	30000	30000	30000		30000	30000	30000	30000	30000	30000	30000	30000	30000	30000
Subbase Layer															
Thickness (in)	25	28	12	12		15	18	13.7	15	8		0 or 12			
Material type	A-3	A-3	A-3	A-3		A-3	A-3	A-3	A-3	A-3		A-3			
Modulus (psi)	13500	13500	13500	13500		13500	13500	13500	13500	13500		13500			
Subgrade															
Material type	SP1- A3	SP1-A-3	SP1-A-3	SP1-A-3	SP1-A-3	SP1-A-3	SP-SM	SM - A-4	SP1-A-3	SP-SM	SP1-A-3	SP1-A-3	SP1- A-3	SP1-A-3	SP1-A-3
Modulus (psi) (backcalc/design - Baladi project)	27739/ 7000	27739/ 7000	27739/ 7000	27739/ 7000	27739/ 7000	27739/ 7000	20400/ 7000	24764/ 5200	27739/ 7000	20400/ 7000	27739/ 7000	27739/ 7000	27739/ 7000	27739/ 7000	27739/ 7000

Note:Gray cells represent assumed values

5.5 VERIFICATION RESULTS

The verification process entails the comparison between the measured and predicted pavement performance of each selected project using DARWin-ME. The results for unbonded, rubblized, composite, and HMA over HMA pavements are presented in this section. The results include an example of the time-series comparison between the predicted and the measured performance. In addition, the predicted distresses for all projects within each rehabilitation strategy were plotted against the measured distresses. These plots give a clear indication if the software over or under predicts the measured performance. Finally, the comparison of the predicted with the measured distresses highlights the need for local calibration of the DARWin-ME performance prediction models. In addition, conclusions can be made regarding the accuracy of the rehabilitations models for use in design.

5.5.1 Unbonded Overlays

The verification results for unbonded overlay projects are summarized in this section. Figure 5-13 shows an example of the time-series distresses for the project JN34120. The predicted performance values are superimposed on the measured distresses. For all the projects, limited distress magnitudes were observed. None of the projects were close to the performance threshold value. It should be noted, that for projects with multiple directions, only one DARWin-ME project file was created because for this study, it was assumed that the as constructed input values were the same for both directions. The time-series results from both directions are compared to the DARWin-ME predicted distresses. The time-series comparison between predicted and measured performance for all unbonded overlay projects are included in Appendix C.

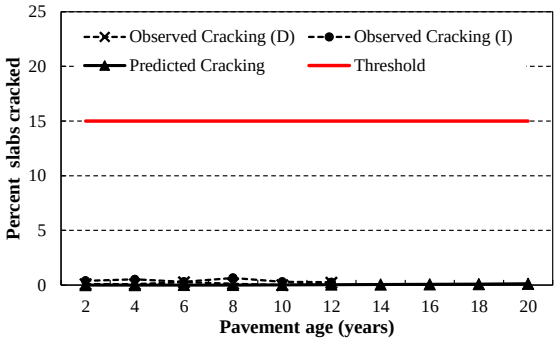

(a) Transverse cracking

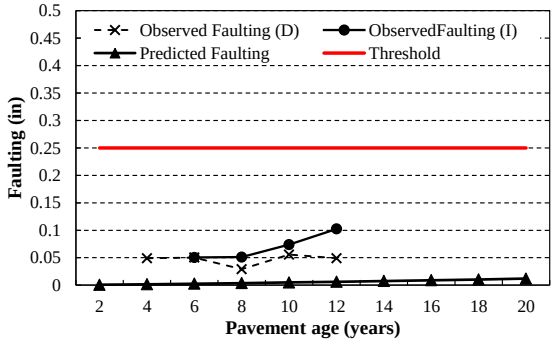

(b) Faulting

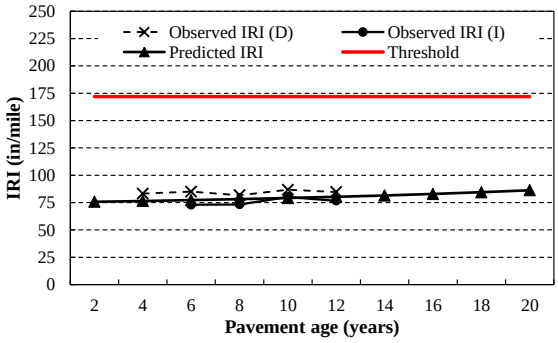

(c) IRI

Figure 5-13 Example of time-series verification results for an unbonded overlay project based on different distresses

Figure 5-14(a) shows that DARWin-ME under predicts the measured cracking for the unbonded overlay projects. The faulting model also under predicts the measured faulting as shown in Figure 5-14(b). The measured and predicted faulting values are minimal and do not reach the threshold limit. It is expected that minimal faulting should be predicted in DARWin-ME because dowels (1.25 inch in diameter) were included in the design for load transfer at the joint. The IRI predicted values (Figure 5-14c) are closer to the measured performance. Based on these results, calibration of all the performance models for unbonded overlay is necessary to improve the accuracy of DARWin-ME for the Michigan conditions.

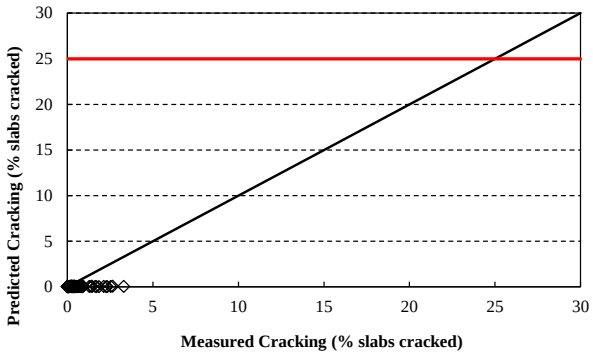

(a) Transverse cracking

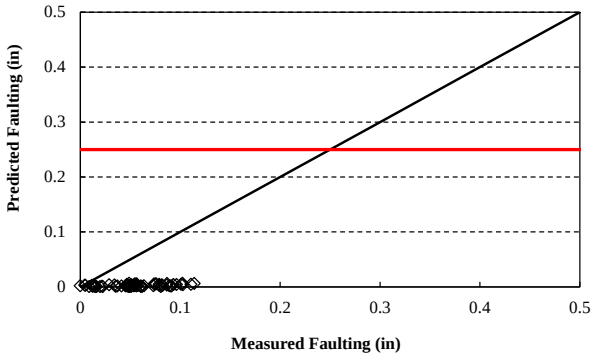

(b) Faulting

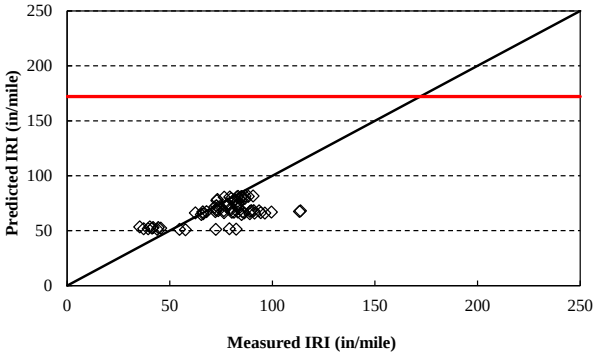

(c) IRI

Figure 5-14 Predicted vs. measured results for all unbonded overlay projects.

5.5.2 Rubblized Overlays

The verification results for rubblized overlay projects are summarized in this section. The verification was performed using two different subgrade moduli (see the back-calculated and design MR values in Table 2-9 which are from MDOT Report Number RC-1531). The back-calculated values were not determined in this study. The subgrade modulus has significant effect on rutting performance. Figure 5-15 shows an example of the time-series comparison between predicted and measured performance for the project JN44109. Figure 5-16 summarizes the predicted vs. measured performance for all rubblized projects using the back-calculated subgrade moduli. Figure 5-17 illustrates the same results with the adjusted recommended design subgrade modulus values. The time-series comparison between predicted and measured performance for all rubblized overlay projects are included in Appendix C

The results in Figure 5-16 and Figure 5-17 illustrate that the predictions are not close to the line of equality. It can be concluded that the design software under-predicts longitudinal cracking for most of the pavement sections. The thermal transverse cracking model under-predicts the measured performance. The minimal amount of thermal transverse cracking predicted by the software could be due to appropriate binder selection for a specific climate. However, this is not observed in the field as each selected project has significant amounts of measured transverse cracking. It should be noted that several of the selected projects were constructed prior to Superpave binder specification were adopted for design. Thus, climatic considerations were not taken into account during binder selection. It is observed that the software over predicts the measured distresses for both rutting and IRI. The design value subgrade MR over predicted rutting more than the backcalculated MR. Therefore, calibration of all the performance models is necessary to improve the accuracy of DARWin-ME for the Michigan conditions. Based on the results, it is also recommended to use backcalculation to determine the subgrade soil condition.

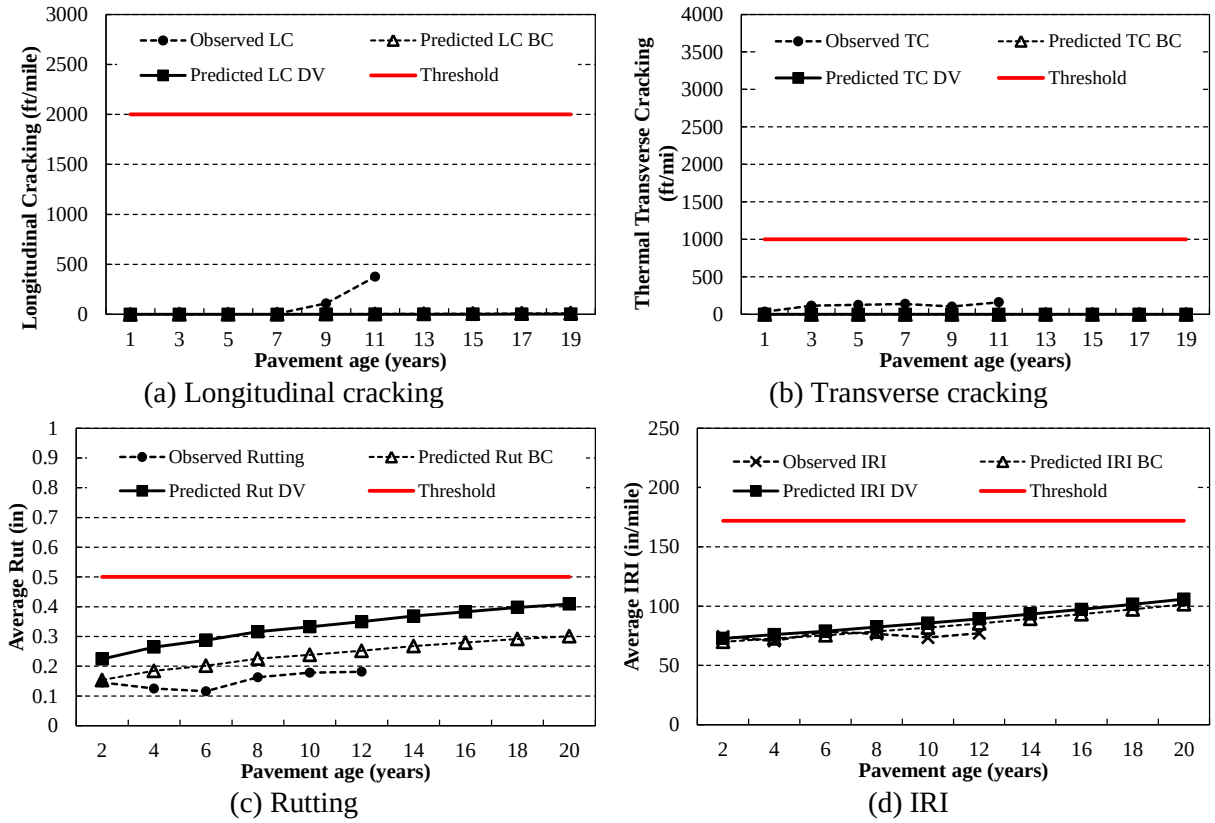

(a) Longitudinal cracking (b) Transverse cracking

(c) Rutting (d) IRI

Figure 5-15 Example of time-series verification results for a rubblized overlay project based on different distresses

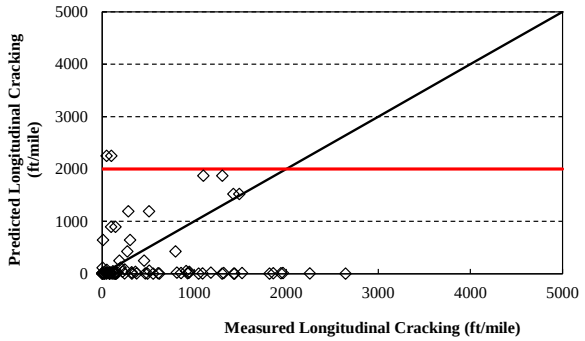

(a) Longitudinal cracking

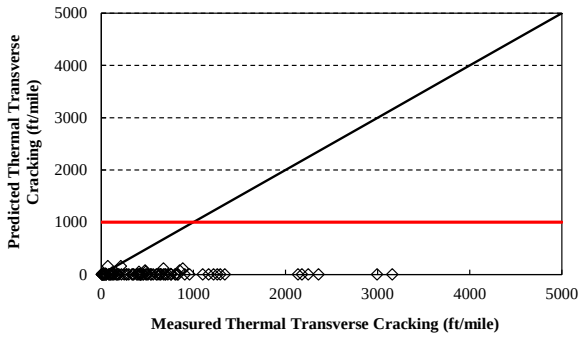

(b) Thermal transverse cracking

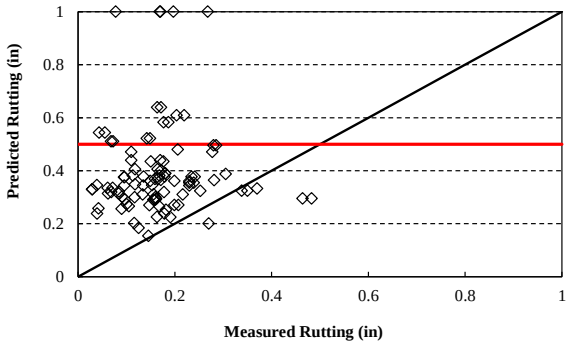

(c) Rutting

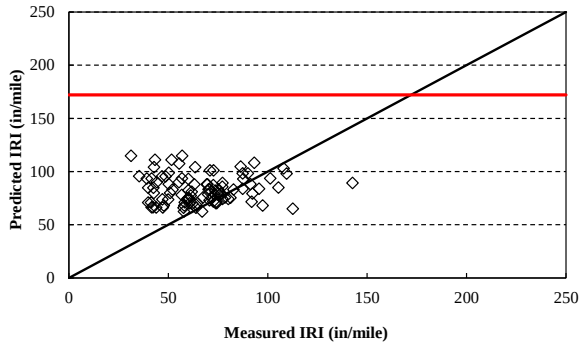

(d) IRI

Figure 5-16 Predicted vs. measured results for rubblized overlay projects using backcalculated subgrade MR

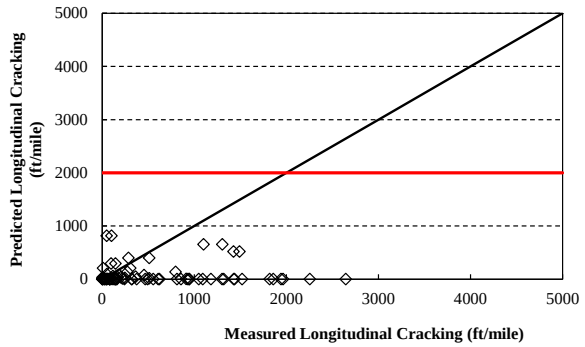

(a) Longitudinal cracking

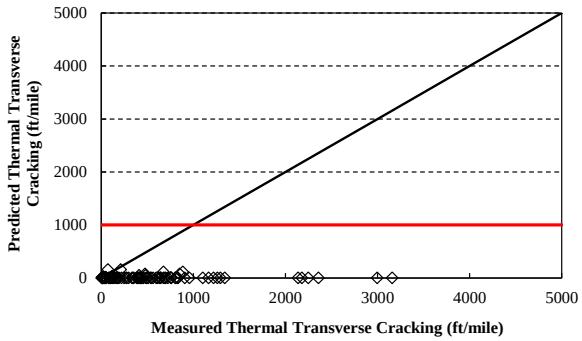

(b) Thermal transverse cracking

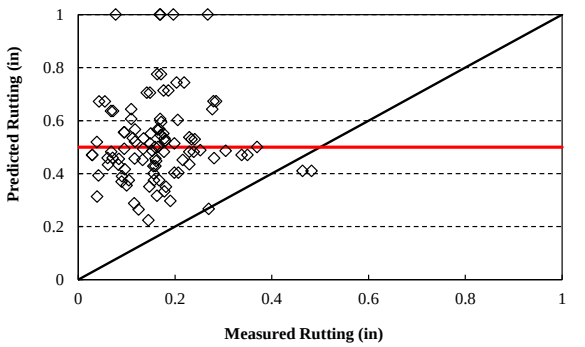

(c) Rutting

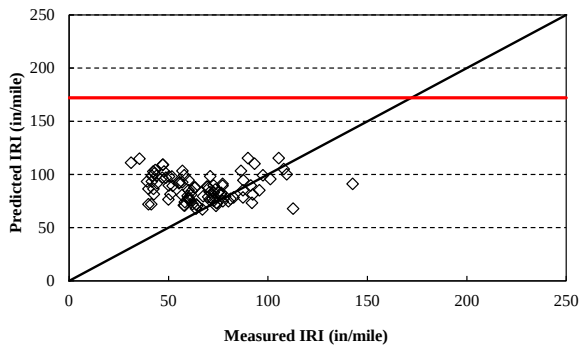

(d) IRI

Figure 5-17 Predicted vs. measured results for rubblized overlay projects using design MR

5.5.3 Composite Overlays

The verification results for composite overlay projects are summarized in this section. Figure 5-18 shows an example of the time-series distresses for the project JN45443. The predicted time series distress values are superimposed on the measured values. Figure 5-19 summarizes the predicted vs. measured performance to determine how well the predictions match measured distress for all selected projects. The time-series comparison between predicted and measured performance for all composite overlay projects are included in Appendix C.

The results in Figure 5-19 illustrate that the predicted performance is not close to the line of equality. It is observed that a bias exists between the predicted and measured performance for both rutting and IRI. The software under-predicts longitudinal cracking. The thermal transverse cracking values were not included for composite pavements because the software predicted values that were identical for all projects. Therefore, calibration of all the models is necessary to improve the accuracy of DARWin-ME for the Michigan conditions.

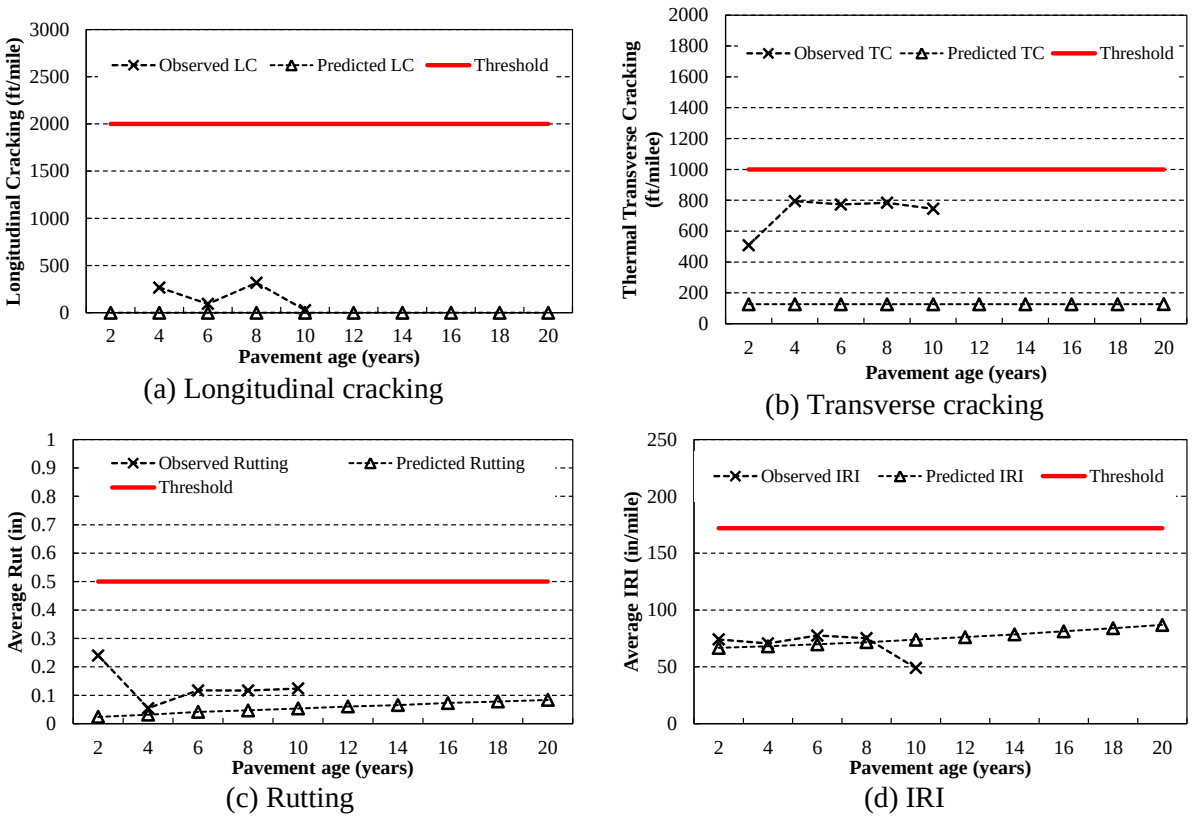

(a) Longitudinal cracking

(b) Transverse cracking

(c) Rutting

(d) IRI

Figure 5-18 Example of time-series verification results for a composite overlay project based on different distresses

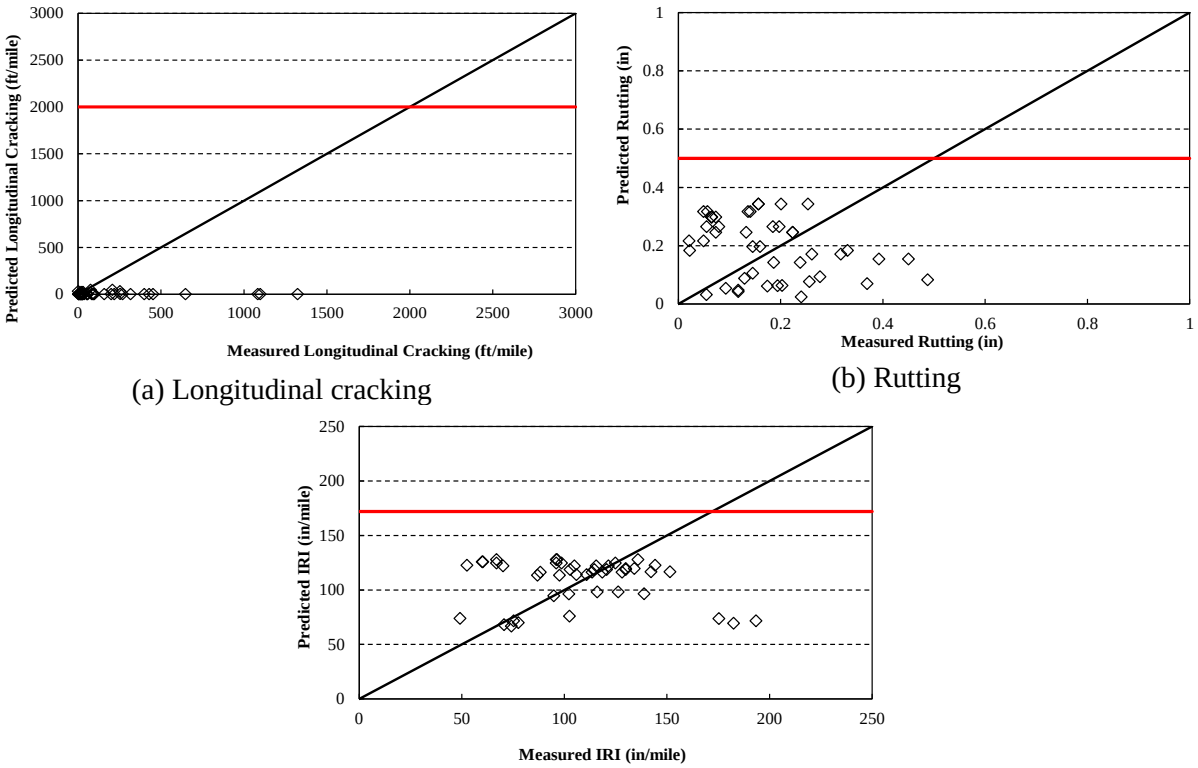

(a) Longitudinal cracking

(b) Rutting

(c) IRI

Figure 5-19 Predicted vs. measured results for all composite overlay projects

5.5.4 HMA over HMA

The verification results for HMA over HMA projects are summarized in this section. As an example, Figure 5-20 shows the measured and predicted distress for the project JN33543. It can be seen that even though a maintenance fix was performed after the 13th year, the propagation of distress is fairly reasonable from year eleven to thirteen for longitudinal cracking. The thermal transverse cracking model under predicts measured thermal transverse cracking. The rutting model over predicts measured rutting. On the other hand, the IRI model predictions are reasonable. Figure 5-21 summarizes the predicted vs. measured performance for all HMA over HMA projects with a poor existing pavement condition rating. Figures5-22 and 5-23 show the results for fair and good existing pavement condition ratings. The DARWin-ME software allows the user to select the condition of the existing HMA pavement layer. Since, the existing HMA pavement condition of the pavement was not known with certainty, the verification of the HMA over HMA performance models was performed using poor, fair, and good conditions. The results in Figure 5-21 also illustrate that the predicted performance is not close to the line of equality. It can be observed that bias exists between the predicted and measured performance for both longitudinal, thermal transverse cracking, rutting and IRI. Therefore, calibration of all the models is necessary to improve the accuracy of DARWin-ME for the Michigan conditions.

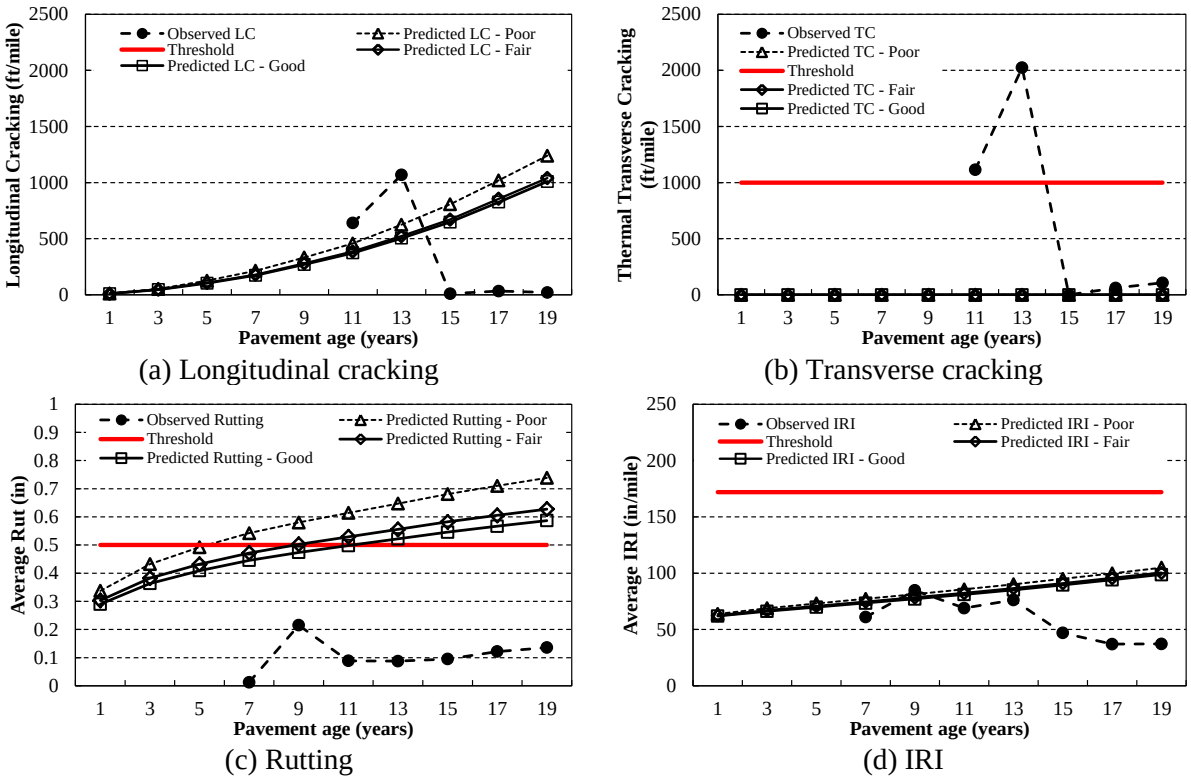

(a) Longitudinal cracking (b) Transverse cracking

(c) Rutting (d) IRI

Figure 5-20 Example of time-series verification results for a HMA over HMA project

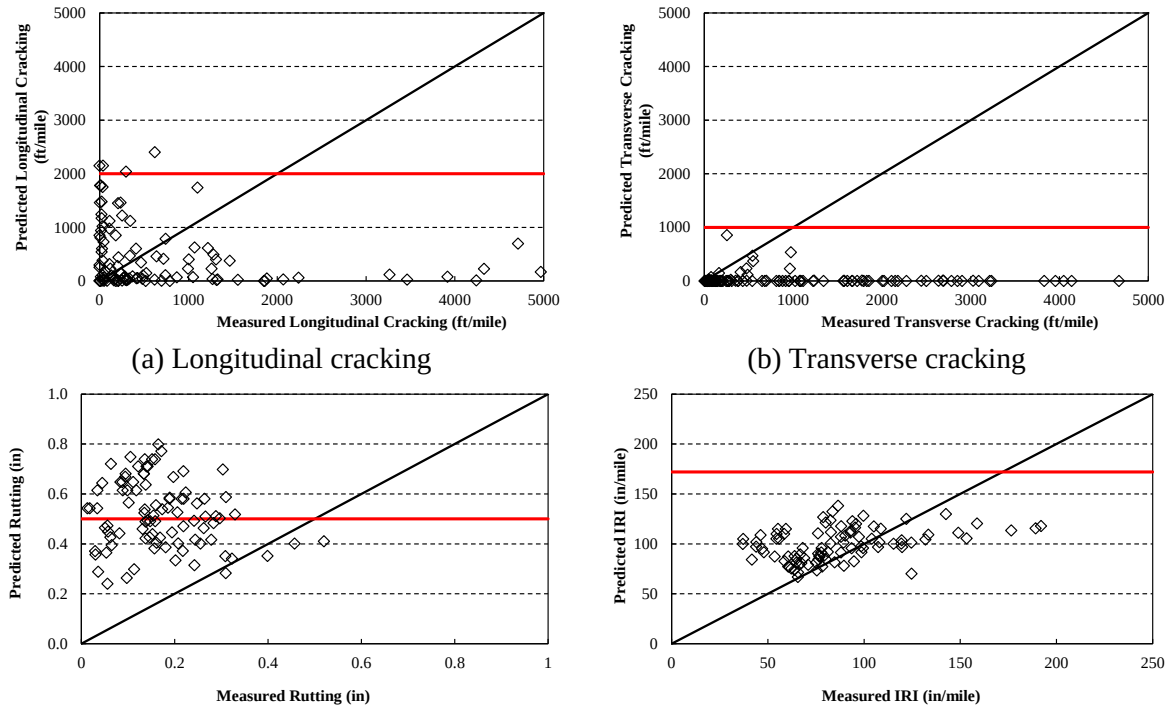

(a) Longitudinal cracking (b) Transverse cracking

(c) Rutting (d) IRI

Figure 5-21 Predicted vs. Measured performance for HMA over HMA with poor existing condition.

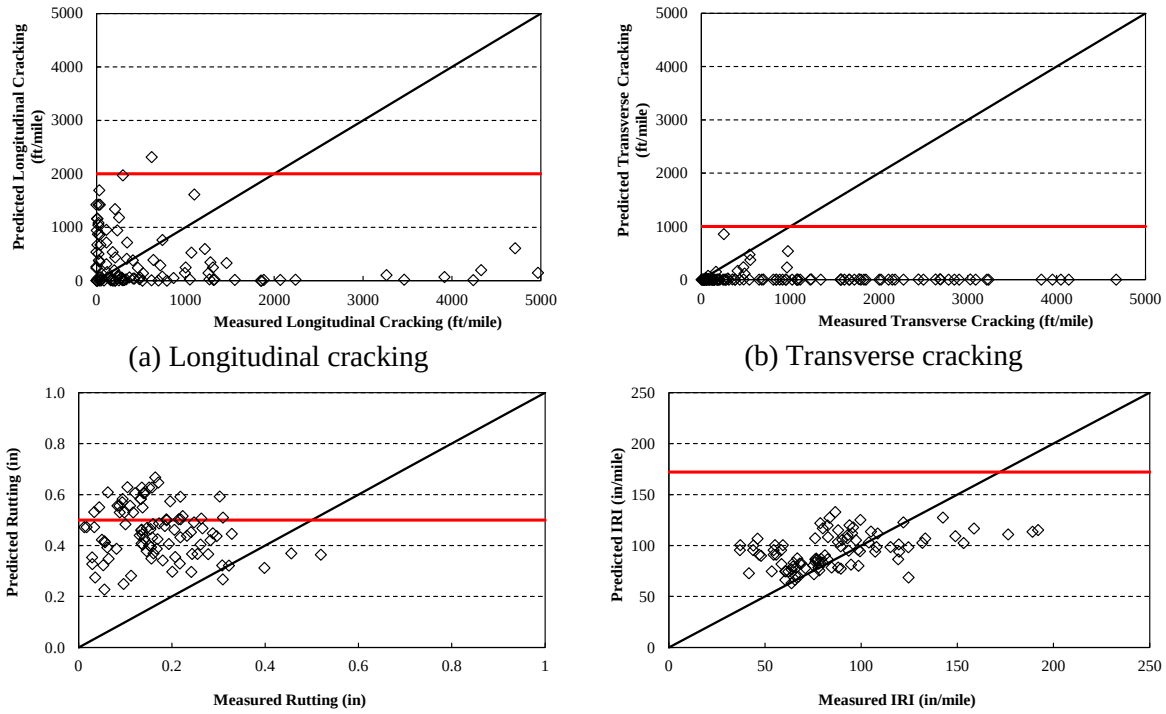

(a) Longitudinal cracking (b) Transverse cracking

(c) Rutting (d) IRI

Figure 22 Predicted vs. Measured performance for HMA over HMA with fair existing condition.

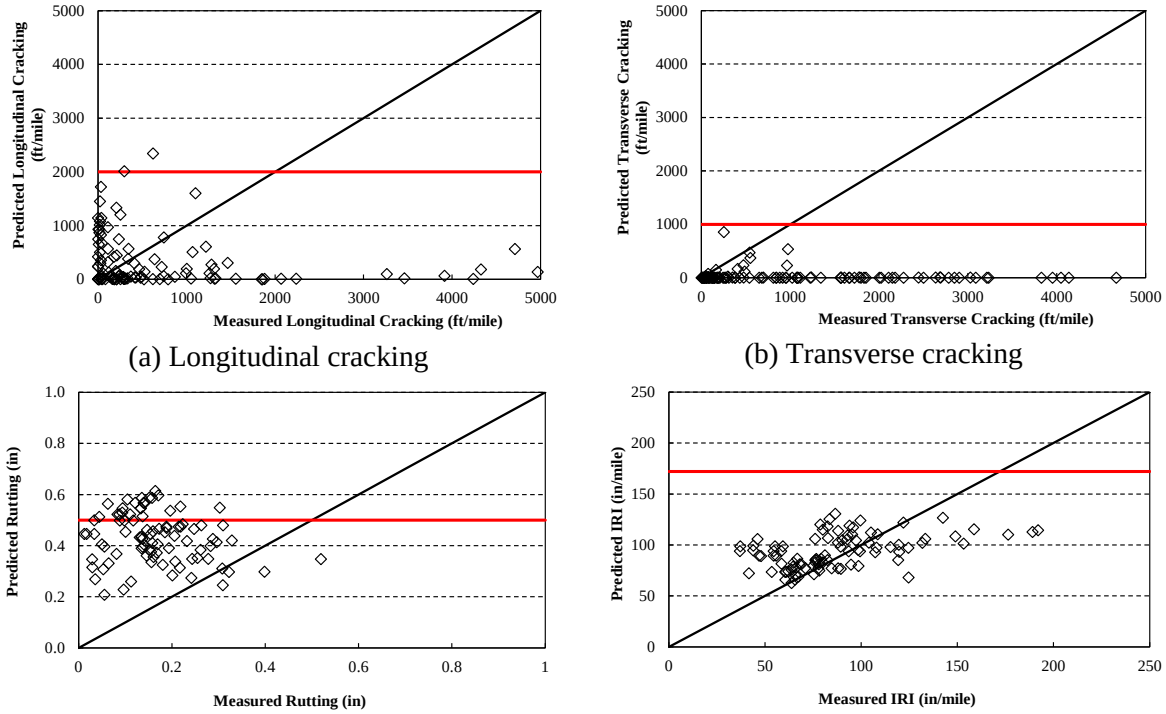

(a) Longitudinal cracking (b) Transverse cracking

(c) Rutting (d) IRI

Figure 23 Predicted vs. Measured performance for HMA over HMA with good existing condition.

5.6 SUMMARY

Verification of the M-E PDG/DARWin-ME performance models are necessary to determine how well the models predict measured pavement performance for Michigan conditions. In this chapter, the following sequential steps for the verification process were presented:

1. Identify projects in different regions in the State based on local pavement design and construction practices.
2. Extract the measured pavement performance data for each project from the MDOT Pavement Management System (PMS) and Sensor database.
3. Obtain all input data related to pavement materials, cross-section, traffic and climatic conditions for the identified projects.
4. Compare the measured and predicted performances for each project to identify the local calibration needs.

The verification of the performance prediction models based on the selected projects for different rehabilitation options show the need for local calibration. This calibration will be executed in Task 3 of the project. It should be noted that work accomplished in this task will facilitate the calibration process due to the following reasons:

- All of the identified projects can be used in the local calibration.
- The custom PMS and sensor databases developed in this task can be used to further identify additional road segments based on distress magnitudes instead of construction records for local calibration (if needed).

CHAPTER 6 - CONCLUSIONS AND RECOMMENDATIONS

6.1 SUMMARY

The main objectives of Part 2 of the project were to determine the impact of various input variables on the predicted pavement performance for the selected rehabilitation design alternatives in the MEPDG/DARWin-ME, and to verify the pavement performance models for MDOT rehabilitation design practice. Therefore, the significant inputs related to material characterization, existing pavement condition, and structural design for the selected rehabilitation options were identified. Subsequently, the accuracy of the rehabilitation performance models was evaluated by comparing measured and predicted performance.

The overarching findings from the sensitivity analyses performed in Part 2 for different rehabilitation options in the MEPDG/DARWin-ME of the study are:

- *HMA over HMA*: the overlay thickness and HMA volumetrics are the most significant inputs for the overlay layer while the existing HMA thickness and pavement condition rating have a significant effect on the predicted pavement performance among the inputs related to the existing pavement structure.
- *Composite pavements*: the overlay thickness and HMA air voids are significant inputs for the overlay layer. In addition, among the inputs related to the existing intact PCC pavement, the existing PCC thickness has a significant effect on the predicted pavement performance.
- *Rubblized pavements*: the HMA thickness, air voids and effective binder content are the most significant inputs for the overlay layer. While none of the inputs related to the existing PCC layer have shown a significant impact on the predicted performance, the results show that the existing PCC layer modulus is important for alligator cracking and IRI.
- *Unbonded overlays*: all overlay (i.e. the new layer) related inputs significantly impact the predicted cracking performance while the modulus of subgrade reaction (*k*-value) is the most important among inputs related to existing layers.

The interaction between overlay air voids and existing pavement thickness significantly impacts all performance measures among HMA rehabilitation options. The interaction between overlay thickness and existing PCC layer modulus has the most significant effect on unbonded overlay predicted performance. It should be noted that all analyses were conducted using input ranges reflecting Michigan practices.

The verification of the performance prediction models based on the selected projects for different rehabilitation options show the need for local calibration. All of the identified projects used for verification will be utilized in Task 3 for local calibration. Based on the results of the analyses, various conclusions and recommendations were made and are presented in the next sections.

6.2 CONCLUSIONS

Based on the results of the analyses performed in Part 2 tasks, various conclusions were drawn. These conclusions can be divided into the following three broad topics:

- Issues related to the MEPDG/DARWin-ME software
- Identification of significant inputs based on sensitivity analyses
- Verification of the MEPDG/DARWin-ME rehabilitation performance models

6.2.1 The MEPDG/DARWin-ME Software Issues

Several issues were encountered while running the MEPDG/DARWin-ME software. These concerns were related to certain structural and material properties. In addition, reasonableness of certain inputs was investigated whenever unusual results were encountered during the analyses. These concerns include:

1. The software internally limits the existing PCC elastic modulus because higher values produce counter intuitive results. Therefore, the recommended value of 3,000,000 psi should be considered as the upper bound limit for elastic modulus.
2. The software reduces the subgrade resilient modulus (MR) value by a fixed factor depending on the soil type; fine or coarse. If the design MR is used as a direct input in the MEPDG/DARWin-ME, the MR values will be reduced internally to reflect laboratory determined MR (for levels 2 and 3). It should be noted that in the DARWin-ME the reduction factor can be specified by the user for level 1 while the software uses an internal reduction factor for unbound layers when using levels 2 & 3.
3. In the MEPDG/DARWin-ME the HMA interlayer modulus and thickness have insignificant impact on the equivalent thickness, especially within the practical range of 1 to 3 inches for interlayer thickness. This implies that the interlayer thickness and stiffness have no significant impact on the predicted performance.

6.2.2 Sensitivity Analyses

The main objective in this task was to evaluate the impact of the inputs specific to various rehabilitation options on the predicted performance. To accomplish this goal, the following types of sensitivity analyses were performed:

1. Preliminary sensitivity
2. Detailed sensitivity
3. Global sensitivity
4. Satellite studies

Each sensitivity analysis has a unique contribution to the overall understanding in determining the impact of design inputs on the predicted pavement performance. The outcome of the preliminary sensitivity resulted in the identification of significant inputs related to the existing pavement layers. Subsequently, these inputs were combined with the

significant inputs for the new pavement layer (overlay) to conduct the detailed sensitivity. The outcome from the detailed sensitivity analyses include the significant main and interactive effects (ANOVA) between the inputs related to the existing and overlay layers. It should be noted that the statistical and practical significant interactive effects were only investigated for the inputs related to the existing layer, overlay layer and a combination of existing and overlay layers.

Finally, the global sensitivity analysis was performed based on the results from the detailed sensitivity analysis. The global sensitivity analysis (GSA) is more robust because of the following reasons:

a. Main and interaction results are based on the entire domain of each input variable.
b. The importance of each input can be quantified using normalized sensitivity index (NSI).
c. Relative importance of each design input can be determined.

In this report, the term "sensitive" implies changes in the output (predicted performance) with respect to change in the input values. On the other hand, the term "significant" implies changes in the design input values that result in substantial changes in the predicted performance.

6.2.2.1 Preliminary sensitivity

Table 6-1summarizes the significant inputs from preliminary sensitivity analyses for the selected rehabilitation options. These inputs only characterize the existing pavement. The results show that existing surface layer thickness and existing pavement structural capacity are the most important inputs for all rehabilitation options.

Table 6-1 List of significant inputs from preliminary sensitivity analysis

Rehabilitation option	Significant inputs
HMA over HMA	• Existing HMA condition rating • Existing HMA thickness
HMA over JPCP (Composite)	• Existing PCC thickness • Existing PCC flexural strength
JPCP over JPCP (Unbonded overlay)	• Existing PCC thickness
CRCP over HMA	• Existing HMA thickness
CRCP over JPCP	• Existing PCC thickness • Existing PCC strength • Subgrade k-value

6.2.2.2 Detailed sensitivity

The detailed sensitivity analyses included the significant variables identified in preliminary analyses in addition to the significant inputs previously identified for new pavement layers.

Full factorials were designed to determine statistically significant main and two-way interaction effects. The results of the sensitivity analyses show that the existing pavement condition rating and existing thickness for HMA over HMA is critical for all performance measures. On the other hand, existing PCC modulus and thickness are important in determining the performance of HMA overlay over intact and rubblized PCC. For a given condition of the existing pavement, HMA overlay volumetric properties, binder type and amount, and thickness play a significant role. In addition, HMA volumetrics, binder type and amount, and thickness should be carefully selected for the overlays to mitigate various distresses whether the existing pavement is intact or rubblized concrete.

For unbonded overlays, the results of the sensitivity analyses show that the existing pavement condition (in terms of *E*) is critical for predicting cracking performance. Higher MOR (within reason) and thickness of overlay will limit the cracking. However, if the existing foundation is weak, a better strategy to reduce the unbonded overlay cracking would be to either increase PCC MOR or thickness, and use concrete with lower CTE. Table 6-2 presents the summary of significant input variable based on the detailed sensitivity analysis.

Table 6-2 List of significant inputs from detailed sensitivity analysis

Rehabilitation option	Significant inputs
HMA over HMA	• Existing HMA condition rating • Existing HMA thickness • Granular base and subgrade modulus • Overlay air voids • Overlay effective binder • Overlay binder PG • Overlay thickness
HMA over JPCP (Composite)	• Existing PCC thickness • Existing PCC flexural strength • Climate • Overlay air voids • Overlay binder PG • Overlay thickness
HMA over JPCP fractured (Rubblized)	• Existing PCC thickness • Existing PCC elastic modulus • Overlay air voids • Overlay effective binder • Overlay binder PG • Overlay thickness
JPCP over JPCP (Unbonded overlay)	• Existing PCC thickness • Existing PCC elastic modulus • Existing modulus of subgrade reaction • Overlay MOR • Overlay thickness • Overlay CTE • Overlay joint spacing

6.2.2.3 Global sensitivity analysis

Four rehabilitation options were considered in global sensitivity analysis (GSA) similar to the preliminary and the detailed sensitivity analyses. First, the relative contributions of the design inputs for various performance measures were identified and discussed. Second, the main effect of design inputs for a base case was investigated. Finally the interactive effect of the design inputs was studied for all performance measures within each rehabilitation option.

The results are summarized based on the main effects determined through the maximum NSI values. The input variables are ranked based on their relative impact on different performance measures. The following are the findings based on the main effects of input variables:

HMA over HMA

- In general, the overlay thickness and HMA volumetrics (air voids and effective binder contents) are the most significant inputs affecting the predicted performance for the overlay layer
- The existing pavement thickness and condition rating have significant effect among the existing pavement related inputs. Table 6-3 shows the list of significant inputs along with the ranking and NSI values.

Table 6-3 List of significant inputs — HMA over HMA

Input variables	Ranking (NSI)
Overlay air voids	1 (6)
Existing thickness	2 (5)
Overlay thickness	3 (4)
Existing pavement condition rating	4 (4)
Overlay effective binder	5 (2)
Subgrade modulus	6 (2)
Subbase modulus	7 (1)

Composite pavement

- The overlay thickness and HMA air voids are the most significant inputs for the overlay layer
- The existing pavement thickness and existing PCC layer modulus have significant effect on predicted performance among the existing pavement related inputs. Table 6-4 shows the list of significant inputs along with the ranking and NSI values.

Table 6-4 List of significant inputs — Composite pavement

Inputs	Ranking (NSI)
Overlay air voids	1 (9)
Overlay thickness	2 (2)
Existing PCC thickness	3 (1)

Rubblized pavement

- The HMA air voids and effective binder content are the most significant inputs for the overlay layer

- For longitudinal cracking and IRI, existing PCC thickness is more important as compared to the existing PCC layer modulus. However, existing PCC layer modulus is more significant for alligator cracking and rutting. Table 6-5 shows the list of significant inputs along with the ranking and NSI values.

Table 6-5 List of significant inputs — Rubblized PCC pavement

Inputs	Ranking (NSI)
Overlay air voids	1 (6)
Overlay effective binder	2 (2)
Overlay thickness	3 (1)

Unbonded overlay

- All overlay related inputs (see Table 6-6) significantly impact the cracking performance
- The existing PCC elastic modulus is the most important input among all inputs related to existing layers. Table 6-6 shows the list of significant inputs along with the ranking and NSI values.

Table 6-6 List of significant inputs — Unbonded PCC overlay

Design inputs	Ranking (NSI)
Overlay PCC thickness (inch)	1 (23)
Overlay PCC CTE (per °F x 10-6)	2 (12)
Overlay PCC MOR (psi)	3 (8)
Overlay joint spacing (ft)	4 (5)
Existing PCC elastic modulus (psi)	6 (1)
Climate	7 (1)

The following are the findings based on the interactive effects of input variables for the selected rehabilitation option:

- The interaction between overlay air voids and existing pavement thickness significantly impacts all performance measures among HMA rehabilitation options. A higher air void in the overlay layers on a thin existing layer thickness seems to be the worst combination for cracking.
- The interaction between overlay thickness and existing PCC layer modulus have the most significant effect on unbonded overlay performance. A thicker overlay may hide the impact of weak existing PCC layer on predicted performance.

All the interactions studied (see Tables 6-7 to 6-10) here are practically and statistically significant. Therefore all of them should be considered in the design and analysis.

Table 6-7 Significant interaction between inputs — HMA over HMA

Interaction	Ranking (NSI)
Overlay air voids and existing thickness	1 (15)
Overlay thickness and existing thickness	2 (10)
Overlay effective binder and existing thickness	3 (7)

Table 6-8 Significant interaction between inputs — Composite pavement

Interaction	Ranking (NSI)
Overlay air voids and existing thickness	1 (44)
Overlay thickness and existing thickness	2 (25)

Table 6-9 Significant interaction between inputs — Rubblized pavement

Interaction	Ranking (NSI)
Overlay air voids and existing thickness	1 (4)
Overlay effective binder and existing thickness	2 (2)
Overlay thickness and existing thickness	3 (1)

Table 6-10 Significant interaction between inputs — Unbonded PCC overlay

Interaction	Ranking (NSI)
Overlay thickness and existing modulus	1 (28)
Overlay MOR and existing modulus	2 (14)
Overlay MOR and existing thickness	3 (6)

6.2.2.4 Satellite studies

Several additional clarification studies were performed to evaluate the sensitivity of input variables in the MEPDG/DARWin-ME. The following are the main findings from the satellite studies:

- HMA base course gradation has a slight effect on the predicted bottom-up alligator cracking while HMA top and leveling course gradations do not significantly impact the predicted performance. Therefore, the average gradation from the specification limits can be used for pavement design.
- The effect of binder rheology (*G** master curve) is important for rutting prediction. Therefore, it is recommended that G* master curve (level 1) should be used if available, especially if rutting is a dominant distress. The variations in *G** master curve could be attributed to different binder sources for the same PG. However, it is anticipated that if a binder from the same source is utilized for mix design at a specific location, the level 1 *G** master curve should not vary significantly. Therefore, an average can be used for multiple *G** master curves. Part 1 of this study addressed this issue in more detail.
- The unbound layer gradations do not have a significant impact on the predicted performance. Based on these results it is recommended that for same material type and climate used in this study, the base and subbase aggregate gradations can be selected within the limits of the specifications.

6.2.3 Verification of the Rehabilitation Performance Models

Verification of the MEPDG/DARWin-ME performance models is necessary to determine how well the models predict the measured pavement performance for Michigan conditions. Results of the verification process support the following conclusions:

- For the unbonded overlay, the MEPDG/DARWin-ME software under-predicts the measured cracking and faulting. The IRI predicted values were closer to the measured performance; however, bias still exists.
- For rubblized pavements, the software under-predicts longitudinal and transverse cracking for most of the pavement sections while it over-predicts the measured distresses for rutting and IRI.
- For composite pavements, the one-to-one plot between the predicted and measured performance for rutting and IRI showed higher variability (i.e., more error). Also, the software under-predicted the longitudinal cracking.
- For HMA over HMA bias exists between the predicted and measured performance for rutting and IRI i.e., the software over predicts the measured performance. While longitudinal cracking showed larger error, thermal transverse cracking was under-predicted.

The validation of the performance prediction models based on the selected projects for different rehabilitation options show the need for local calibration. This calibration will be executed in Part 3 of the research study. It should be noted that work accomplished in this task will facilitate the calibration process due to the following reasons:

- All of the identified projects can be used in the local calibration.
- The custom PMS and sensor databases developed in this task can be used to further identify additional road segments based on distress magnitudes instead of construction records for local calibration (if needed).

6.3 RECOMMENDATIONS

The following are the recommendations based on the findings from Part 2:

1. For unbonded overlays, the existing PCC elastic modulus input should not exceed a value of 3,000,000 psi.
2. An average HMA gradation from the specification limits should be used for pavement design.
3. The average *G** master curve (level 1) should be used if available for a binder from a source, especially if rutting is the dominant distress.
4. For unbound layers, base and subbase aggregate gradations should be selected within the limits of the specifications.
5. It is recommended that the following rehabilitation option in the DARWin-ME should be used for design until local calibration is performed.
    a. HMA over HMA
    b. Composite overlays
    c. Rubblized overlays
    d. Unbonded PCC overlays
6. The use of falling weight deflectometer (FWD) is recommended to characterize the existing pavement, especially for flexible pavements with high traffic volume. The FWD testing guidelines for sensor configuration, number of drops, testing frequency and temperature measurements are outlined in Chapter 3. The guidelines are

recommended in the short-term while modifications should be made in the long-term based on the local experience.

7. The use of ground penetration radar (GPR) for estimating the existing pavement layer thicknesses in conjunction with FWD is recommended to enhance the back-calculation accuracy and testing efficiency.
8. The load pulse of the MDOT FWD equipment should be used to calculate the frequency based on the equation: $f = \frac{1}{2t}$.
9. Further investigation is needed during the local calibration of the performance models (Part 3 of the study) to evaluate the appropriateness of both backcalculated and design subgrade MR values.

6.4 IMPLEMENTATION

Based on the conclusions and recommendations of Part II study, the following are recommendations for the implementation of the DARWin-ME in the state of Michigan:

- Increase the use of FWD for backcalculation of layer moduli to characterize existing pavement conditions for all the rehabilitation options adopted in Michigan is warranted, especially for high traffic volume roads (interstates and freeways).
- PMS distress data and unit conversion is also necessary to ensure compatibility between MDOT measured and DARWin-ME predicted distresses in the long-term for implementation of the new design methodology (see Tables 6-11 and 6-12). The units can be converted by using the equations mentioned in Chapter 5. The results of conversion should be stored separately in the database for the selected PD's listed Chapter 5. Sensor data (IRI, rut depth and faulting) do not need any further conversion because of their compatibility with DARWin-ME.

Table 6-11 Flexible pavement distresses

Flexible pavement distresses	MDOT units	DARWin-ME units	Conversion needed?
IRI	in/mile	in/mile	No
Top-down cracking	miles	ft/mile	Yes
Bottom-up cracking	miles	% area	Yes
Thermal cracking	No. of occurrences	ft/mile	Yes
Rutting	in	in	No
Reflective cracking	None	% area	No

Table 6-12 Rigid pavement distresses

Rigid pavement distresses	MDOT units	DARWin-ME units	Conversion needed?
IRI	in/mile	in/mile	No
Faulting	in	in	No
Transverse cracking	No. of occurrences	% slabs cracked	Yes

- The significant input variables that are related to the various rehabilitation options and summarized in this report should be an integral part of a database for construction and material related information. Such information will be beneficial for future design projects and local calibration of the performance models in the DARWin-ME. Table 6-13 summarizes the testing needs for the significant input variables obtained from the sensitivity analysis performed in Chapter 4.

Table 6-13 Testing needs for significant input variables for rehabilitation

Pavement layer type	Significant input variables	Lab test[1]	Field test
Overlay	HMA air voids	Yes	
	HMA effective binder	Yes	
	PCC CTE (per °F x 10-6)	Yes	
	PCC MOR (psi)	Yes	
Existing	HMA thickness		Extract core
	Pavement condition rating		Distress survey
	Subgrade modulus		FWD testing
	Subbase modulus		FWD testing
	PCC thickness		Extract core
	Existing PCC elastic modulus (psi)		FWD

[1] Either use current practice or AASHTO test methods

REFERENCES

CHAPTER 2

1. Haider, S. W., H. K. Salama, N. Buch, and K. Chatti, "Significant M-E PDG Design Inputs for Jointed Plain Concrete Pavements in Michigan," presented at the Fifth International Conference on Maintenance and Rehabilitation of Pavements and Technological Control, Park City, Utah, USA, 2007, pp. 79-84.
2. Haider, S. W., H. K. Salama, N. Buch, and K. Chatti, "Influence of Traffic Inputs on Rigid Pavement Performance Using M-E PDG in the State of Michigan," presented at the Fifth International Conference on Maintenance and Rehabilitation of Pavements and Technological Control, Park City, Utah, USA, 2007, pp. 85-90.
3. Buch, N., K. Chatti, S. W. Haider, and A. Manik, "Evaluation of the 1-37A Design Process for New and Rehabilitated JPCP and HMA Pavements, Final Report," Michigan Department of Transportation, Construction and Technology Division, P.O. Box 30049, Lansing, MI 48909, Lansing, Research Report RC-1516, 2008.
4. Haider, S. W., N. Buch, and K. Chatti, "Evaluation of M-E PDG for Rigid Pavements—Incorporating the State-of-the-Practice in Michigan," presented at the 9th International Conference on Concrete Pavements San Francisco, California, USA, 2008, pp.
5. Buch, N., S. W. Haider, J. Brown, and K. Chatti, "Characterization of Truck Traffic in Michigan for the New Mechanistic Empirical Pavemnet Design Guide, Final Report," Michigan Department of Transportation, Construction and Technology Division, P.O. Box 30049, Lansing, MI 48909, Lansing, Research Report RC-1537, 2009.
6. Haider, S. W., N. Buch, K. Chatti, and J. Brown, "Development of Traffic Inputs for Mechanistic-Empirical Pavement Design Guide in Michigan," *Transportation Research Record*, vol. 2256, pp. 179-190, 2011.
7. Baladi, G. Y., T. Dawson, and C. Sessions, "Pavement Subgrade MR Design Values for Michigan's Seasonal Changes, Final Report," Michigan Department of Transportation, Construction and Technology Division, P.O. Box 30049, Lansing, MI 48909, Lansing, Research Report RC-1531, 2009.
8. Baladi, G. Y., K. A. Thottempudi, and T. Dawson, "Backcalculation of Unbound Granular Layer Moduli, Final Report," Michigan Department of Transportation, Construction and Technology Division, P.O. Box 30049, Lansing, MI 48909, Lansing, 2010.
9. Schwartz, C. W., R. Li, S. Kim, H. Ceylan, and R. Gopalakrishnan, "Sensitivity Evaluation of MEPDG Performance Prediction," NCHRP 1-47 Final Report, 2011.
10. Zhou, C., B. Huang, X. Shu, and Q. Dong, "Validating MEPDG with Tennessee Pavement Performance Data," *Journal of Transportation Engineering*, vol. 139, pp. 306-312, 2013.
11. NCHRP Project 1-37A, "Guide for Mechanistic-Empirical Design of New and Rehabilitated Pavement structures," National Cooperative Research Program (NCHRP), Washington D.C. Final Report, 2004.

12. NCHRP Project 1-40B, "Local Calibration Guidance for the Recommended Guide for Mechanistic-Empirical Pavement Design of New and Rehabilitated Pavement Structures," Final NCHRP Report 2009.
13. AASHTO, "Mechanistic-Empirical Pavement Design Guide: A Manual of Practice: Interim Edition," American Association of State Highway and Transportation Officials 2008.

CHAPTER 3

1. AASHTO, "Mechanistic-Empirical Pavement Design Guide: A Manual of Practice: Interim Edition," American Association of State Highway and Transportation Officials 2008.
2. NCHRP Project 1-37A, "Guide for Mechanistic-Empirical Design of New and Rehabilitated Pavement structures," National Cooperative Research Program (NCHRP), Washington D.C. Final Report, 2004.
3. Tompkins, D., P. Saxena, A. Gotlif, and L. Khazanovich, "Modification of Mechanistic-Empirical Pavement Design Guide Procedure for Two-Lift Composite Concrete Pavements," 2012.
4. Smith, K. D., J. E. Bruinsma, M. J. Wade, K. Chatti, J. M. Vandenbossche, and H. T. Yu, "Using Falling Weight Deflectometer Data with Mechanistic-Empirical Design and Analysis, Volume 1: Final Report," Federal Highway Administration, 1200 New Jersey Avenue, SE, Washington, DC 20590 2010.
5. Pierce, L. M., K. D. Smith, J. E. Bruinsma, M. J. Wade, K. Chatti, and J. M. Vandenbossche, "Using Falling Weight Deflectometer Data with Mechanistic-Empirical Design and Analysis, Volume 3: Guidelines for Deflection Testing, Analysis, and Interpretation," Federal Highway Administration, 1200 New Jersey Avenue, SE, Washington, DC 20590 2010.
6. Chatti, K., M. Kutay, and L. Lei, "Relationships between Laboratory-Measured and Field-Derived Properties of Pavement Layers," 2011.

CHAPTER 4

1. Buch, N., K. Chatti, S. W. Haider, and A. Manik, "Evaluation of the 1-37A Design Process for New and Rehabilitated JPCP and HMA Pavements, Final Report," Michigan Department of Transportation, Construction and Technology Division, P.O. Box 30049, Lansing, MI 48909, Lansing, Research Report RC-1516, 2008.
2. Haider, S. W., N. Buch, and K. Chatti, "Evaluation of M-E PDG for Rigid Pavements—Incorporating the State-of-the-Practice in Michigan," presented at the 9th International Conference on Concrete Pavements San Francisco, California, USA, 2008, pp.
3. Schwartz, C. W., R. Li, S. Kim, H. Ceylan, and R. Gopalakrishnan, "Sensitivity Evaluation of MEPDG Performance Prediction," NCHRP 1-47 Final Report, 2011.
4. Kutay, E. and A. Jamrah, "Preparation for Implementation of the Mechanistic-Empirical Pavement Design Guide in Michiagn: Part 1 - HMA Mixture Characterization," Michigan Department of Transportation, 425 West Ottawa, P.O. Box 30050 Lansing, MI 48909, Lansing, Research Report ORBP OR10-022, 2012.

5. NCHRP Project 1-37A, "Guide for Mechanistic-Empirical Design of New and Rehabilitated Pavement structures," National Cooperative Research Program (NCHRP), Washington D.C. Final Report, 2004.
6. Rauhut, J. B., A. Eltahan, and A. L. Simpson, "Common Characteristics of Good and Poorly Performing AC Pavements," Federal Highway Administration, FHWA-RD-99-193, December 1999.
7. Khazanovich, L., D. M, B. R, and M. T, "Common Characteristics of Good and Poorly Performing PCC Pavements," Federal Highway Administration, FHWA-RD-97-131, 1998.
8. Haider, S. W., N. Buch, K. Chatti, and J. Brown, "Development of Traffic Inputs for Mechanistic-Empirical Pavement Design Guide in Michigan," *Transportation Research Record*, vol. 2256, pp. 179-190, 2011.
9. Buch, N., S. W. Haider, J. Brown, and K. Chatti, "Characterization of Truck Traffic in Michigan for the New Mechanistic Empirical Pavemnet Design Guide, Final Report," Michigan Department of Transportation, Construction and Technology Division, P.O. Box 30049, Lansing, MI 48909, Lansing, Research Report RC-1537, 2009.
10. AASHTO, "Mechanistic-Empirical Pavement Design Guide: A Manual of Practice: Interim Edition," American Association of State Highway and Transportation Officials 2008.
11. Weckman, G., D. Millie, C. Ganduri, M. Rangwala, W. Young, M. Rinder, and G. Fahnenstiel, "Knowledge extraction from the neural ‘black box’in ecological monitoring," *Journal of Industrial and Systems Engineering*, vol. 3, pp. 38-55, 2009.